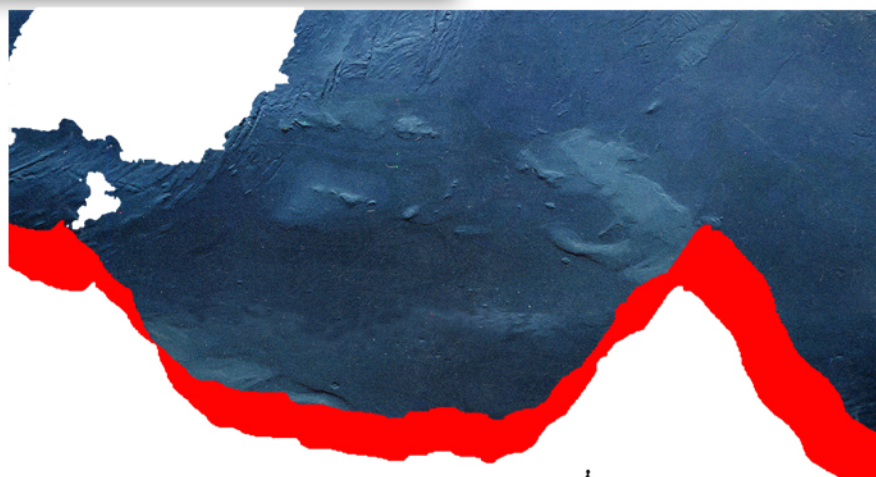


STRUCTURAL CONTROLS ON MAGMA TRANSPORT AND



THE GEOLOGICAL SOCIETY
OF AMERICA



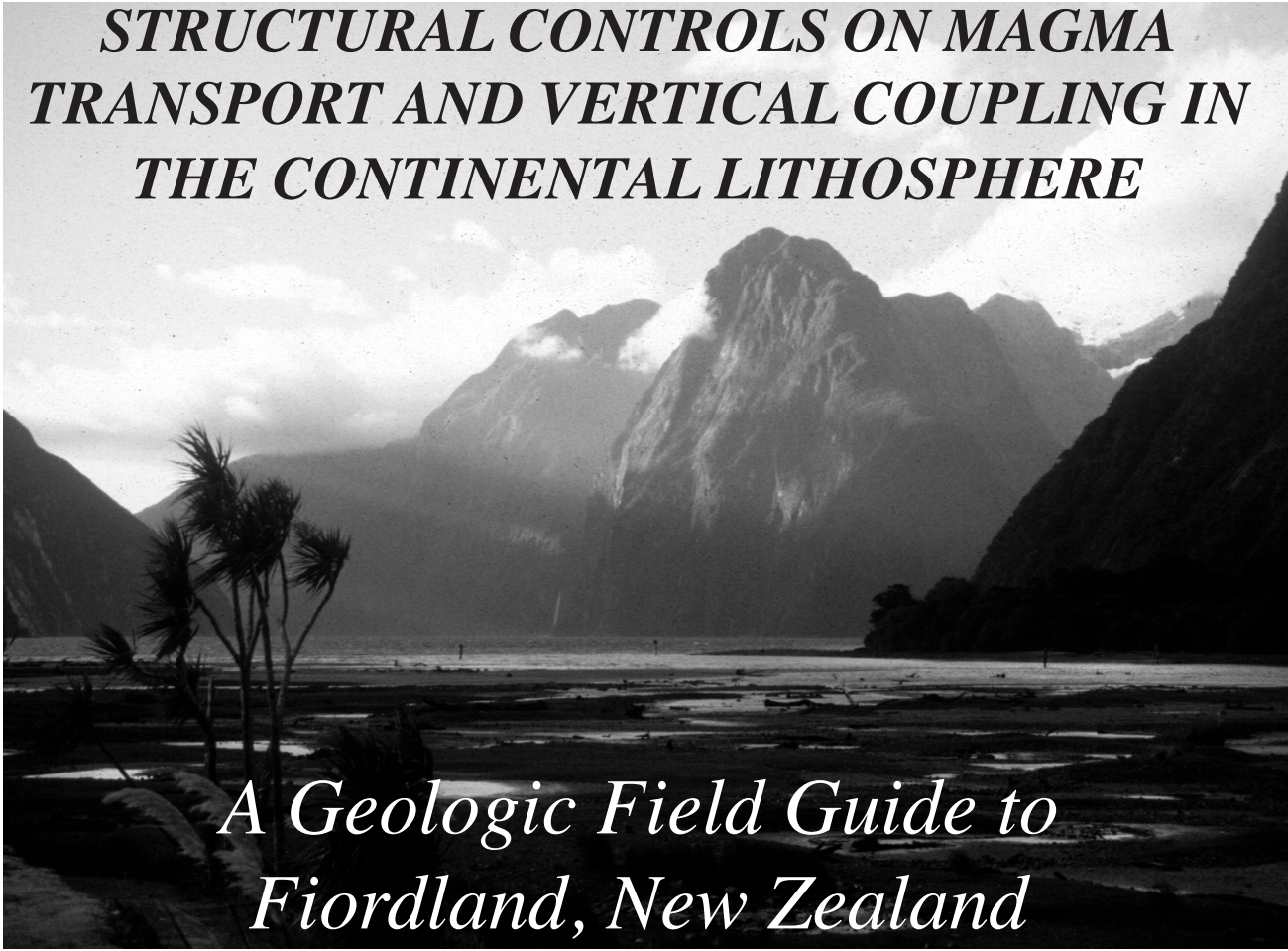
**KEITH KLEPEIS
GEOFFREY CLARKE
TRACY RUSHMER
ANDREW TULLOCH**



VERTICAL COUPLING IN THE CONTINENTAL LITHOSPHERE

APRIL 26 - MAY 6 2003 - NEW ZEALAND

***STRUCTURAL CONTROLS ON MAGMA
TRANSPORT AND VERTICAL COUPLING IN
THE CONTINENTAL LITHOSPHERE***



***A Geologic Field Guide to
Fiordland, New Zealand***

Keith Klepeis

Department of Geology, University of Vermont, U.S.A.

Geoffrey Clarke

School of Geosciences, University of Sydney, Australia

Tracy Rushmer

Department of Geology, University of Vermont, U.S.A.

Andrew Tulloch

Institute of Geological and Nuclear Sciences, New Zealand

Geological Society of America Field Forum
April 26-May 6, 2003

Cover artwork by Javier Pelcastre and Carmelina Mora, Cancún, Mexico

Acknowledgements

This Field Forum was made possible through the assistance of numerous people, agencies and businesses in the U.S., Australia and New Zealand. We are indebted to the Geological Society of America for sponsoring the Field Forum. We especially thank Edna Collis for her support and assistance in managing aspects of the logistics, accounts and the guidebook. Travel grants from the Geological Society of America's Pretorius Fund helped students attend the meeting. We also thank the U.S. National Science Foundation for generous funding that aided student participation at the Field Forum and helped with some of the logistics of running the trip in New Zealand. We especially thank Arthur Goldstein and David Fountain for their enthusiastic support and encouragement. We also are grateful to Ian Turnbull and Nick Mortimer at the Institute of Geological and Nuclear Sciences in Dunedin for many helpful discussions and assistance during our years of work in Fiordland. Rupert Sutherland also provided valuable insights and discussions. They have inspired us with their enthusiasm and provided valuable encouragement and commentary.

We also thank our current and former students, whose work has been vital to our understanding of Fiordland geology: Julie Hollis (1996), Tim Patrick (1996), Helen Degeling (1997), Nathan Daczko (1997); Louise Turner (1998), James Stevenson (2000), Alex Papadakis (2000), Alex Claypool (2000-2001), Ben Dockrill (2000), Jelte Harnmeijer (2001), Dale Walker (2001), Stephen Marcotte (2002-2003), and W. Corey Simonson (2002-2003). Angelo Antignano (2000-2002) performed experiments on the Pembroke diorite at the University of Vermont. We also thank our colleagues for their assistance and expertise. The work of Nathan Daczko during the pursuit of his PhD was instrumental to our understanding of northern Fiordland. Richard White provided valuable assistance in George Sound and during work on the Anita Shear Zone at Poison Bay. Nigel Kelly provided assistance at Caswell Sound. Julie Hollis provided expertise and assistance both in the field near Milford Sound and, with Trevor Ireland at ANU, in working out the geochronology of the high grade granulites. George Gehrels and Jeff Vervoort at the University of Arizona provided geochronologic data from Caswell Sound and south of Milford Sound. Bill Collins provided helpful discussions and assistance during work north and south of Milford Sound.

We thank the Department of Land Conservation in Te Anau for permission to visit and sample localities mentioned in the text. In addition, we thank Jeff Shanks and Sean Mullay of *Milford Helicopters* for their years of support, they are two of the best helicopter pilots we have ever encountered. We offer our warm thanks to Paul Norris of *Real Journeys* for his assistance and for helping us organize the *Milford Wanderer* and other support for this trip. We thank the captain and crew of the *Milford Wanderer* for their expertise and assistance guiding us through the waterways and coastlines of Fiordland. We also thank Jennifer and Dave Kluken at Milford Sound Lodge for their assistance and understanding of the special needs of geologists on field trips. Gabriela Mora-Klepeis' help as the logistical assistant and field coordinator of this trip was extremely valuable. We also thank Javier Pelcastre and Carmelina Mora for the artwork used on the cover of this guidebook and at the Field Forum.

The work that formed the foundation of this Field Forum was funded by Australian Research Council grants to K.K. and G.C. (ARC-A10009053), National Science Foundation grants to K.K. and T.R. (EAR-0087323) and (EAR-0313626), an ARC grant to G.C. (ARC discovery project DP0342862), and grants from the Geological Society of America, and support from the Institute of Geological and Nuclear Sciences, the University of Sydney, and the University of Vermont.

<u>Participant List</u>	<u>e-mail</u>	<u>Affiliation</u>
Andrew Allibone	andrew.allibone@jcu.edu.au	James Cook University
Geoffrey Clarke	geoffc@mail.usyd.edu.au	University of Sydney
Maria Luisa Crawford	mcrawfor@brynmawr.edu	Bryn Mawr College
William Crawford	wcrawfor@brynmawr.edu	Bryn Mawr College
Nathan Daczko	ndaczko@mail.utexas.edu	University of Texas at Austin
Jonathan Davidson	J.P.Davidson@durham.ac.uk	University of Durham
Michael Dungan	michael.dungan@terre.unige.ch	Université de Geneve
James Dunlap	Jim.Dunlap@anu.edu.au	Australian National University
Joel Fitzherbert	joelf@mail.usyd.edu.au	University of Sydney
George Gibson	George.Gibson@ga.gov.au	Geoscience Australia
Scott Giorgis	scott@geology.wisc.edu	University of Wisconsin, Madison
Arthur Goldstein	agoldste@nsf.gov	National Science Foundation
Bradley Hacker	hacker@geol.ucsb.edu	University of California, Santa Barbara
Jacqui Halpin	jacqui_halpin@hotmail.com	University of Sydney
Simon Harley	sharley@glg.ed.ac.uk	University of Edinburgh
Steve Israel	sisrael@eos.ubc.ca	University of British Columbia
Keith Klepeis	kklepeis@uvm.edu	University of Vermont
Jeffrey Lee	jeff@caliente.geology.cwu.edu	Central Washington University
Stephen Marcotte	smarcotte@zoo.uvm.edu	University of Vermont
Robert Miller	rmiller@geosun.sjsu.edu	San Jose University
Gabriela Mora-Klepeis	gmora@zoo.uvm.edu	University of Vermont
Alberto Patino-Douce	klington@gly.uga.edu	University of Georgia
Robert Price	rprice@zoo.uvm.edu	University of Vermont
Peter Robinson	probinso@els.mq.edu.au	Macquarie University
Tracy Rushmer	trushmer@zoo.uvm.edu	University of Vermont
Jinny Sisson	jinnys@rice.edu	Rice University
Harold Stowell	hstowell@wgs.geo.ua.edu	University of Alabama
Rupert Sutherland	R.Sutherland@gns.cri.nz	IGNS, Wellington
Andrew Tulloch	A.Tulloch@gns.cri.nz	IGNS, Dunedin
Ian Turnbull	I.Turnbull@gns.cri.nz	IGNS, Dunedin
Cees Van Staal	cvanstaa@NRCan.gc.ca	University of Ottawa
Julie Vry	Julie.Vry@vuw.ac.nz	Victoria University of Wellington
Tina White	TinaM@mail.utexas.edu	University of Texas at Austin
Robert Wiebe	bob.wiebe@fandm.edu	Franklin and Marshall College
Carlos Zuluaga	zuluua001@bama.ua.edu	University of Alabama
Horst Zwingmann	Horst.Zwingmann@csiro.au	CSIRO, Australia

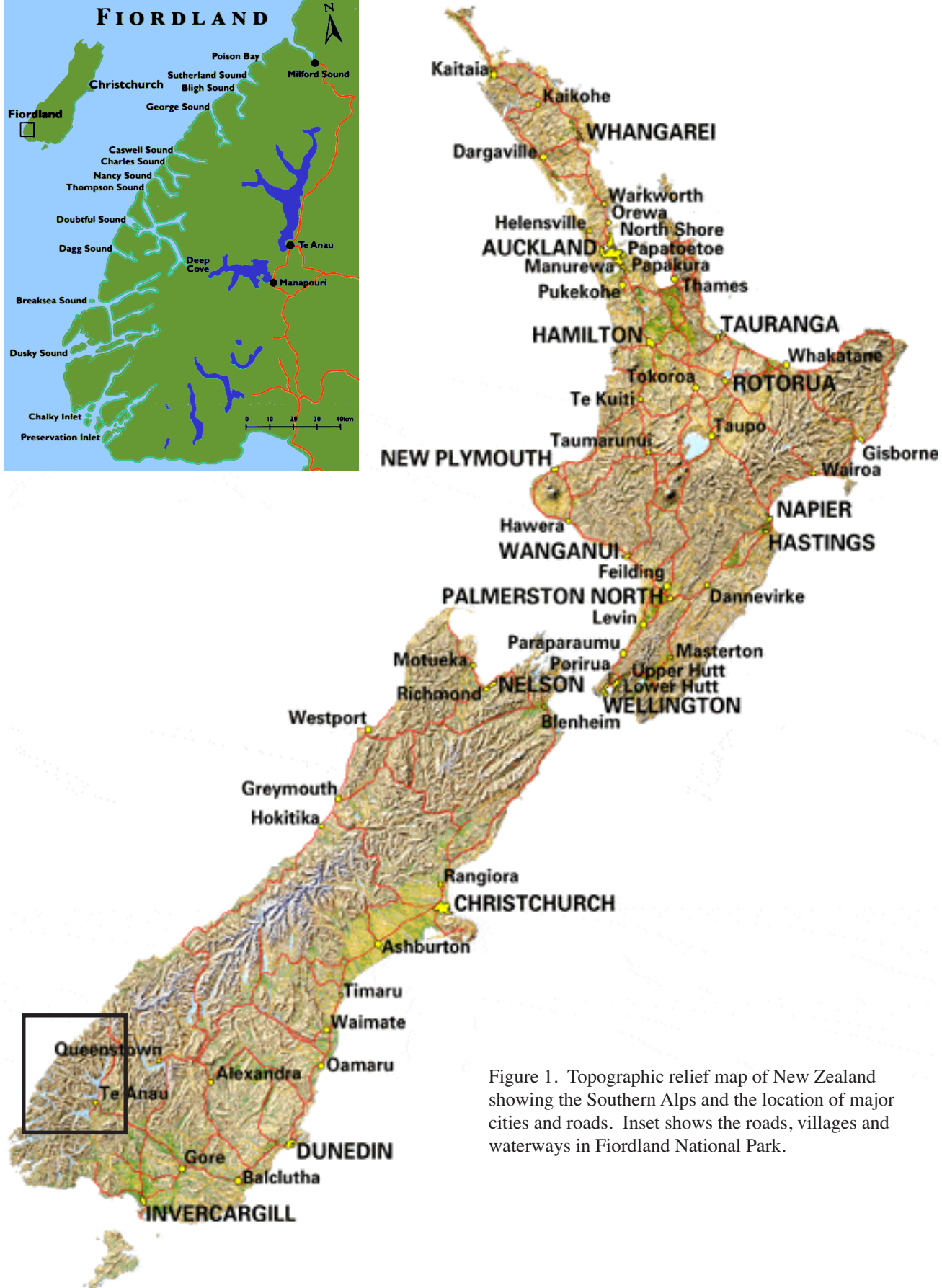


Figure 1. Topographic relief map of New Zealand showing the Southern Alps and the location of major cities and roads. Inset shows the roads, villages and waterways in Fiordland National Park.

Prospective Itinerary

April 26: Arrive in Dunedin, New Zealand (Fig. 1), by 5 p.m. for dinner and orientation.

April 27: Chartered bus to Milford Sound, stopping to examine magma mingling textures and mafic intrusions in the upper crust of an early Mesozoic island arc.

April 28–30: Orientation; short in-house conference where participants present and discuss relevant work; outcrop examination of lower crustal granulites, high-*P* migmatites, granulite facies mineral assemblages, and lower crustal shear zones; access by helicopter if weather permits.

May 1: Examine coastal exposures of Milford Sound aboard the *Milford Wanderer*. Includes boundaries of the granulite belt and early Mesozoic arc and lower crustal shear zones showing variable styles of strain partitioning.

May 2: George Sound. Examine migmatite textures, metamorphic assemblages, and intrusive contacts inside a mafic-intermediate lower crustal batholith. Relationships here contrast with those found below the batholith.

May 3: Caswell Sound. Examine a mid-crustal fold-thrust belt and its relationship to magmatism at and above the uppermost contact of the batholith.

May 4: Crooked Arm. Examine sheeted ultramafic, gabbroic and dioritic intrusions, evidence of the partial melting of mafic lower crust and extensional shear zones that evolved at garnet granulite facies conditions.

May 5: Continued examination of Crooked Arm leaving boat by noon. Bus and ferry to the town of Te Anau for dinner and overnight.

May 6: Travel to Dunedin (5 hours). Flights out after 1 p.m.

Logistical Notes. For five days, we will be living aboard the *Milford Wanderer* (a fully enclosed, comfortable boat with three decks, 35 berths, tendercraft, and a crew of five) to access remote sites along the waterways of Fiordland National Park. After the first night in a motel in Dunedin, we'll stay three nights at the Milford Lodge (comfortable budget accommodation) where we'll visit field sites and hold an informal conference. We may use short helicopter trips if weather permits. While aboard the *Milford Wanderer*, we'll visit outcrops using small boats and anchor in protected areas for the evening. Dinners (6–7 p.m.) will be followed by informal discussions. Participants should be physically fit and comfortable walking on steep, rocky terrain. Limited roadside access will involve short walks (<0.5 km). Elsewhere we will be in mountain valleys (<1500 m) or landing on coastal outcrops. Participants should be prepared for wind, rain, and cool (5–10 °C, 40–50 °F) temperatures. A list of recommended clothing will be provided.

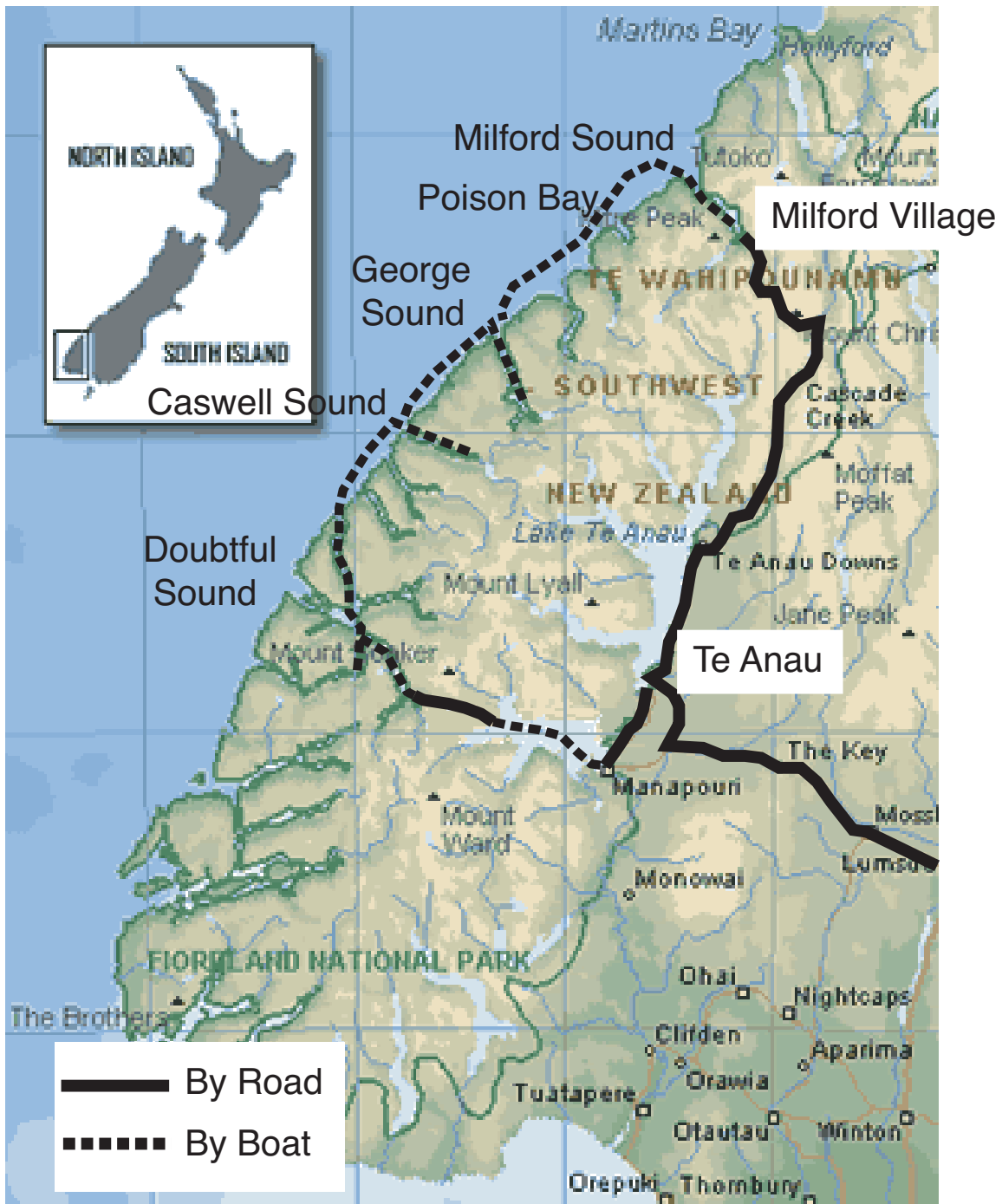


Figure 2. Map showing the route of the Field Forum.

Introduction and Aims of the Field Forum

The mechanisms by which magma is generated, segregated and transported through continental crust and how these processes affect the mechanical evolution of orogens are two of the least understood issues of continental dynamics. Numerical models of convergent orogens show that periodic magmatism and rapidly changing thermal and structural regimes in the lower crust strongly influence the behavior of the entire lithosphere. However, few field sites allow us to examine directly structural and magmatic features that evolved simultaneously within large sections of the lower crust. This lack of exposure has severely inhibited our ability to determine the effects of feedbacks among magmatic, metamorphic and deformation processes on lithospheric evolution for specific tectonic scenarios.

The deeply eroded, Early Cretaceous granulite belt of Fiordland, New Zealand provides us with an unusual opportunity to examine structural, metamorphic and magmatic processes at very deep levels of an ancient orogen (25-50 km paleodepths). This belt contains rare exposures of high-pressure migmatites and lower crustal structural features that enable us to observe directly how magma is generated, segregated and transported through the continental crust and how these processes affect the vertical coupling of deformation within an ancient orogen.

The aim of this field forum is to provide a group of investigators working on these topics with the opportunity to examine structures controlling the transfer of magma and displacements vertically through a thermally and mechanically evolving crustal column. We will use one of the world's best field examples to visit sites that record these processes in the lower crust. Our intent is that the spectacular preservation of rock textures and structures in Fiordland will stimulate new ideas and provide a basis for us to reevaluate our understanding of melt generation and escape from the lower crust and how migrating magma interacts with deformation at the lithospheric scale.

These exposures allow us to address the following specific issues:

- 1) Evidence of rapidly evolving thermal and structural regimes in the lower crust during a 35 million year period and the effects of these changes on the evolution of the lithosphere.
- 2) Evidence of fluid and melt sources and changing mechanisms of magma segregation and transport through the lower crust.
- 3) Feedback mechanisms among crustal melting, granulite facies metamorphism and deformation.
- 4) The effects of the crustal melting and magmatism on vertical coupling/decoupling processes within the lithosphere.
- 5) Flow patterns in natural lower crustal shear zones and their relationship to deformation and magma transport processes.
- 6) Space-time controls on deformation partitioning and strain localization processes in the lower crust.

This field guide is organized by geographic locality, beginning with Milford Sound in the north and ending with Doubtful Sound in the South (Fig. 2). Descriptions of the geology of these areas are preceded by summaries of the regional geologic settings of Fiordland and the South Island, and the overall structure and geologic history of Fiordland rocks.

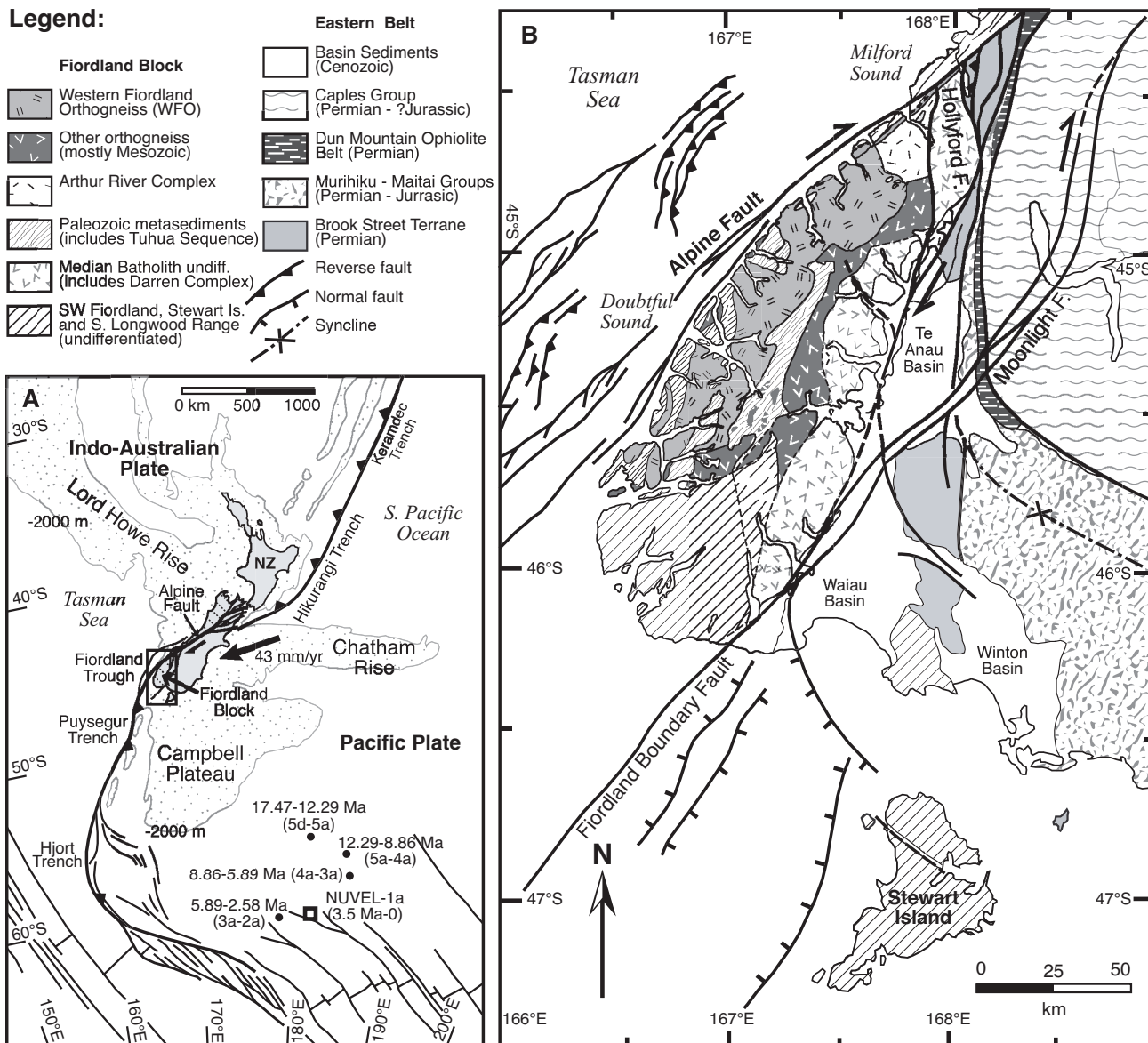


Figure 3. (a) Tectonic setting of New Zealand. Indo-Australian-Pacific plate slip vector indicated (arrow). The Pacific plate has rotated counterclockwise relative to a fixed Australian plate about Euler poles (black dots) that have changed position with time (Walcott, 1998). Time periods and magnetic anomalies (in parentheses) for each pole of motion are indicated. The instantaneous, present-day Euler Pole (NUVEL-1a) is from DeMets (1994). Inset shows location of the Fiordland region. (b) Map showing the geology and structure of the Fiordland Block and Eastern sedimentary belt. High-*P* granulites occur in the Arthur River Complex and Western Fiordland Orthogneiss. The Fiordland Block is outlined by the Alpine, Hollyford, Moonlight, and Fiordland Boundary faults (Norris and Carter, 1980; Norris and Turnbull, 1993). Offshore structures in the Tasman Sea are from Lebrun et al. (2000). Major lithologic divisions are from Bradshaw (1990).

Regional Setting of South Island

The geology of the south island of New Zealand can be divided into Eastern and Western provinces (Landis and Coombs, 1967; Bishop et al., 1985; Turnbull, 2000). A belt of rocks that are referred to as the Median Tectonic Zone (Kimbrough et al., 1993, 1994) or the Median Batholith (Fig.

3; Mortimer et al., 1999) separate these two provinces. Most of the Eastern Province formed within a convergent setting and contains arc-volcanic rocks, arc-derived sedimentary sequences, and accretionary complexes of Permian-Cretaceous age (MacKinnon, 1983; J.D. Bradshaw, 1989; Mortimer et al., 1995). The Western Province is composed of Lower Paleozoic paragneiss cut by Devonian and Carboniferous granitoids (Muir et al., 1998; Wandres et al., 1998; Ireland and Gibson, 1998). Rocks within this province preserve a polyphase mid-Paleozoic history that includes low-P/high-T metamorphism followed by medium-P/high-T metamorphism. Paleozoic events occurred when ancestral New Zealand lay within or outboard of the Pacific margin of Gondwana (Wood, 1972; Carter et al., 1974; Ireland and Gibson, 1998; Mortimer et al., 1999).

The Median Tectonic Zone or Median Batholith (Fig. 3) is a comparatively narrow belt of tectonically disrupted arc-related rocks with U-Pb zircon ages that mostly fall into two age groups: 247–195 Ma and 157–131 Ma (J.Y. Bradshaw, 1990; Kimbrough et al., 1993, 1994). Late Triassic plutons that intrude the Eastern Province indicate that this province and the Median Tectonic Zone were together by this time (Williams and Harper, 1978; Mortimer et al., 1999). Rocks of the Median Tectonic Zone and the Western Province are intruded by stitching plutons of the Early Cretaceous 126–116 Ma Western Fiordland Orthogneiss / Separation Pt. Suite (J.Y. Bradshaw, 1990; Kimbrough et al., 1994). Mafic dikes that intrude Lower Paleozoic host gneiss in the Western Province near Milford Sound suggest that the amalgamation of the Median Tectonic Zone with Gondwana may have occurred as early as ~136 Ma and probably by ~129 Ma (Hollis et al., 2003).

Summary of the Geologic History of Fiordland

In this field guide we focus on a Mesozoic history of lower crustal magmatism, high grade metamorphism and both contractional and extensional deformation that occurred when Fiordland formed part of the Gondwana margin (Fig. 4). However, it is important to keep in mind that the Fiordland rocks also record a history of Paleozoic convergence as well as Cenozoic tectonism. To interpret the effects of Mesozoic events, we must also be able to recognize the effects of all stages in the geologic history of the region. In this section we summarize the main geologic intervals recorded in the Fiordland rock record.

Paleozoic Convergence

Gabbroic to dioritic orthogneisses and metasediments of northern and central Fiordland record a history of both Paleozoic and Early Cretaceous orogenesis. Paleozoic tectonism involved contractional deformation, low to high grade metamorphism, and pluton emplacement within the Pacific margin of Gondwana from ~481 to ~334 Ma (Oliver, 1980; Gibson et al., 1988; Ireland and Gibson, 1998). Crustal thickening and tectonic burial during this period are indicated by medium to high pressure (P=7–9 kbar) kyanite-bearing assemblages that overprint lower pressure (P=3–5 kbar) sillimanite-bearing assemblages in Paleozoic metasediments (Gibson, 1990).

Early Cretaceous Magmatism, Metamorphism, and Convergence

Superimposed on Paleozoic structures and mineral assemblages is a record of Early Cretaceous arc-related pluton emplacement, high-P upper amphibolite-granulite facies metamorphism, and intense contractional deformation (J.Y. Bradshaw, 1989; Brown, 1996; Clarke et al., 2000; Klepeis et al., 2003). These events coincided with the emplacement of a major batholith and the accretion of outboard terranes

(including the MTZ, Fig. 4) onto the Pacific margin of Gondwana (Mattinson et al., 1986; McCulloch et al., 1987; Tulloch and Kimbrough, 1989; Mortimer et al., 1999). Most of the accreted terranes now make up the Eastern Province of SW New Zealand.

During the period 126-116 Ma, the lower crust now represented by rocks in northernmost Fiordland accumulated at least 10 km (thickness) of mafic-intermediate magma (Mattinson et al., 1986). The first phases were gabbroic with minor ultramafic compositions; later phases were dominated by diorite. This intrusion formed a >3000 km² batholith called the Western Fiordland Orthogneiss (WFO, Fig. 3) and has been interpreted to have added sufficient heat to the lower crust to partially melt host gneisses (Daczko et al., 2001b). At the time of this intrusion, the lower crust was composed of older (>126 Ma) mafic-intermediate intrusive phases of the early Mesozoic arc (Hollis et al., 2003), and Paleozoic gneisses of Gondwana margin affinity (Tulloch et al., 2000).

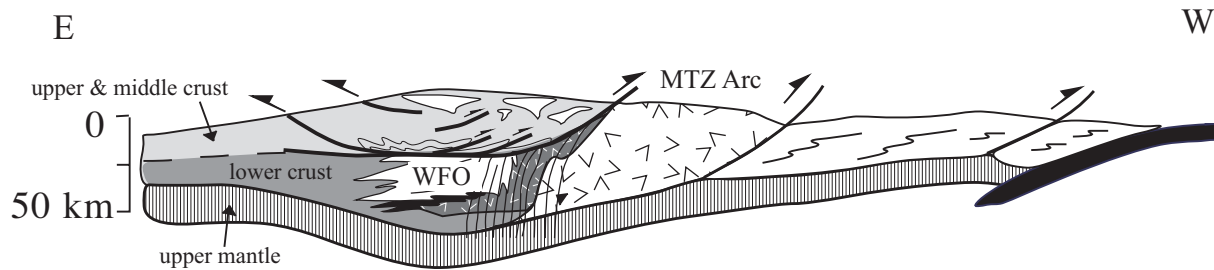


Figure 4. Schematic cross-section showing a convergent setting between the Gondwana continental margin and an early Mesozoic arc (MTZ) after Klepeis et al. (2003). WFO is the Western Fiordland Orthogneiss batholith.

The ages of major intrusive features and of Cretaceous deformation and metamorphism are well constrained by published geochronology (Mattinson et al., 1986; McCulloch et al., 1987; Gibson and Ireland, 1995; Muir et al., 1998; Ireland and Gibson, 1998; Nathan et al., 2000; Tulloch et al., 2000; Hollis et al., 2003). Published dates and analyses of zircon from within the section reveal two distinctive periods of Early Cretaceous magmatism and deformation: 1) the emplacement of mafic-intermediate magma into the lower crust (150-116 Ma) and the partial melting of lower crustal host gneisses; and 2) contractional deformation and the emplacement of sodic, high Sr/Y granitoids in the middle and upper crust (116-105 Ma). The mafic dikes and plutons that make up the Arthur River Complex near Milford Sound record magmatism, melting and deformation that occurred during these two periods. The first period included emplacement of the Western Fiordland Orthogneiss, which intruded the Arthur River Complex (Mattinson et al., 1986; Bradshaw, 1990). U-Pb ion probe dates on zircons from the Arthur River complex have yielded some Paleozoic protolith ages (355±10 Ma) and metamorphic ages at ~134 Ma and ~120 Ma (Tulloch et al., 2000). Garnet-pyroxene-plagioclase-bearing assemblages within the Arthur River Complex and the Western Fiordland Orthogneiss give metamorphic pressures (P=12-16 kbar) indicative of lower crustal paleodepths (Blattner, 1978; J.Y. Bradshaw, 1989; Clarke et al., 2000; Daczko et al., 2001a).

Mid-Cretaceous Extension

By 108-105 Ma extension affected parts of the Fiordland belt and other areas (J.D. Bradshaw, 1989; Tulloch and Kimbrough, 1989; Gibson and Ireland, 1995; Spell et al., 2000). The Doubtful Sound shear zone is formed during this period (Gibson et al., 1988; Gibson and Ireland, 1995). In northern Fiordland, the Anita Shear Zone (Fig. 5) contains several superposed fabrics that formed

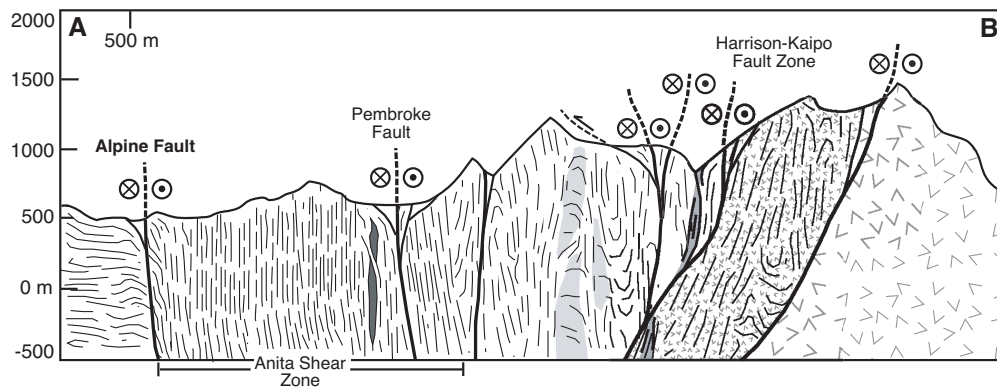
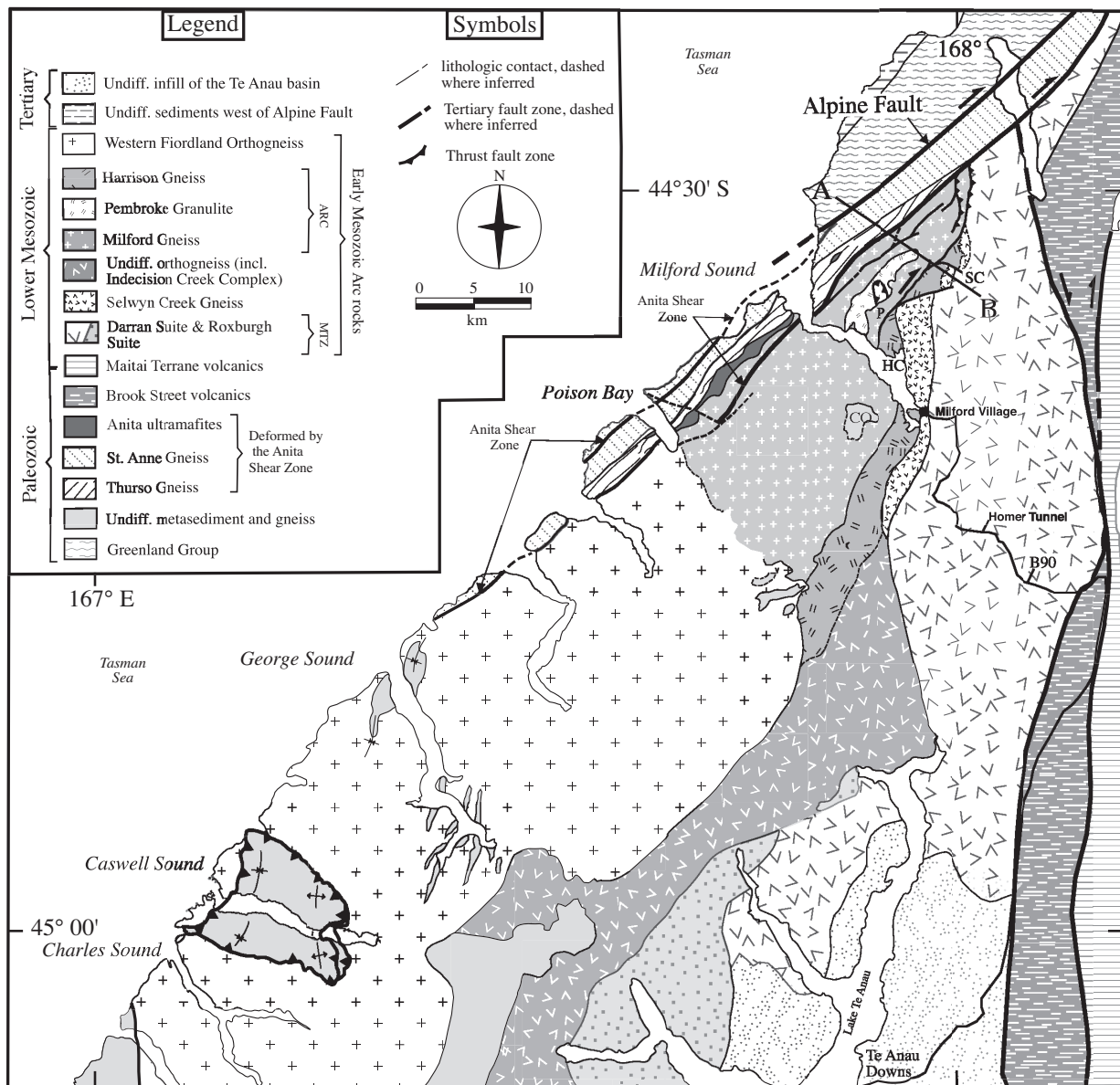


Figure 5. Geologic map of north-central Fiordland showing the major lithologic subdivisions. Map was constructed using data from Bradshaw (1989; 1990), Blattner (1991), Turnbull (2000), Daczko et al. (2002), Claypool et al. (2002) and Klepeis and Clarke (2003). P is Pembroke Valley, CO is Camp Oven Creek, ARC is the Arthur River Complex, MTZ is the Median Tectonic Zone, SC is Selwyn Creek, HC is Harrison Cove, B90 is Bridge 90. Profile (A-B) is after Claypool et al. (2002).

during or after this period (Hill, 1995; Klepeis et al., 1999; Nathan et al., 2000). K-Ar ages of hornblende (Nathan et al., 2000) and U-Pb dates of apatite (Mattinson et al., 1986) suggest that the granulites had cooled to 300-400°C by ~90 Ma. This last phase preceded inception of seafloor spreading in the Tasman Sea (~84 Ma) by ~15 Ma (Gaina et al., 1998) and was accompanied by the formation of extensional metamorphic core complexes elsewhere in New Zealand (Tulloch and Kimbrough, 1989).

Late Cretaceous-Cenozoic Tectonic History

Late Cretaceous extension and rifting associated with the breakup of Gondwana led to the opening of the Tasman Sea basin between Australia and New Zealand by ~84 Ma (Gaina et al., 1998). By approximately 52 Ma, sea floor spreading along the central Tasman ridge system had ended (Gaina et al., 1998) and a new period of rifting initiated in the southwest Tasman Sea region south of New Zealand (Weissel et al., 1977). Here, the Pacific-Australia plate boundary developed as a spreading center at least by 47-45 Ma (Sutherland et al., 2000). From 30 to 11 Ma, the spreading direction became progressively more oblique and the boundary eventually evolved into a transform as the relative pole of rotation between the Pacific and Australian plates migrated southward (Lamarche et al., 1997). Spreading ceased and oblique subduction initiated beneath the continent between 12 and 10 Ma (Davey and Smith, 1983). Later, clockwise rotation of the Euler pole (Fig. 3a) resulted in strike-slip motion along most of the plate boundary, followed by transpression (Sutherland, 1995). Near the end of the Miocene (~6.4 Ma), a decrease in the obliquity of plate convergence resulted in an increase in the rate of convergence and the uplift of the Southern Alps (Walcott, 1998).

Approximately 70-75% of motion arising from the current regime of oblique convergence between the Australian and Pacific plates is accommodated by orogen-parallel slip along the Alpine Fault (Sutherland et al., 2000; Norris and Cooper, 2001). This fault links the E-dipping Puysegur trench to the south with the west-dipping Hikurangi subduction zone to the north (Fig. 3a). Four hundred and sixty kilometers of offset have accumulated along the Alpine Fault (Wellman, 1953). Uplift rates are estimated at 5-12 mm/year (Bull and Cooper, 1986; Walcott, 1998). Plate motion vectors near the central section of the Southern Alps have been calculated from global plate models at rates of 39-45 mm/yr at azimuths of 071°-083° (Chase, 1978; Walcott, 1979; 1998; DeMets et al., 1994). Late Quaternary slip rates indicate that 27 ± 5 mm/year of strike-slip occurs on the Alpine Fault north of Milford Sound (Sutherland, 1994). Dip-slip rates show variation along strike of the Alpine Fault with a maximum of >10 mm/year in the central section and decreasing to zero near Milford Sound (Norris and Cooper, 2001). These estimates imply late Quaternary rates of shortening as high as 25 ± 3 mm/year may be accommodated away from the southernmost (onshore) segment of the Alpine Fault. Other estimates suggest shortening rates across the Alpine Fault range from 10-16 mm/yr (Walcott, 1998).

April 27-May 1

Milford Sound and Adjacent Areas

The Milford Road Exposures

The upper crustal part of an Early Mesozoic Arc. The road from Te Anau to Milford Sound (Fig. 5) crosses a series of fault-bounded terranes composed of Permian-Early Cretaceous plutonic, volcanic

and volcanoclastic rocks of the Median Tectonic Zone or Median Batholith. This batholith represents part of an early Mesozoic magmatic arc that initially formed outboard of Gondwana during 247-131 Ma subduction-related magmatism (Fig. 4; Kimbrough et al. 1994; Muir et al. 1998; Tulloch and Kimbrough, 2003). Prior to Late Cenozoic faulting, the Median Batholith extended >500 km from Stewart Island (Fig. 3b; Allibone and Tulloch, 1997) through Fiordland to the northwest corner of the South Island. Onshore, extensive rain forest cover commonly obscures field relationships, and it was not until recently that the extent and continuity of the composite marginal batholith was recognized (Mortimer et al., 1999).

On the eastern side of the Median Batholith, low grade volcanoclastic rocks of the Brook Street Terrane and the Maitai Terrane represent arc-derived volcanoclastic rocks and accretionary complexes that accreted onto the margin of Gondwana during the early Mesozoic (Figs. 3b, 5; J.D. Bradshaw 1989; Mortimer et al. 1999; Turnbull, 2000). This eastern side also contains low-K, high-Na rocks of the *Separation Point Suite* (Tulloch 1988; Muir et al., 1995; Tulloch and Kimbrough, 2003). In easternmost Fiordland the plutonic suite is dominated by tonalite, granodiorite, and granite (Tulloch and Rabone, 1993). In western Fiordland the suite includes gabbro, diorite and monzodiorite of the Western Fiordland Orthogneiss (J.Y. Bradshaw, 1990). Tilted sedimentary sequences of the early Cenozoic Te Anau Basin (Figs. 3b, 5) rest unconformably on top of the Median Batholith.

Claypool et al. (2002) found that the terranes and high-grade gneisses that occur as fault-bounded wedges in Fiordland were shuffled vertically and squeezed up between curved reverse and oblique-slip faults (Figs. 5b, 6). The Arthur River Complex and the Darran Complex constitute two of these wedges that have been displaced relative to one another (Fig. 6). Displacement on these faults have disrupted

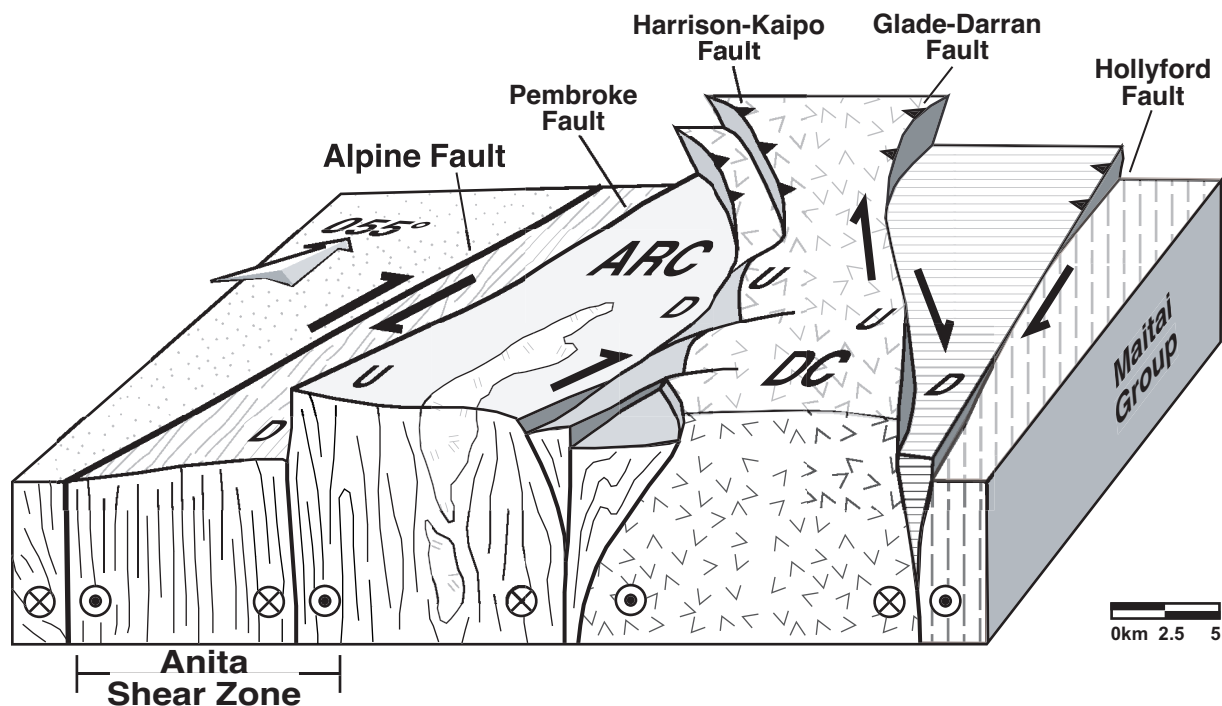


Figure 6. Block diagram of region north of Milford Sound showing fault-bounded terranes of northern Fiordland after Claypool et al. (2002). Oblique-slip and reverse motion have resulted in the vertical displacement of the Arthur River Complex (ARC) and the Darran Complex (DC) relative to adjacent wedges.

most of the original intrusive contacts along the margins of the Darran Suite, although we will visit one site (Harrison Cove) where the contact between the Darran Suite and the Arthur River Complex may be gradational.

The eastern side of the Median Batholith along the Milford road includes leucogabbro, gabbro and diorite of the Darran Suite (Fig. 5; Williams and Harper, 1978; Kimbrough et al., 1994; Mortimer and others, 1999; Blattner and Graham, 2000). This unit is composed of unmetamorphosed gabbro and diorite that represent the shallow, upper crustal part of the early Mesozoic arc. Most of the Darran Suite is only weakly deformed. However, its western margin, exposed near Milford Sound is highly deformed. We will stop at localities along the road to examine the intrusive relationships between the various phases of the Darran Suite. At Bridge 90 (B90; Fig. 5), a coarse-grained gabbro host was intruded by fine-grained amphibolite dikes followed by dioritic and felsic veins (Fig. 7a). Rectangular blocks of competent layered orthogneiss are intruded and surrounded by veins that display flaser textures and undulate margins (Fig. 7b). The delicate features preserved in these exposures contrast with the highly deformed and metamorphosed intrusive rocks that formed at the roots of the early Mesozoic arc, and are now exposed in northern and central Fiordland.



Figure 7. Photographs of gabbro and diorite intrusions of the Darran Suite exposed at Bridge 90 along the Te Anau-Milford Road. See Figure 5 for location.

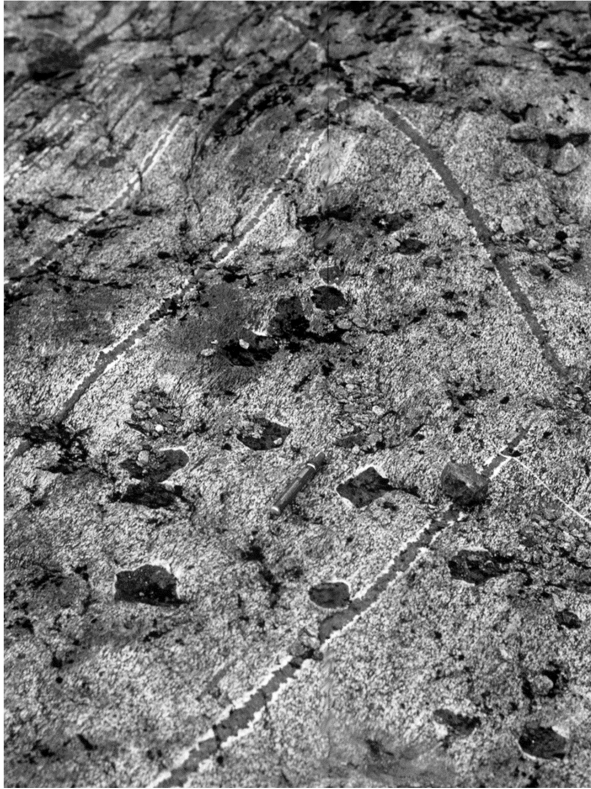


Figure 8. Photograph showing the lattice array of leucosomes and garnet trains in migmatitic metadiorite exposed in the Pembroke Valley. See Figure 5 for location.

The Pembroke Granulite

Migmatite and Garnet Granulite Dehydration Zones. North of Milford Sound, the Pembroke Granulite (Fig. 5) forms a large pod that is enveloped by the Milford Gneiss. Gabbroic gneiss forms the majority of the Pembroke Granulite (>70% of 0.75 km² area studied) and is generally found in the lower reaches of the Pembroke Valley (P, Fig. 5). Dioritic gneiss is generally found in the upper reaches of the Pembroke Valley, but may also outcrop as pods within the gabbroic gneiss. Ultramafic gneiss is subordinate to the other two components of the Pembroke Granulite and is generally found as small pods, up to 50 m across, most commonly within the dioritic gneiss. The eastern and western margins of this pod are poorly exposed. However, on the basis of relationships preserved along the upper reaches of the Harrison Valley (HC, Fig. 5), the boundaries are inferred to parallel to the NNE-strike of the dominant foliation (Fig. 5b) near Milford Sound.

Migmatitic dioritic gneiss displays a penetrative foliation composed of aggregates of hornblende, clinopyroxene, orthopyroxene, clinozoisite, plagioclase and small amounts of biotite and quartz. Leucosome in these rocks occurs as trains or patches of euhedral garnet partially surrounded by aggregates of equidimensional plagioclase (Fig. 8). Where most extensively developed, these garnet-bearing leucosomes contain two components: (1) a septum of linked garnet poikiloblasts, enclosed by (2) a zone of plagioclase and quartz-bearing leucosome, which is in turn surrounded by the host dioritic gneiss. The large garnet-bearing leucosomes form a lattice-like network where leucosome is either drawn out parallel to or cuts the foliation (Fig. 8). These textures provide evidence that some of the original melt exploited and migrated along and across foliation planes following partial melting of the lower crust.

In all areas of the Pembroke Granulite, the percentage of leucosome is low ($\leq 10\%$) and there is no disruption of stromatic layering (Fig. 9d). These observations support our interpretation that the volume of melt produced during partial melting of hornblende-bearing gneiss remained relatively low ($\leq 10\%$). They also suggest that the segregation of melt from migmatitic source rocks was efficient. Stromatic leucosome feed laterally into larger discordant veins that cut the foliation at high angles. These features suggest that original partial melt was efficiently extracted from the migmatite by arrays of discordant veins.

To test possible mechanisms of melt generation in gneisses below the batholith, piston-cylinder experiments were performed on an unmelted sample of dioritic gneiss at $P=14$ kbar and $T=800-975^{\circ}\text{C}$ (Antignano et al., 2001; Antignano, 2002; Klepeis et al., 2003). The mineral assemblage consisted of

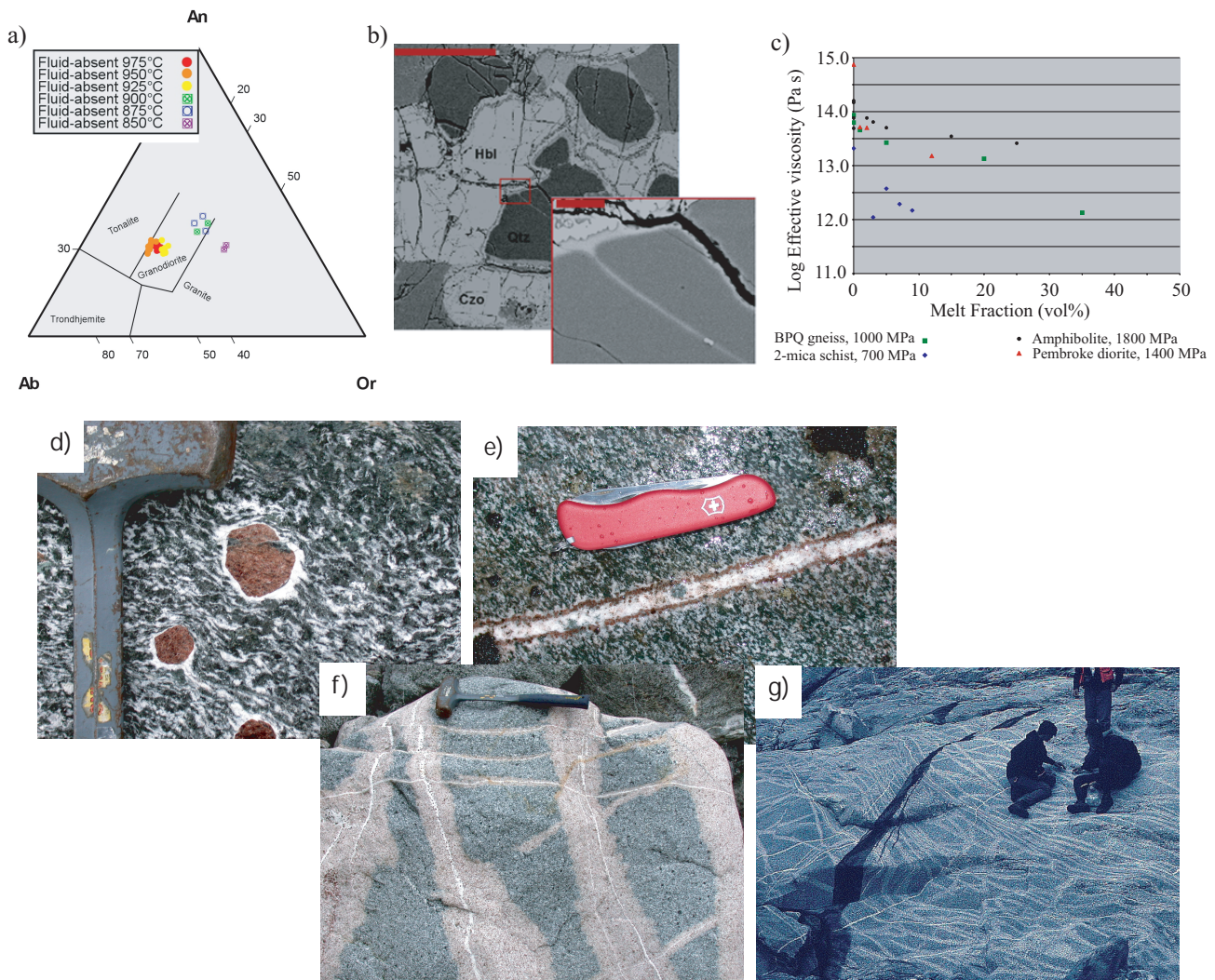


Figure 9. a) Compositions of partial melts in metadiorite plotted on an Ab-An-Or diagram. b) Backscatter image showing textural evidence of the melting reaction: hornblende + clinozoisite + quartz + plagioclase \Rightarrow clinopyroxene + garnet + melt + plagioclase +/- Fe-oxides in solid diorite core experiment. Reaction products surround quartz grain and melt is observed in a fracture (red box). Scale is 200 microns. Inset shows close-up of melt fracture in quartz grain, product clinopyroxene is shown in top left corner. Black crack is due to unloading of experiment. Scale is 20 microns. c) Effective viscosity vs. melt fraction plot showing results from solid-media deformation experiments. Metadiorite sample displayed a high effective viscosity compared to pelite under subsolidus conditions and is similar to amphibolite (Rushmer, 1995) and biotite-plagioclase-quartz (BPQ) gneiss (Holyoke and Rushmer, 2002) with partial melt present (Antignano, 2002). d) Migmatitic dioritic gneiss showing leucosome surrounding peritectic garnet. e) Garnet-bearing leucosome filling extension fracture in gabbroic gneiss. f) Granulite facies dehydration haloes surrounding leucosome and fracture networks. Haloes contain clinopyroxene + garnet assemblage that replaces hornblende-bearing assemblage in gabbroic gneiss. g) Reorientation of extension fractures record ductile deformation following brittle failure of the lower crust.

plagioclase + quartz with hornblende, clinzoisite and biotite as the hydrous phases. At $T=825^{\circ}\text{C}$, biotite undergoes melting in the absence of free water (fluid-absent), followed by reaction of hornblende and clinzoisite resulting in garnet + melt as reaction products. Melt compositions initially are granitic due to the influence of biotite but become granodioritic to tonalitic with increasing temperature as the

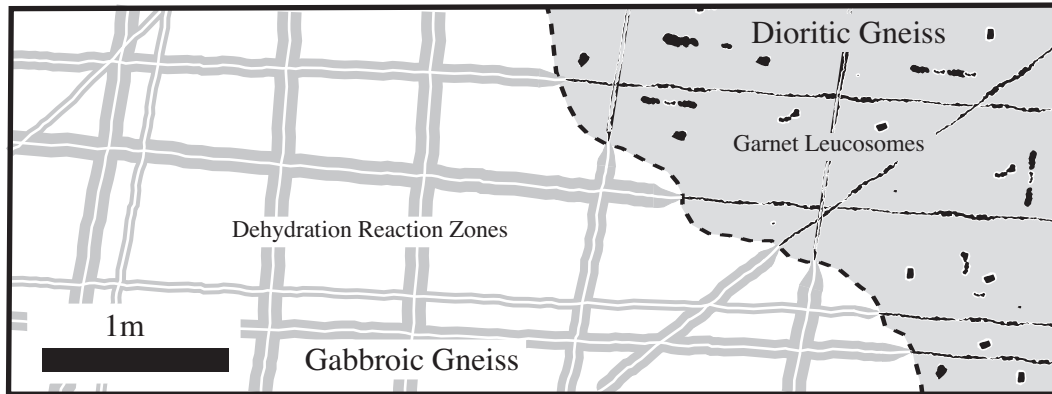


Figure 10. Structural form map showing the physical links that occur between garnet-bearing leucosomes in migmatitic dioritic gneiss and garnet-, clinopyroxene-bearing dehydration zones that surround dehydration zones in gabbroic gneiss (after Daczko et al., 2001b).

main reaction shifts to fluid-absent melting of hornblende \pm clinzoisite (Fig. 9a). Calculated water activities of the melts are low (0.39 to 0.12) and trace element data from experimentally produced glasses show high Sr/Y ratios. Melt fractions remained low (≤ 10 vol%) at all temperatures up to $T=975^{\circ}\text{C}$ (Fig. 9c). This suggests that although partial melting occurred in large parts of the section below the batholith, the volume of melt produced probably remained low. These results may explain the low percentage of leucosome observed in mafic lower crust in the field (Fig. 9d) and contrasts with the

much higher melt fractions observed in migmatitic paragneiss above the batholith.

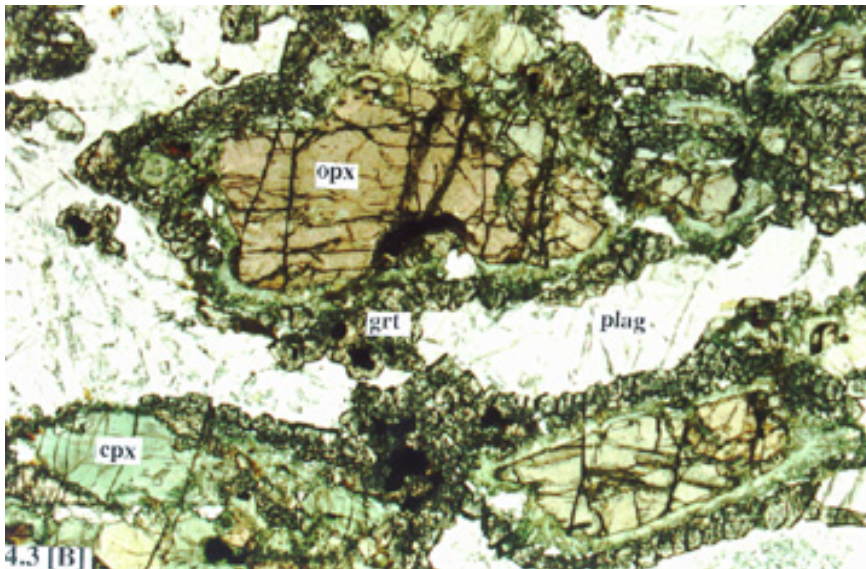


Figure 11. Thin section photo of orthopyroxene enclosed by random symplectic intergrowth of clinopyroxene, clinzoisite, biotite and rutile, which is enclosed by a corona of garnet in dehydration zone exposed at Pembroke Valley. See Figure 5 for sample location. After Clarke et al. (2000).

Across contacts between the migmatitic dioritic gneiss and adjacent, non-migmatitic gabbroic gneiss, a physical connectivity exists between leucosome in the migmatite and veins in the metagabbro (Fig. 10). This physical connectivity revealed how migrating partial melts interacted chemically with gabbroic gneiss during their migration. Over distances of a few centimeters, leucosome in stromatic migmatite changes into thin (2-5 cm) planar veins that are surrounded by garnet-,

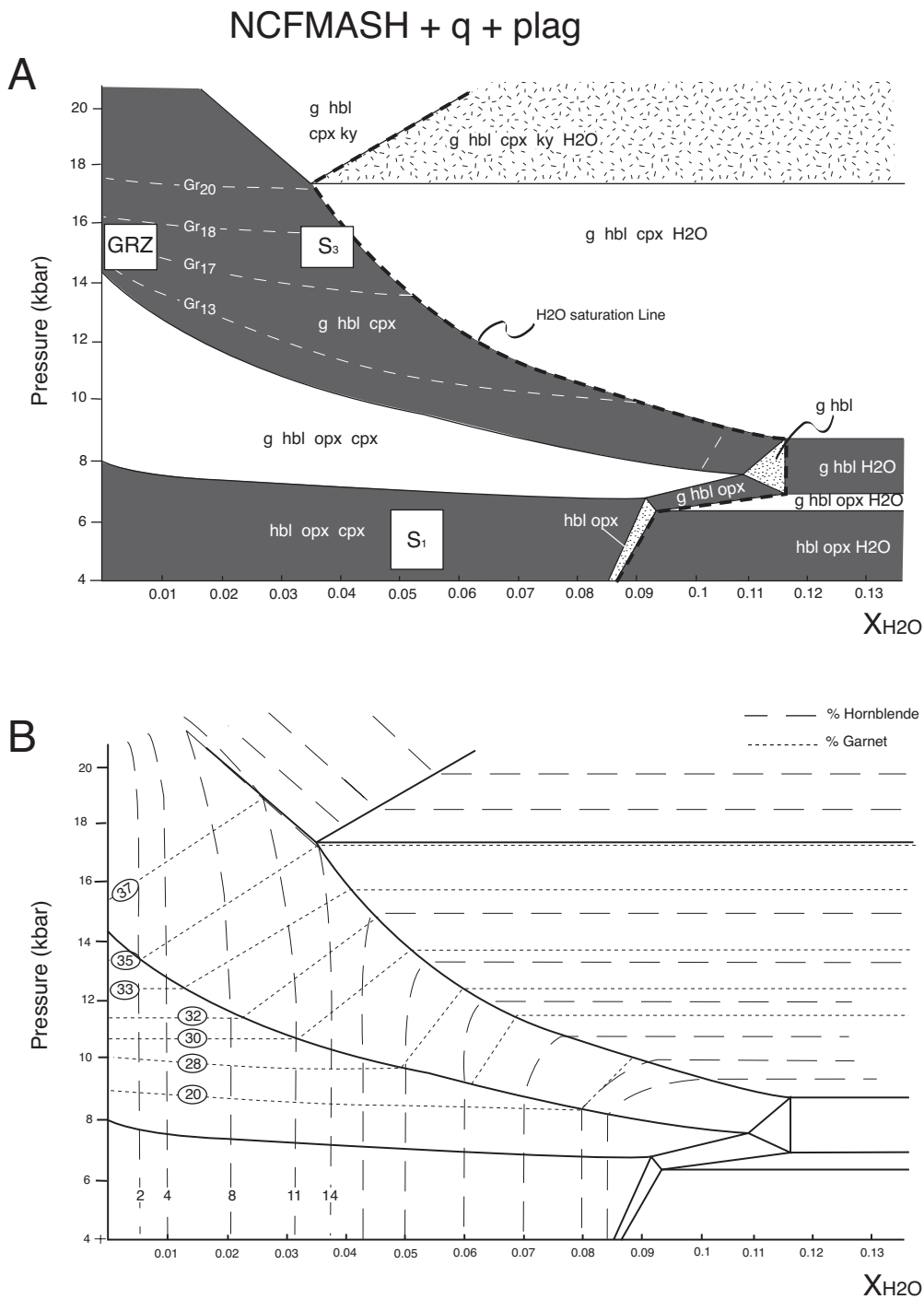


Figure 12. P - X_{H_2O} pseudosection for $T=750^\circ\text{C}$ and $P=4\text{--}20$ kbar constructed in the system $\text{CaO-Na}_2\text{O-FeO-MgO-Al}_2\text{O}_3\text{-SiO}_2\text{-H}_2\text{O}$ using THERMOCALC (v2.6) and the “20 April 1996” internally-consistent thermodynamic dataset from $\text{Al}_2\text{O}_3 = 26.8$, $\text{CaO} = 24.5$, $\text{MgO} = 21.2$, $\text{FeO} = 17.3$, $\text{Na}_2\text{O} = 10.2$, $\text{H}_2\text{O} = 0.0$ ($X_{H_2O} = 0$) to $\text{Al}_2\text{O}_3 = 25.03$, $\text{CaO} = 22.9$, $\text{MgO} = 19.8$, $\text{FeO} = 16.2$, $\text{Na}_2\text{O} = 9.6$, $\text{H}_2\text{O} = 6.5$ ($X_{H_2O} = 0.13$). These rock compositions match XRF whole rock analyses of gabbroic gneiss in the Pembroke Granulite. The pseudosection is drawn for quartz and plagioclase in excess. Minerals included in the construction of the grid were garnet (g), hornblende (hb), clinopyroxene, kyanite (ky), orthopyroxene (opx), clinopyroxene (cpx), plagioclase and quartz. GRZ is garnet reaction zone. After Clarke et al. (2000).

clinopyroxene-bearing dehydration zones in adjacent gabbroic gneiss (Figs. 10, 9e, 9f, 9g). These dehydration zones record the recrystallization of hornblende-bearing assemblages to garnet granulite at conditions of $T > 750^{\circ}\text{C}$ and $P = 13\text{-}16$ kbar (Figs. 11, 12; Clarke et al., 2000). The garnet granulite dehydration zones only occur in the gabbroic gneiss and are physically continuous with leucosome in the migmatitic dioritic gneiss (Fig. 10).

Garnet and rutile are absent from gabbroic gneiss that encloses the garnet reaction zones. Orthopyroxene and hornblende are mostly absent from the inner garnet reaction zones, whereas they are common in the host gabbroic gneiss and in outer parts of the garnet reaction zone (near the garnet reaction zone/ host gabbroic gneiss boundary, Fig. 11). Clinopyroxene, plagioclase, quartz and opaque minerals are present in both areas of rock. Plagioclase is less abundant in the garnet reaction zones, when compared with the host gabbroic gneiss. Small grains of kyanite commonly occur in plagioclase. Modal contents of clinopyroxene and quartz increase with the transformation of host gabbroic gneiss to garnet reaction zone. Thus, the two-pyroxene hornblende granulite to garnet-clinopyroxene granulite transformation involves the breakdown of orthopyroxene and hornblende, in the presence of plagioclase, to form garnet and clinopyroxene, and the breakdown of ilmenite to form rutile. The following reaction approximates the transformation (Fig. 12; see also Blattner, 1976; Oliver, 1977; Bradshaw, 1989b):



Using a natural, unmelted sample of the dioritic gneiss Antignano et al. (2001) and Antignano (2002) used piston cylinder experiments to establish that the dilatational strains associated with melting involving the reaction of hornblende and clinozoisite were high enough to fracture matrix feldspar and quartz (Fig. 9b). In addition, the experiments showed that calculated water activities for these melts are low enough (0.39 to 0.12) to cause dehydration (Antignano et al., 2001; Antignano, 2002).

Zircon ages (81.8 ± 1.8 Ma) from a post-tectonic dike located in the Pembroke Valley indicate that high-grade granulite and upper amphibolite facies metamorphism in the Arthur River Complex terminated in the mid-Cretaceous (Hollis et al., 2003). In addition, K-Ar ages on hornblende (Gibson et al., 1988; Nathan et al., 2000) and U-Pb dates on apatite (Mattinson et al., 1986) indicate that the Western Fiordland Orthogneiss and Arthur River Complex had cooled to $300\text{-}400^{\circ}\text{C}$ by ~ 90 Ma.

Deformation. A series of nearly vertical 1-3 meter-wide dextral and sinistral shear zones (Fig. 13) deform all vein arrays and garnet-bearing dehydration zones in metagabbro and metadiorite (Fig. 9g). The shear zones display two orientations. The sinistral set contains a mylonitic foliation that strikes to the east and dips steeply to the south. A penetrative, gently southwest-plunging mineral lineation defined by attenuated clusters of amphibole and clinozoisite occurs on these foliation planes. Sense of shear indicators within this set include oblique foliations (Fig. 14), asymmetric recrystallized tails on feldspar porphyroclasts, and microfaulted garnet. These structures all record sinistral displacements parallel to a shallowly plunging mineral lineation. The second set of minor shear zones is subordinate in size and abundance to the first set. This second set contains a mylonitic foliation that strikes to the northwest and displays shallow to moderate dips to the southwest. A gently west- and northwest-plunging amphibole and clinozoisite mineral lineation occurs on foliation planes. Sense of shear indicators within this subordinate set all show dextral displacements.

The steep shear zones are all deformed and transposed by a series of gently southeast-dipping shear zones that approximately parallel the dominant gneissic foliations of the western domain (Fig.

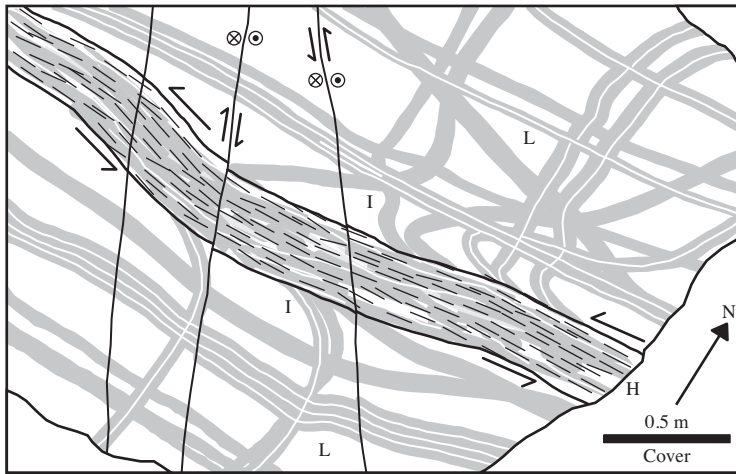


Figure 13. Sketch of a mylonitic sinistral shear zone that deforms garnet reaction zones (shaded lines). Note well defined shear zone boundaries. Exposure located in the Pembroke Valley. See Fig. 5 for location.

15). Each shear zone displays a mylonitic foliation consisting of the assemblage hornblende, clinozoisite, garnet and biotite. Stretched aggregates of garnet and plagioclase and aligned hornblende form down-dip, southeast-plunging mineral lineations on foliation planes. Daczko et al. (2001a) inferred that the metamorphic mineral assemblages within these shear zones equilibrated at peak conditions of $P=14.1 \pm 1.2$ kbar and $T=674 \pm 36^\circ\text{C}$.

The zone of mylonite that occurs in the central part of each of the gently dipping shear zones is approximately 7-10 meter thick. These central mylonite zones, all of which are approximately

parallel, are vertically stacked on top of one another at a spacing of approximately 50-100 meters (Fig. 16). The total thickness of this shear zone stack is unknown but available exposure suggests that it is at least 1 km thick. Between the stacked shear zones thin (<1 meter thick) mylonitic shear bands dip to the southeast and northwest and sweep into parallelism with the central mylonite zones located above and below them. These shear bands envelop asymmetric pods of coarse-grained metagabbro and metadiorite that form imbricated, antiformal stacks that also dip to the southeast and northwest (Fig. 16b). The displaced pods display an older, recrystallized gneissic foliation that is truncated by the margins of the shear bands. Lineations on foliation planes within the shear bands display similar trends but steeper plunges than the lineations that occur in the central mylonite zones. The sense of shear in all

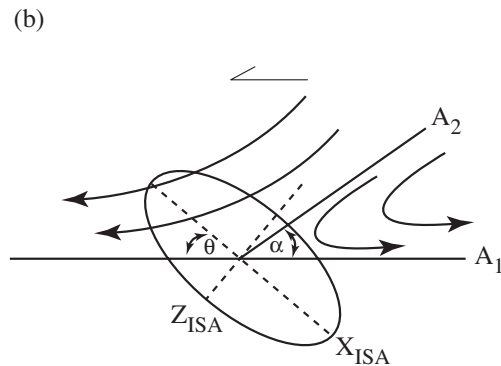
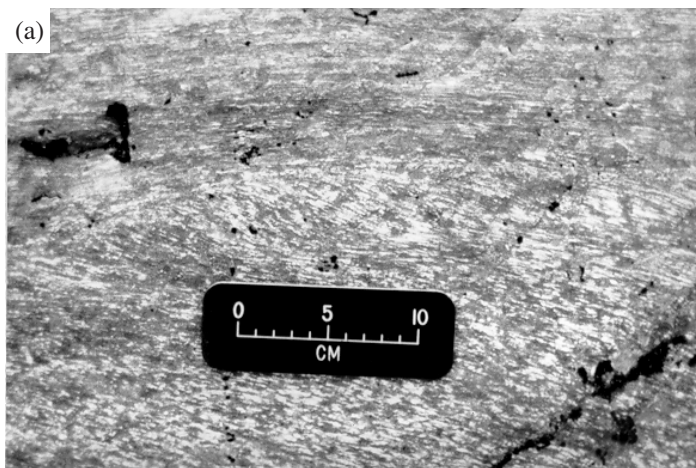


Figure 14. Photo of a sinistral shear zone showing attenuated and flattened mineral clusters that define a mylonitic foliation at top of photo. Central part of photograph (above scale) shows an oblique foliation enveloped by mylonitic in a low strain lens. Progressive anticlockwise rotation of oblique foliation from low to high strain areas gives a sinistral shear sense for the shear zone. Cartoon showing relative orientation of the flow apophyses (A_1, A_2), instantaneous strain axes (X_{ISA}, Z_{ISA}) and the angles between these elements for a sinistral transpressional flow regime.



Figure 15. Map of ductile thrust fault and related structures. Inset shows pattern of vertically stacked, subhorizontal thrusts and their location within Pembroke Valley. After Daczko et al. (2001a).

asymmetric hornblende and clinozoisite fish, asymmetric tails of biotite and hornblende on garnet porphyroblasts, asymmetric boudinage and minor shear zones. These indicators provide evidence of oblique sinistral displacements parallel to the moderately south- and southwest-plunging mineral lineations that occur on the western side of the shear zone. This sense of shear is consistent with the sinistral displacements recorded by steep minor shear zones of the Pembroke Valley. In addition to a dominantly sinistral shear sense, the involvement of folds at all scales provide evidence of a component of shortening across the shear zone.

of these mylonite zones and shear bands is top-to-the-northwest regardless of the dip of mylonitic foliations. This style of displaced, imbricated pods that override one another in these shear zones is diagnostic of layer-parallel shortening and thickening in zones of contraction.

Camp Oven Creek

The dominant structural grain east and west of the Pembroke Valley is controlled by a steep, penetrative NNE-striking upper amphibolite facies foliation (Fig. 17). Hornblende and biotite mineral lineations mostly plunge moderately to the south and southwest with some localities also displaying near vertical plunges. This foliation represents part of a steep, 10-15 km wide, NNE-striking zone that parallels the western margin of the Median Batholith. Klepeis and Clarke (2003) introduced the new name Indecision Creek Shear Zone for this zone of intense deformation.

Daczko et al. (2002b) showed that metamorphic conditions accompanying deformation that produced the steep foliation at Milford Sound involved cooling from 750-800°C to 650-700°C with little corresponding change in pressure (Figs. 18, 19). Figure 20 shows a P-T path for mafic orthogneiss of the Arthur River Complex.

Outcrop-scale sense of shear indicators occur mostly in zones of intermediate or low strain where the degree of transposition is less than in the high strain areas. These low-intermediate strain zones occur mainly along the western boundary of the shear zone. Exceptions to this relationship occur in zones of mylonite, where sense of shear indicators are abundant. Sense of shear indicators include

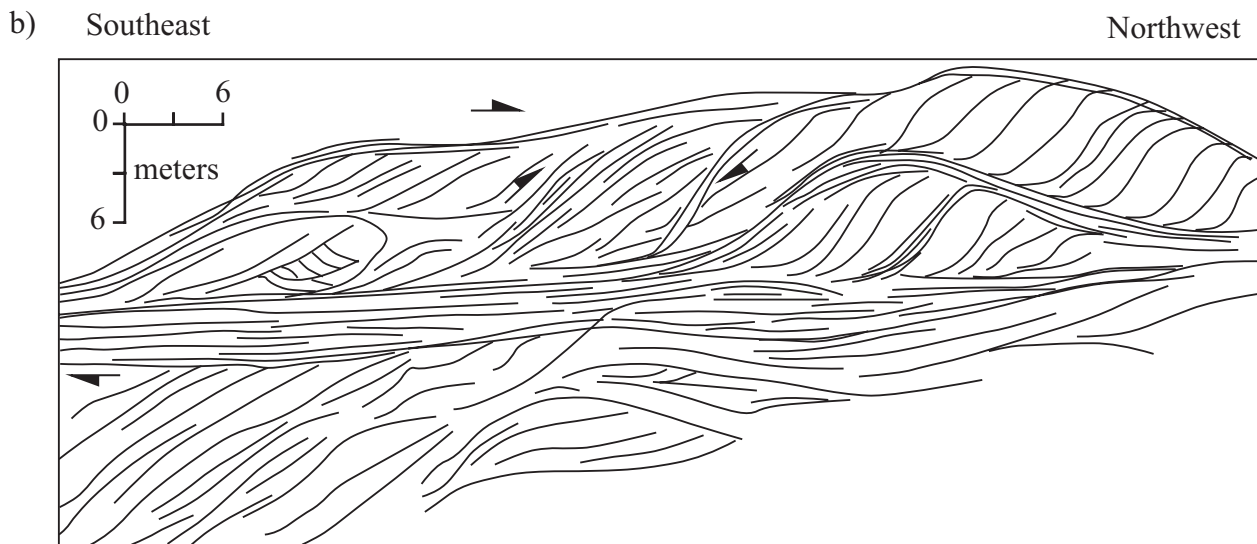
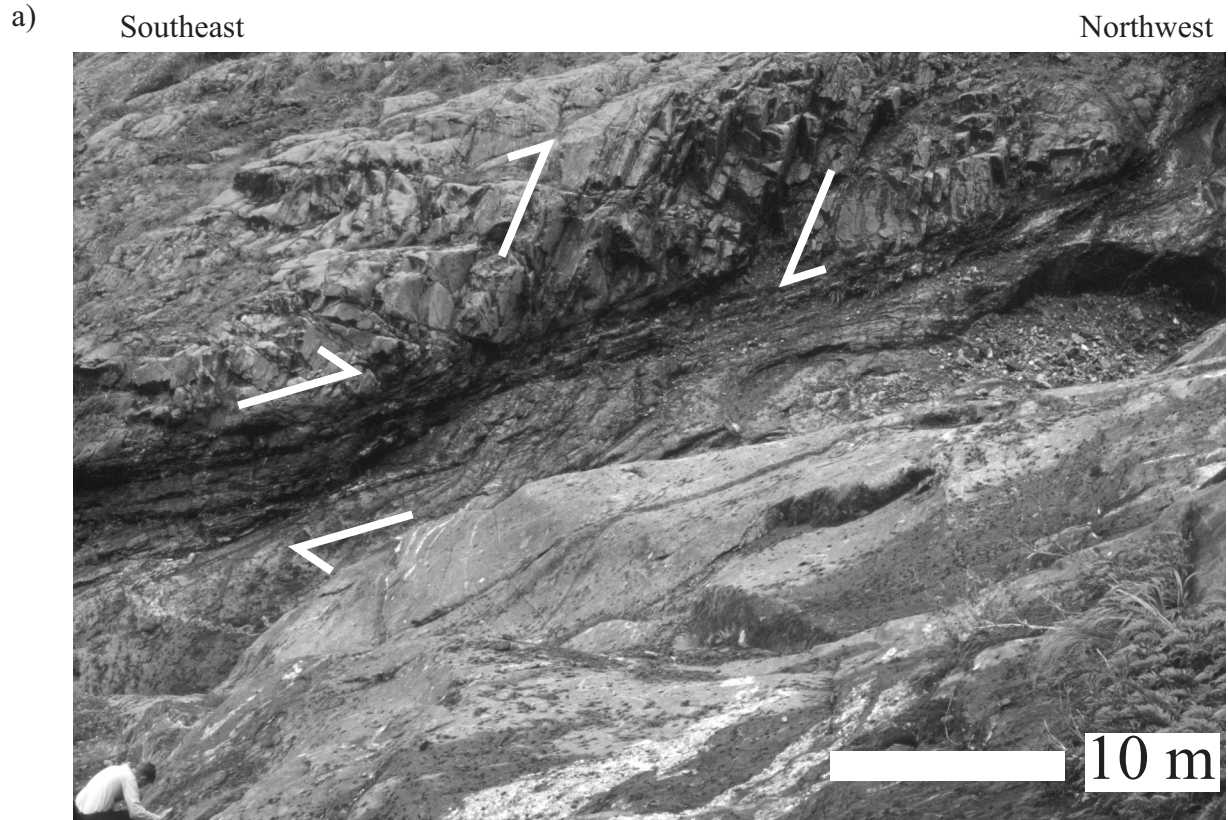


Figure 16. Sectional view of an outcrop-scale thrust duplex that deforms the Pembroke Granulite. Arrows show relative senses of displacement on mylonitic shear zones. Southeast is to the left. After Klepeis and Clarke (2003).

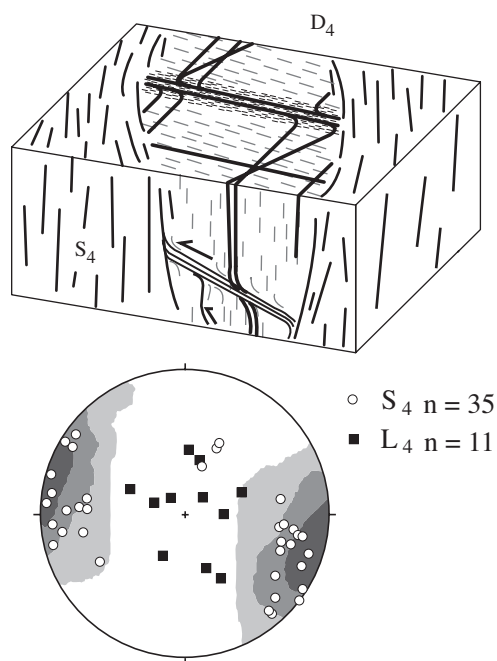


Figure 17. Sketch showing structural relationship between the steep upper amphibolite facies foliation at Milford Sound and the shear zones exposed in the Pembroke Valley. Lower diagram is an equal-area stereonet showing poles to foliation (circles) and steeply plunging down-dip hornblende mineral lineations (squares).

surfaces parallel the steep north-northeast-striking foliation of the Indecision Creek Shear Zone that occurs farther east.

In some parts of the Camp Oven Creek exposures the steep axial planar leucosomes truncate and offset the folded leucosomes (Fig. 23). This relationship suggests that melt represented by the folded leucosome did not feed the second set of leucosomes but were below the solidus during deformation. However, the occurrence of leucosome parallel to the axial planes of folds suggests that these younger structures reflect melt migration during deformation in the Indecision Creek Shear Zone. The folds reflect a component of shortening across the Indecision Creek Shear Zone. Fold tightness and the degree of transposition increases east of Camp Oven Creek.

U-Pb geochronologic data also indicate that high-grade metamorphism accompanied Early Cretaceous magmatism and crustal melting. Thin, high-U metamorphic rims enclose Paleozoic and Early Cretaceous magmatic cores in the Milford Gneiss, the Harrison Gneiss, the Selwyn Creek Gneiss, and Paleozoic gneiss at Camp Oven Creek (Figs. 21, 22; Tulloch et al., 2000; Hollis et al., 2003). These ages are interpreted to reflect the influx of heat that accompanied the emplacement of the mafic-intermediate Western Fiordland Orthogneiss (Tulloch et al., 2000; Hollis et al., 2003). This interpretation is consistent with the range of crystallization ages from the Western Fiordland Orthogneiss (126-116 Ma) and with the spatial distribution of zircon displaying metamorphic rims in migmatite and granulite facies rocks below the batholith.

South of Milford Sound at Camp Oven Creek (CO, Fig. 5) mafic dikes of the Milford Gneiss intrude rafts of Paleozoic host rock. Published U-Pb ages from this and other units of the Arthur River Complex reflect a history of Early Cretaceous magmatism and Early Cretaceous metamorphism and melting. Tulloch et al. (2000) analyzed zircon cores from the Arthur River Complex near Milford Sound and obtained both Early Carboniferous (~360 Ma) and Early Cretaceous (~134 Ma) U-Pb ages (Fig. 21). Hollis et al. (2003) obtained 136-129 Ma U-Pb ages from the cores of magmatic zircon in the Arthur River Complex and showed that these ages most likely reflect the crystallization of Early Cretaceous dikes and plutons (Fig. 22). These data combined with evidence of an intrusive relationship between the mafic dikes of the Milford Gneiss and migmatitic Paleozoic host rock (Fig. 23) at Camp Oven Creek suggest that the Arthur River Complex was emplaced into crust composed of a mixture of MTZ arc rocks and Paleozoic rocks of Gondwana.

At Camp Oven Creek stromatic migmatite (Fig. 23) in a Paleozoic host contains folded leucosome that parallels a folded foliation. This foliation contains the assemblage biotite, hornblende, clinozoisite, plagioclase, and quartz. A second set of leucosomes that is not folded forms spaced arrays that parallel the axial surfaces of the folds. The folds plunge gently to the south and their axial

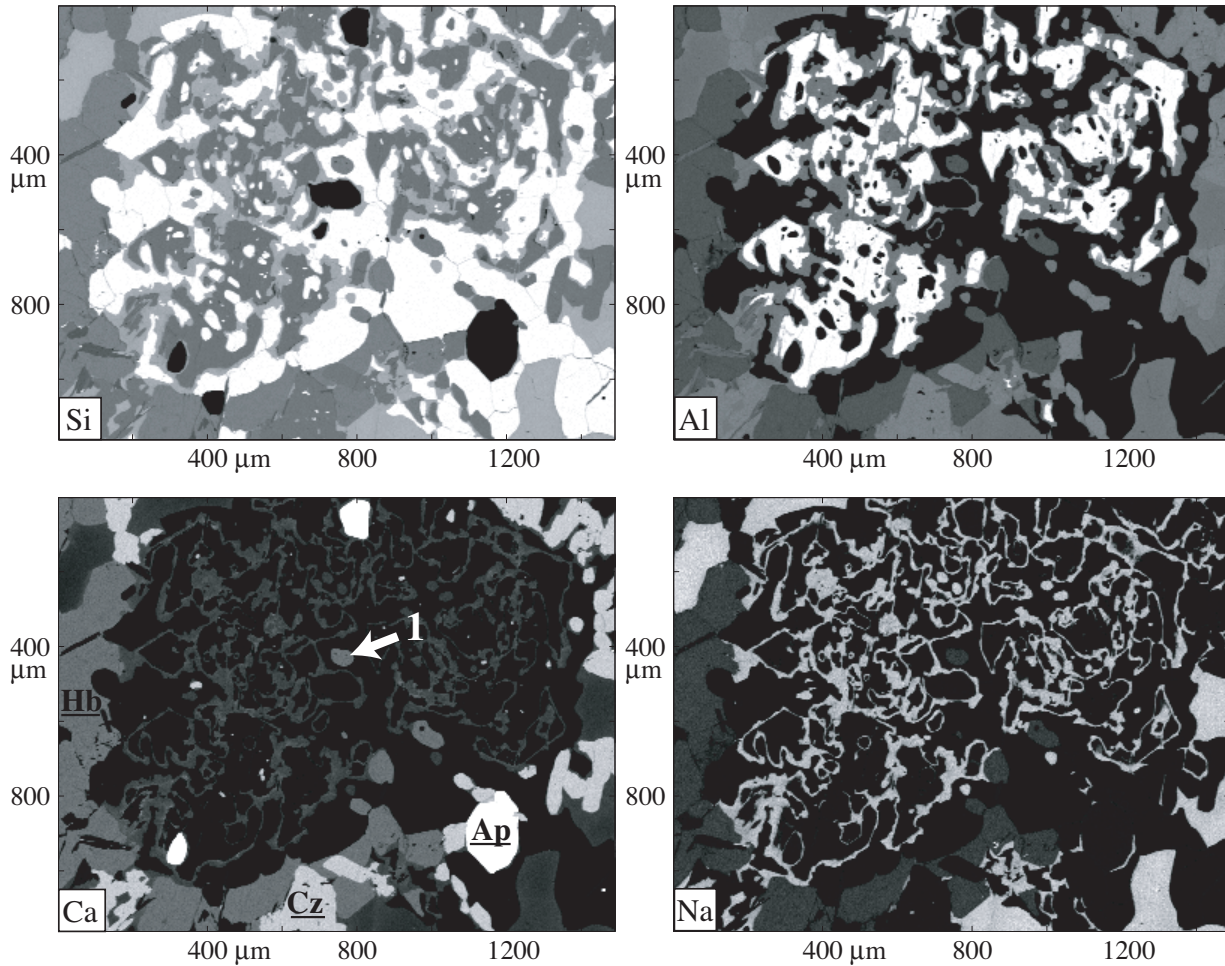


Figure 18. Matrix corrected maps of oxide weight percent for SiO_2 , Al_2O_3 , CaO and Na_2O of a kyanite, quartz and plagioclase symplectite. The maps are approximately $1000 \times 1500 \mu\text{m}$. Grey scale is black for minimum elemental concentration and white for maximum elemental concentration. Minimum and maximum ranges: SiO_2 is 0-100 wt.%, Al_2O_3 is 0-63 wt.%, CaO is 0-28 wt.%, Na_2O is 0-13 wt.%. The white colored mineral on the Si map is quartz. The white mineral on the Al map is kyanite. The white mineral on the Ca map labelled with 'Ap' is apatite. The light-grey mineral on the Ca map labelled with 'Cz' is clinozoisite. The dark-grey mineral on the Ca map labelled with 'Hb' is hornblende. The brightest mineral on the Na map is plagioclase. Arrow labelled with '1' points to a hornblende inclusion within the symplectite.

Selwyn Creek

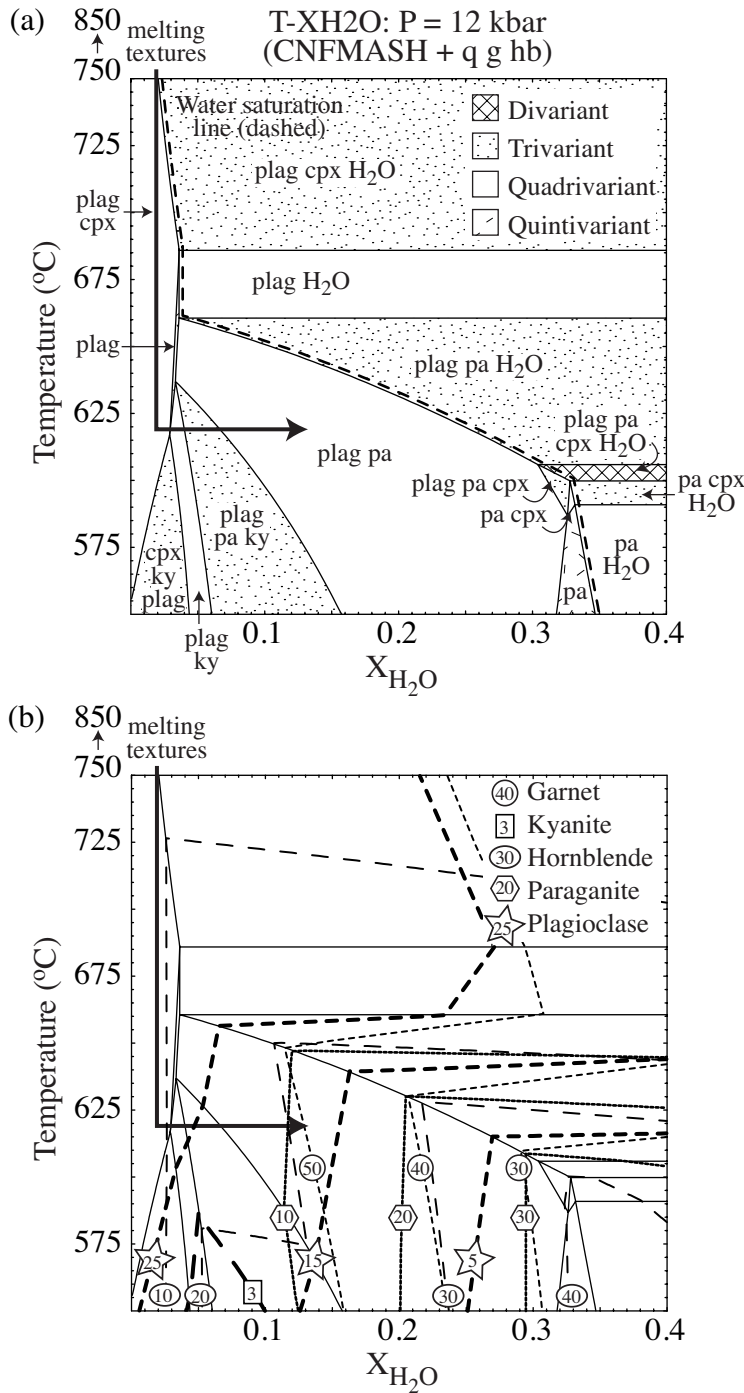


Figure 19. T - X_{H_2O} pseudosection for $P = 12$ kbar and $T = 550$ - 750°C , constructed in the model system CNFMASH ($\text{CaO}-\text{Na}_2\text{O}-\text{FeO}-\text{MgO}-\text{Al}_2\text{O}_3-\text{SiO}_2-\text{H}_2\text{O}$) using THERMOCALC. After Daczko et al. (2002b).

East of the Harrison-Kaipu fault zone is a narrow, 1-2 km wide unit composed of hornblende diorite and garnet-biotite gneiss intruded by amphibolitic to felsic dikes. At Selwyn Creek (SC, Fig. 5) some of these dikes are discordant to a steep amphibolite facies foliation that dominates most of the adjacent Arthur River Complex (Claypool et al., 2002). Others are highly deformed and transposed parallel to a penetrative NNE-striking foliation. Most of the Selwyn Creek exposures are composed of interlayered mafic and felsic gneiss. Evidence for partial melting of dioritic gneiss occurs in the form of discordant veins and patches of leucosome (Fig. 24) that contain peritectic garnet developed along their margins. Some of these leucosomes are folded. Within these gneisses an assemblage of garnet-hornblende-bioite-plagioclase-clinzoisite-paragonite-quartz yielded estimates of the peak of metamorphism at $P=11$ - 13 kbar, $T=560$ - 650°C (Dockrill, 2000). A crystallization age of ~ 154 Ma for the main dioritic part of the Selwyn Creek Gneiss suggests that these rocks also were emplaced during an early phase of magmatism in the Median Batholith (Fig. 22; Hollis et al., 2003) and likely represent deformed parts of the Darran Suite.

Zones of high strain in the Selwyn Creek Gneiss display tight to isoclinal, steeply plunging folds. In these areas, fold hinges and isolated pods that contain older foliations are enveloped and transposed parallel to a steep north-northeast-striking foliation (Fig. 25). The pods that are enveloped by the steep foliation occur at all scales. The largest of them preserves the thrust zones, migmatite and garnet dehydration zones of the Pembroke Granulite (Fig. 17). This steep foliation parallels the boundaries of the Indecision Creek Shear Zone.

Harrison Cove

East of the Pembroke Granulite and west of the Selwyn Creek Gneiss, most of the Harrison Gneiss (Fig. 5) is composed of banded metadiorite with discontinuous sheets of mafic to felsic compositions in gradational contact with the more mafic Milford Gneiss. The dominant mineral assemblage in this unit includes hornblende, plagioclase and clinozoisite, with or without scapolite, garnet, biotite, and phengitic white mica. Hornblende, plagioclase, and clinozoisite define a penetrative gneissic foliation, which is locally folded. A pronounced compositional banding is defined by alternating, discontinuous mafic and felsic layers. The mafic layers tend to be comparatively thin (150 to 600 mm thick) and have assemblages similar to those described for the more mafic Milford Gneiss near the Pembroke Granulite, but with less garnet. The felsic bands are comparatively thick (up to several meters wide), and have mineral assemblages dominated by plagioclase, quartz and hornblende.

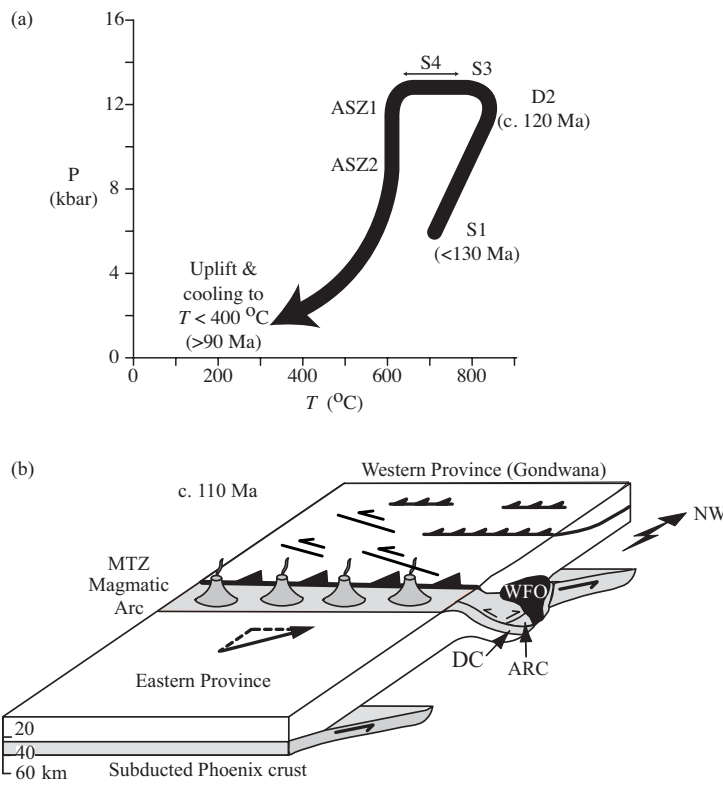


Figure 20. P-T path for mafic orthogneiss of the Arthur River Complex at Milford Sound. ASZ1, 2 are the two phases of mylonite exposed in the Anita Shear Zone (after Klepeis et al., 1999).

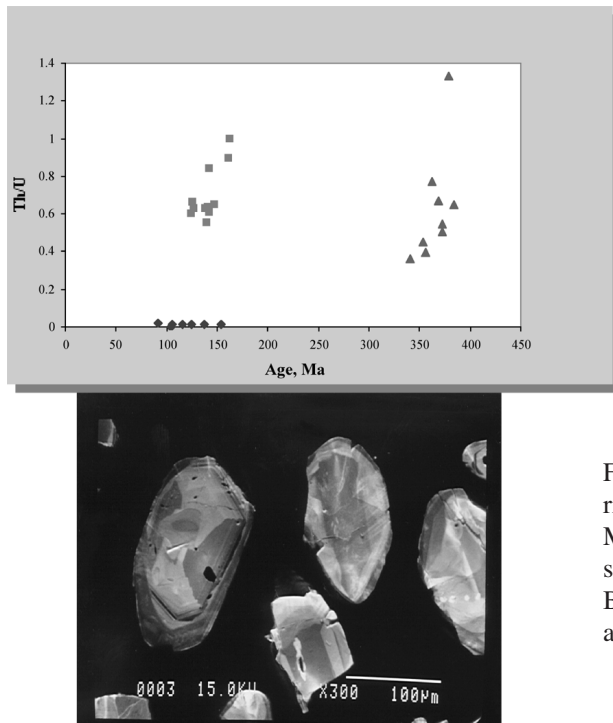


Figure 21. Th/U ion probe data from zircon cores and rims collected from the Arthur River Complex at Milford Sound. After Tulloch et al. (2000). CL image shows sector zoned and oscillatory zoned zircon cores. Both core types have high-U rims that show average ages of ~ 120 Ma. See text for discussion.

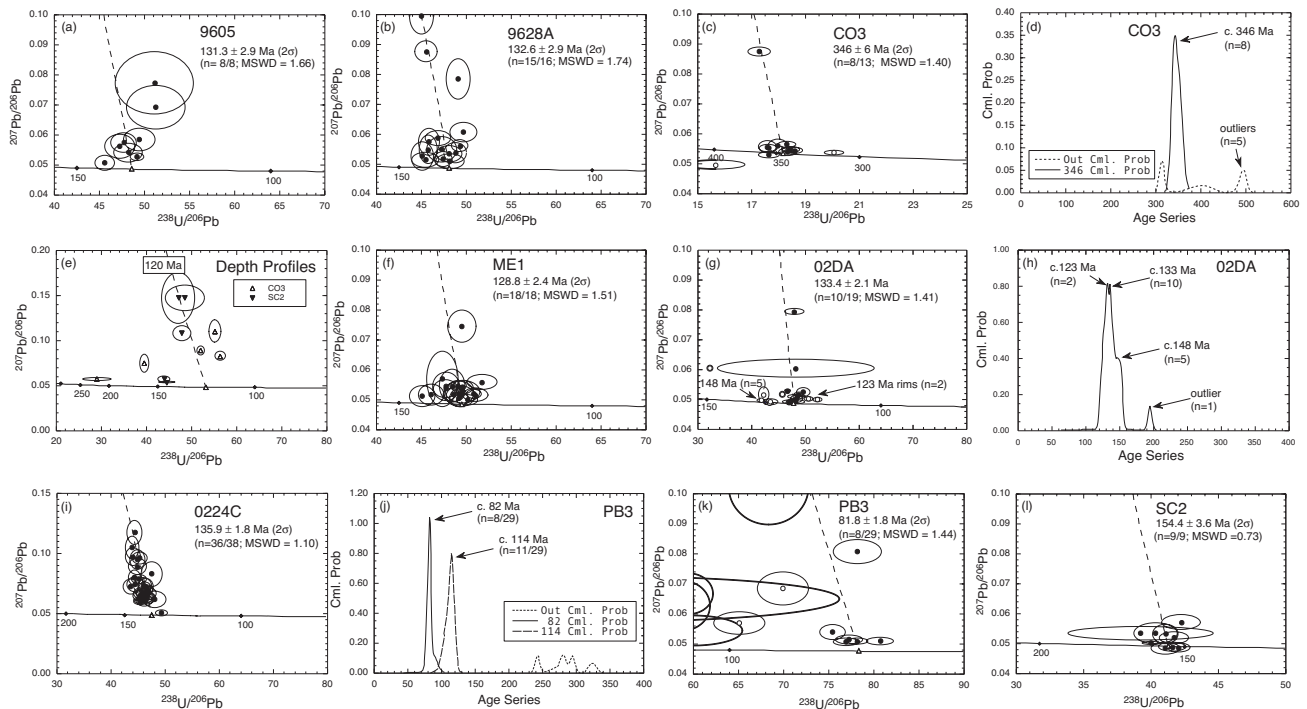


Figure 22. Tera-Wassberg plots of SHRIMP zircon data from (a) 9605, (b) 9628A, (c) CO3 cores, (e) depth profiles of grain surfaces (rims) of CO3 and SC2, (f) ME1, (g) O2DA, (i) O224C, (k) PB3, and (l) SC2 cores, and cumulative probability plots of age populations from (d) CO3, (h) O2DA, and (j) PB3. Samples are described in Hollis et al. (2003).

The eastern boundary of the Harrison Gneiss north of Milford Sound is defined by a 2 km-wide fault zone named the Harrison-Kaipō fault zone (Blattner, 1991; Claypool et al., 2002). This fault zone contains vertical to moderately NW-dipping en echelon faults, tight, variably-plunging folds, and upper greenschist facies shear zones that deform the Harrison Gneiss and separate it from rock units, including the Darran Suite to the east (Fig. 5, 6). In some areas, the Harrison Gneiss-Darran Suite contact has been reported as gradational (Blattner, 1991; Clarke et al., 2000). One area where a gradational contact may be preserved is at Harrison Cove (HC, Fig. 5) where splays of the Harrison-Kaipō fault zone cut southwest and away from the Darran Complex. Thirty-three kilometers northeast of Milford Sound, the Harrison-Kaipō fault curves and abuts against the Pembroke fault.

At Harrison Cove, the transition zone is a few hundred meters wide and contains domains with ophitic textures enveloped by deformed amphibolite dikes. In these deformed zones, coarse-grained (5-10 mm) hornblende, clinozoisite, rutile, plagioclase and quartz define a foliation co-planar with the steep foliation that dominates the Arthur River Complex near Milford Sound. White mica pseudomorphs plagioclase. Garnet occurs in felsic domains as symplectic intergrowths with plagioclase, quartz, ilmenite and rutile. Ophitic textures in these rocks are defined by large clinopyroxene and orthopyroxene phenocrysts (up to 100 mm length), hornblende, plagioclase, ilmenite, and biotite. Limited effects of metamorphism can be recognized in a narrow transition zone near the contact with the Harrison Gneiss.

Coastal Milford Sound

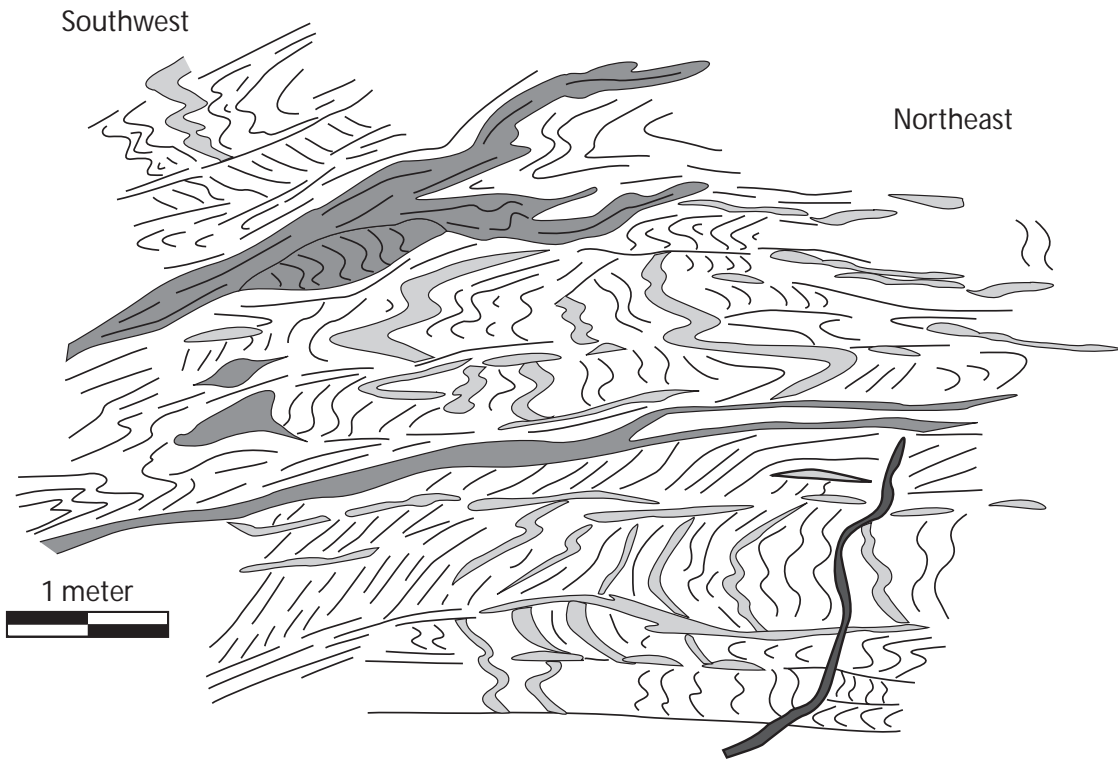
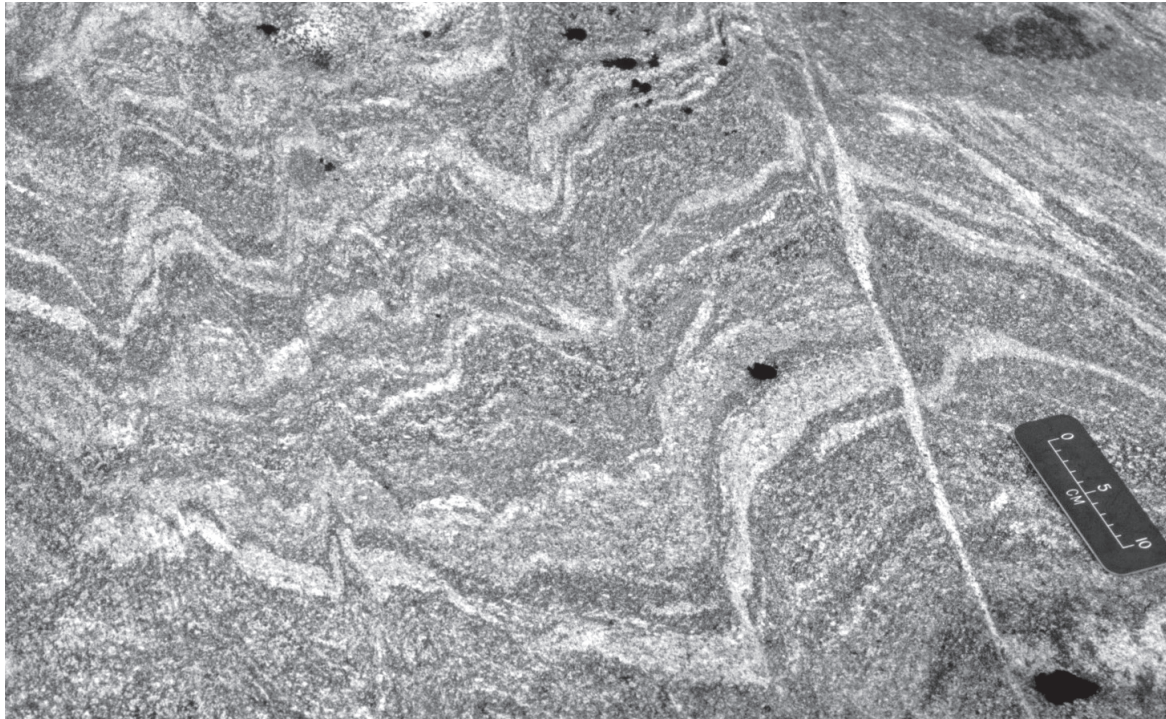


Figure 23. Stromatic migmatite in dioritic gneiss at Camp Oven Creek (CO, Fig. 5). Note folded foliation-parallel leucosome cut by discordant leucosome that parallel the axial planes of folds. Texture is interpreted to represent the migration of melt, now represented by the axial planar leucosome, during folding. Sketch constructed by S. Marcotte. After Klepeis and Clarke (2003).

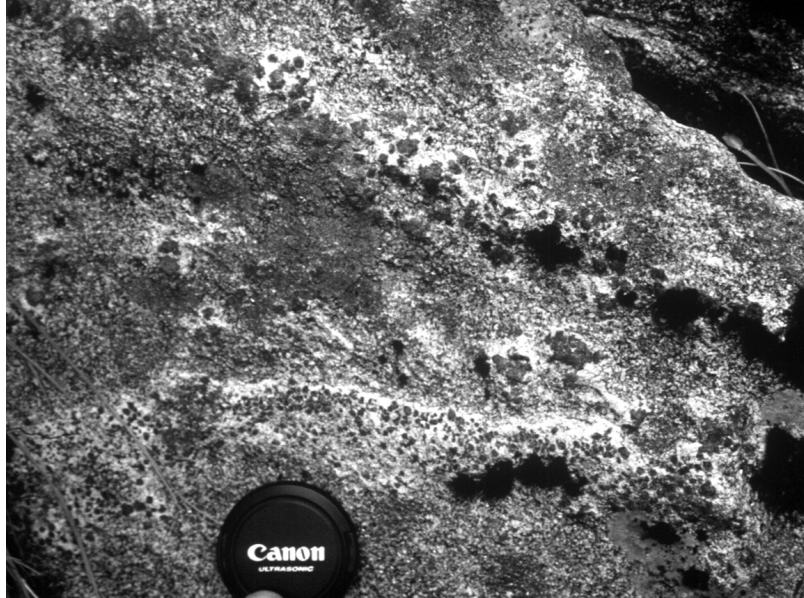


Figure 24. Photograph of peritectic garnet surrounded by quartz and plagioclase in leucosome in Selwyn Creek Gneiss.

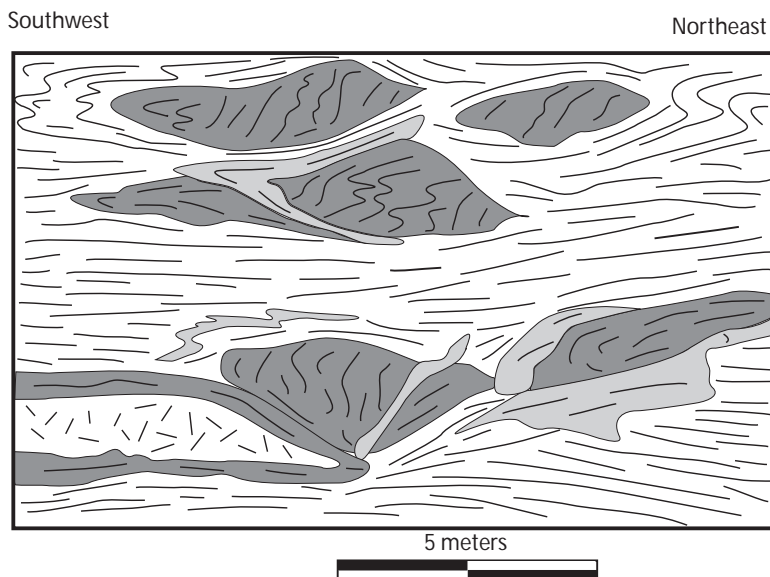


Figure 25. Structural form map of a zone of high strain within the Indecision Creek Shear Zone located in Selwyn Creek Gneiss (Fig. 5). After Klepeis and Clarke (2003).

NNE-striking foliation. Paleozoic, low-medium P, kyanite-bearing metasediments and orthogneisses occur to the west of the shear zone (Wood, 1972; Gibson, 1990; Blattner, 1991). Cretaceous high-P (~12-13 kbar) granulite facies assemblages and metabasic to metadioritic plutons of the Milford Gneiss occur to the east (Mattinson et al., 1986; Bradshaw, 1989; Clarke et al., 2000). Previous work (Blattner, 1991; Hill, 1995; Klepeis et al., 1999) has shown that the Anita Shear Zone comprises superposed foliations displaying mylonitic to cataclastic textures reflecting conditions ranging from upper

Most of Milford Sound contains exposures of the mafic, hornblende-rich Milford Gneiss. This unit contains steep mafic dikes and a steep gneissic and upper amphibolite facies foliation that forms the dominant structural grain of the sound (Fig. 26). In areas where this foliation is weakly developed deformed garnet-bearing dehydration zones can be recognized. Elsewhere, the steep foliation is defined by aligned hornblende, plagioclase, clinozoisite, phengitic white mica and rutile, with or without garnet, clinopyroxene and biotite. In these latter areas, sheets of diorite and coarse-grained leucogabbro and ultramafic dikes were deformed and transposed parallel the foliation (Fig. 26). Hollis et al. (2003) obtained 136-129 Ma zircon ages from the Milford Gneiss, which they interpreted as the range of emplacement ages for magmatic protoliths in this unit. The garnet-dehydration zones and older structures that are well preserved in the Pembroke Valley were mostly destroyed by the intensity of recrystallization that accompanied formation of this steep foliation.

The Anita Shear Zone

Western Boundary of the Granulite Belt. The western boundary of the granulite belt coincides with the Anita Shear Zone (Figs. 5, 27). This shear zone is 3.5-4 km-wide and is dominated by a steep to subvertical,

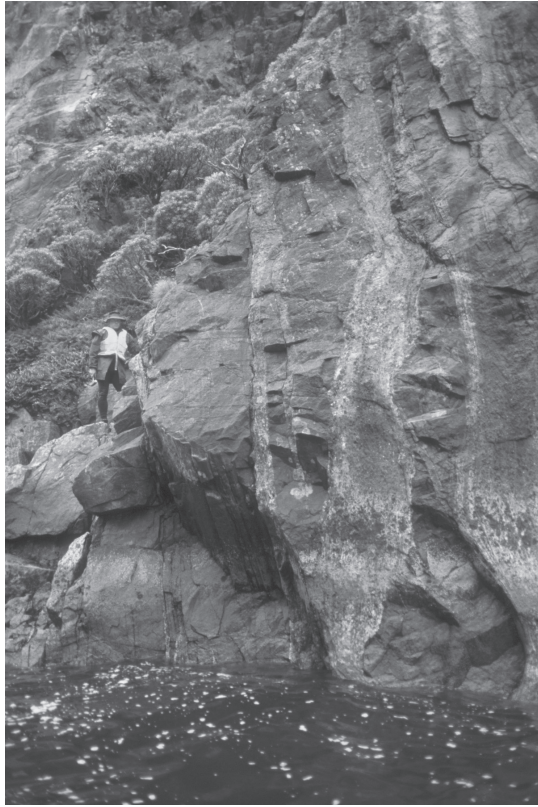


Figure 26. Photograph of vertical mafic dikes in the Milford Gneiss along the coast of Milford Sound. Dikes parallel steep upper amphibolite foliation that dominates the sound.

amphibolite to greenschist facies metamorphism. The Alpine Fault and Pembroke Fault (Fig. 5) reactivate the steep margins of Anita Shear Zone on its western and eastern sides, respectively (Blattner, 1991; Claypool et al., 2002).

Two fiords, Milford Sound and Poison Bay (Fig. 27), provide nearly continuous exposure across the Anita Shear Zone and its wall rocks along sections oriented orthogonal to its NNE-strike. Milford Sound exposes the eastern boundary of the shear zone, whereas Poison Bay contains exposures of both its western and eastern boundaries. The eastern boundary (Fig. 27) is marked by a narrow 1-2 meter-wide, NNE-striking subvertical zone where older fabrics of the Milford Gneiss are cut by steep to subvertical mylonitic foliations of the shear zone. West of this boundary, all intrusive contacts and coarse-grained foliations that occur in the Milford Gneiss are recrystallized and transposed by shear zone mylonitization.

The western boundary of the Anita Shear Zone at Poison Bay lies within the Paleozoic (protolith age) Saint Anne Gneiss (Fig. 27). This unit comprises interlayered metapelitic and metapsammitic rocks with rare mafic layers and minor felsic to mafic dikes and plutons. The dominant structure in these Paleozoic rocks is a weakly developed foliation that parallels bedding planes. Mineral lineations within the rocks

outside the shear zone are rare to absent. Kyanite grains are misaligned within foliation planes suggesting static metamorphic growth.

Superposed Mylonitic Fabrics. The oldest recognizable foliation within the Anita Shear Zone is a subhorizontal to gently east or west-dipping compositional layering (S_1^{SAG}) in the Thurso Gneiss (Figs. 27, 28a). A narrow (<1 m thick) metaconglomerate layer, complete with cobble size clasts parallels the subhorizontal compositional layering. This layering is intensely deformed into tight to isoclinal, recumbent to inclined, gently NE-plunging folds (F_2^{ASZ}). Many of these folds are rootless and all have axial planes that lie parallel to a gently to moderately dipping mylonitic to ultramylonitic foliation (S_2^{ASZ} ; Fig. 27, 28c). S_2^{ASZ} formed during the first phase of intense mylonitic deformation in the Anita Shear Zone. In the Thurso and Saint Anne gneisses S_2^{ASZ} is defined by the assemblage garnet, biotite, plagioclase, quartz, amphibole, clinozoisite and rutile. A penetrative, gently to moderately NNW- and SSE-plunging mineral lineation (L_2^{ASZ}) occurs on S_2^{ASZ} foliation planes within the shear zone. These lineations are defined by aligned amphibole in the Milford Gneiss. The orientation of L_2^{ASZ} - S_2^{ASZ} within the shear zone sharply contrasts with the orientation of structural elements (S_1^{SAG} on the west, S_1^{ARC} on the east) measured outside of the Anita Shear Zone (Figs. 27, 28).

Overprinting the gently to moderately-dipping L_2^{ASZ} - S_2^{ASZ} fabric in the Anita Shear Zone, is a

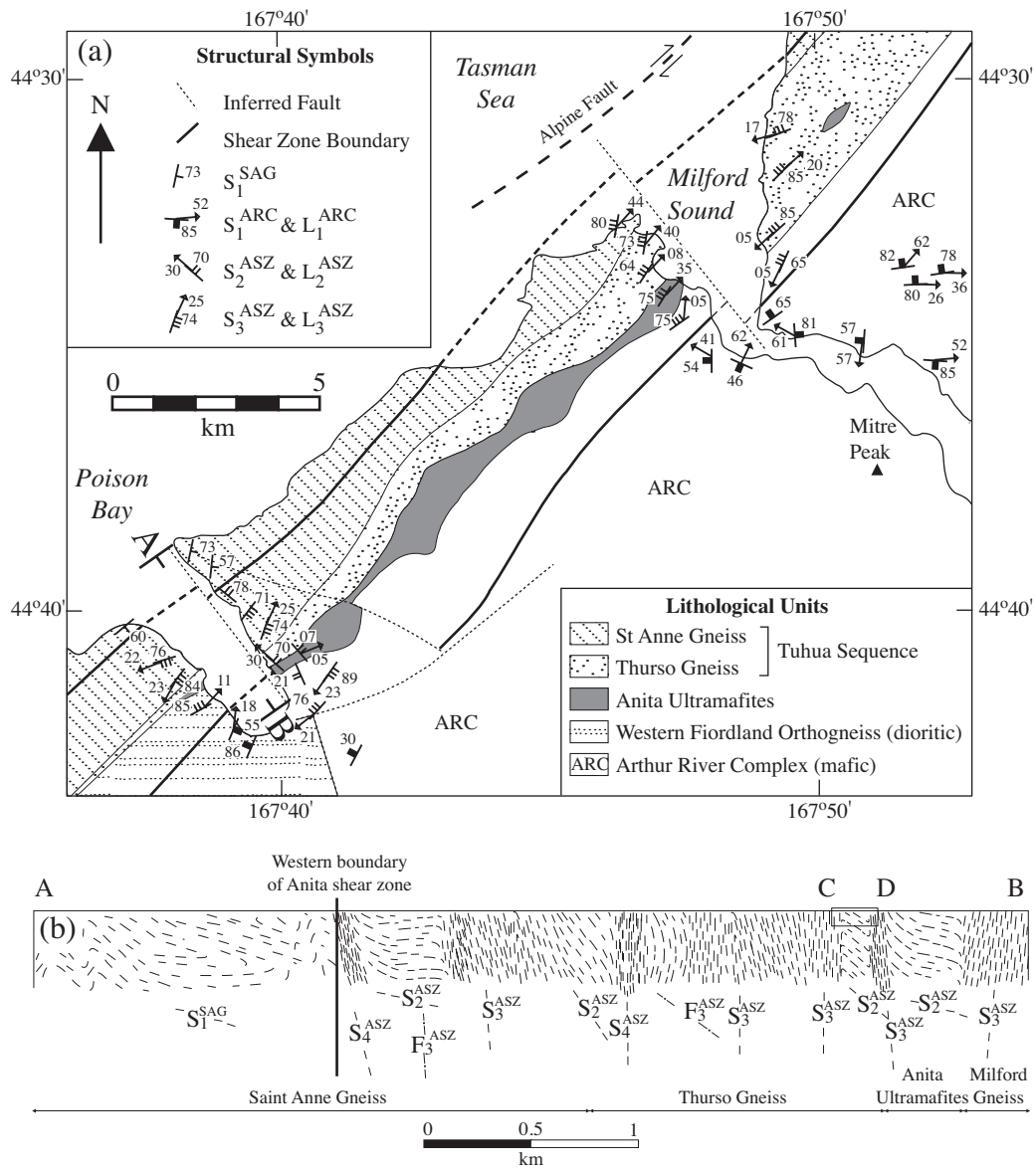


Figure 27. (a) Structural map of the Anita Shear Zone showing major lithologic units within and outside the shear zone boundaries (bold lines). (b) Cross-section (A-B) constructed for northern shore of Poison Bay showing regional-scale variations in the occurrence and orientation of different foliations within and outside the shear zone. After Klepeis et al. (1999).

subvertical, NNE-striking mylonitic foliation (S_3^{ASZ} ; Fig. 28d). This foliation cuts the older L_2^{ASZ} - S_2^{ASZ} fabric at high angles (Fig. 29). In the Thurso and Saint Anne gneisses, S_3^{ASZ} is defined by flattened and aligned garnet, plagioclase, quartz, amphibole, biotite, clinozoisite and titanite. In the Milford Gneiss, S_3^{ASZ} is defined by the assemblage plagioclase, quartz, amphibole, epidote and titanite. Titanite, which is characteristic of the S_3^{ASZ} assemblage, does not occur within the S_2^{ASZ} assemblage anywhere in the shear zone. Preliminary U-Pb dates on this titanite produced a Late Cretaceous-early Tertiary age range of 61-55 Ma (e.g. Fig. 30). A penetrative mineral lineation (L_3^{ASZ}), defined by aligned amphibole in the Milford Gneiss and aligned biotite, amphibole and quartz-plagioclase aggregates in the Thurso and Saint Anne Gneisses occurs on S_3^{ASZ} planes. L_3^{ASZ} is subhorizontal to gently NE- or SW-plunging at high to near orthogonal angles to the L_2^{ASZ} mineral lineation (Fig. 31). The L_3^{ASZ} - S_3^{ASZ} fabric parallels both boundaries of the shear zone and is the most penetrative fabric in the shear zone. Across the entire

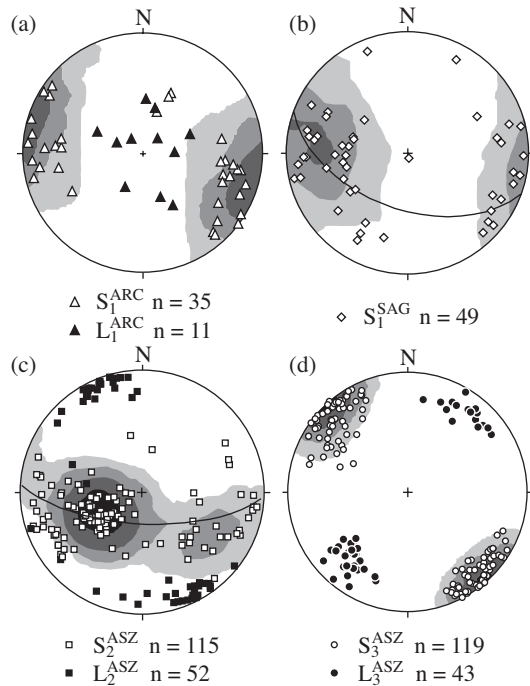


Figure 28. Lower hemisphere equal area stereoplots of structural data from Milford Sound and Poison Bay. Contour intervals are 3% per 1% area. (a) Pre-Anita Shear Zone structural elements east of the shear zone. (b) Pre-Anita Shear Zone structural elements from west of the Anita Shear Zone at Poison Bay. (c) D_2^{ASZ} structural elements (poles to S_2^{ASZ} and L_2^{ASZ}) within the shear zone at Poison Bay. (d) D_3^{ASZ} structural elements (poles to S_3^{ASZ} and L_3^{ASZ}) within the shear zone at Milford Sound and Poison Bay. After Klepeis et al. (1999).



Figure 29. View of a vertical section of outcrop showing a gently SE-dipping S_2^{ASZ} foliation sharply truncated by a vertical S_3^{ASZ} foliation at Poison Bay.

width of the Anita Shear Zone, S_3^{ASZ} occurs together with upright to gently inclined, NE- and SW-plunging folds (F_3^{ASZ}) of S_2^{ASZ} . The interlimb angles of these folds vary from open to isoclinal within the shear zone (Fig. 31).

The youngest phase of deformation within the Anita Shear Zone (D_4^{ASZ}) produced narrow (<10 meters wide) subvertical greenschist facies shear zones that crosscut D_2^{ASZ} and D_3^{ASZ} structures. These minor shear zones are distinguished from D_3^{ASZ} mylonites on the basis of mineral assemblage (S_4^{ASZ} is dominated by muscovite), the occurrence of cataclastic textures and a crenulation cleavage in pelitic schists, and crosscutting relations. D_4^{ASZ} is best developed in the Saint Anne Gneiss near the western boundary of the shear zone and on both sides of the Anita ultramafite. Within the Saint Anne Gneiss, S_4^{ASZ} is defined almost entirely by coarse-grained muscovite. Near the ultramafite D_4^{ASZ} structures are steep, NNE-striking brittle fault zones that contain subhorizontal slickenlines on fault planes. Cataclastic textures, intensely fractured olivine grains and talc in the Anita ultramafite, and fractured garnet, epidote and chlorite in the Milford Gneiss are visible in thin section. Numerous other brittle faults (D_4^{ASZ}) offset lithological contacts and the shear zone boundaries. These faults are parallel and slightly oblique to the walls of Milford Sound and Poison Bay.

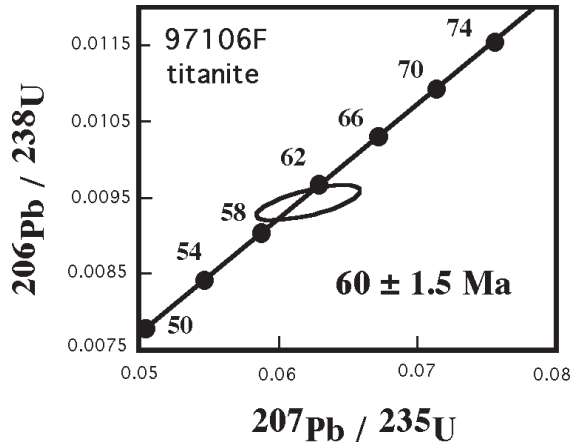


Figure 30. Concordia diagram showing U-Pb isotopic data from titanite in the Anita Shear Zone.

Kinematics. In a previous study, Klepeis et al. (1999) used systems of rotated porphyroclasts and asymmetric microstructures from localities at Poison Bay to compare the kinematics of ductile flow that produced the L_2^{ASZ} - S_2^{ASZ} and L_3^{ASZ} - S_3^{ASZ} fabrics. An abundance of deformed pebble-sized feldspar porphyroclasts in a fine-grained matrix within the Thurso Gneiss and a deformed conglomerate layer provided a means of determining sense of shear in the shear zone. Observations of clast and tail shape were made on three mutually perpendicular surfaces cut relative to the dominant L-S fabric elements in each domain. This study found a wide array of both σ -type, δ -type, and complex σ - δ -type systems indicating both sinistral and dextral senses of shear viewed on surfaces oriented parallel to stretching lineation and perpendicular to foliation.

A statistical analysis of over 300 grains for D_2^{ASZ} and over 200 grains for D_3^{ASZ} shows that the dextral shear sense was dominant for both deformation events. This shear sense defines the sense of forward rotation (dextral) for each strain domain (examples of strain domains shown in Fig. 31). D_2^{ASZ} , however, involved top-down-to-the-SE sense of shear whereas D_3^{ASZ} involved subhorizontal, NNE-SSW dextral displacements nearly orthogonal to L_2^{ASZ} (Fig. 31) In addition to asymmetric tails on feldspar clasts,

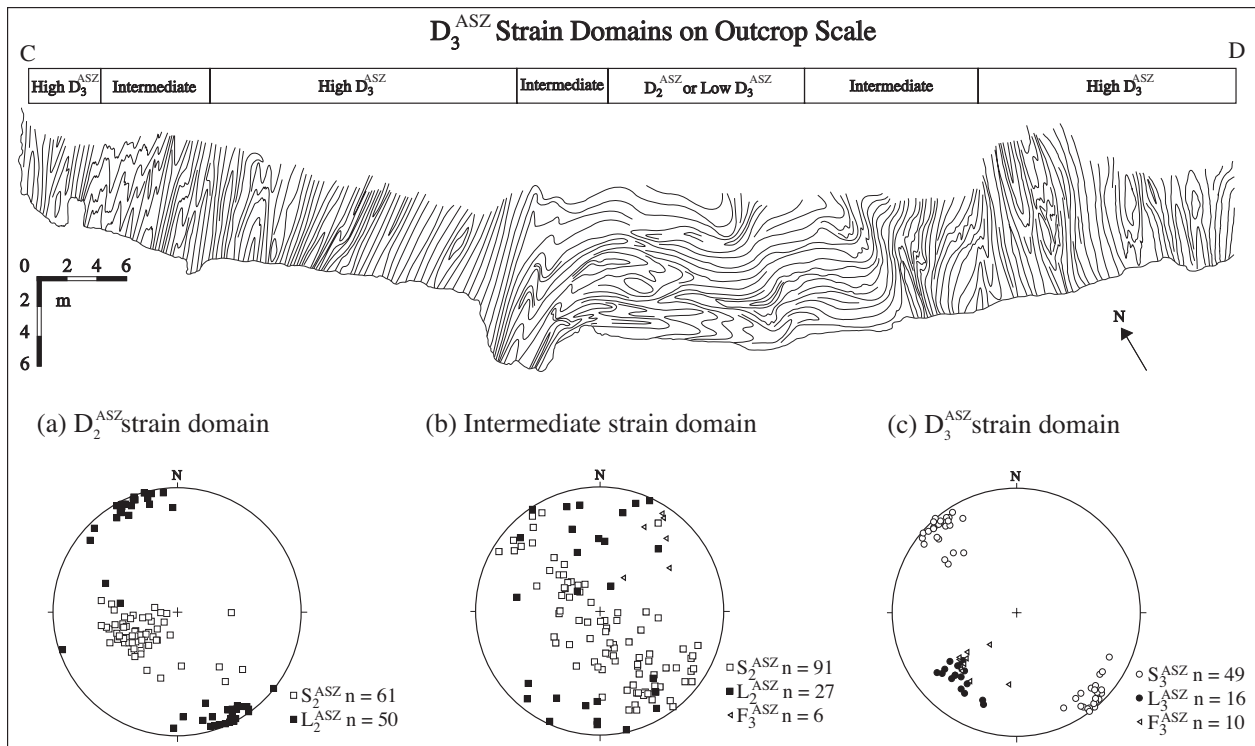


Figure 31. NW-SE cross-section showing foliation trajectories at outcrop site 97106 at Poison Bay. Foliation trajectories show the changing orientations and geometries of D_2^{ASZ} and D_3^{ASZ} mylonites within the shear zone. See Fig. 27 for section location.

numerous other kinematic indicators are present in both D_2^{ASZ} and D_3^{ASZ} strain domains. These include C' shear bands, fractured and microfaulted feldspar grains macroscopic δ -tails on large mafic clasts, mica fish, and minor shear zones that parallel the main foliation in each domain.

May 2

George Sound

The Western Fiordland Orthogneiss Batholith, George Sound (Figs. 5, 32, 33) provides us with near continuous exposure along a NW-SE section (Fig. 34) through the Western Fiordland Orthogneiss (WFO). Most of this batholith is composed of sheeted dioritic intrusions, numerous felsic-mafic dikes and folded rafts of deformed and metamorphosed country rock. At the NW end of George Sound, one large (4-5 km wide) raft is composed of foliated and folded schists, marble and gneiss of the George Sound Paragneiss. Within a 500 m wide zone near the contact between the raft and the WFO, intrusive relationships and delicate migmatitic textures are well preserved (Figs. 33, 34). This contact zone escaped much of the deformation and recrystallization that followed emplacement of the WFO. At the SE end of George Sound at Anchorage Cove (Fig. 33), another raft of migmatitic paragneiss is intensely deformed and recrystallized.

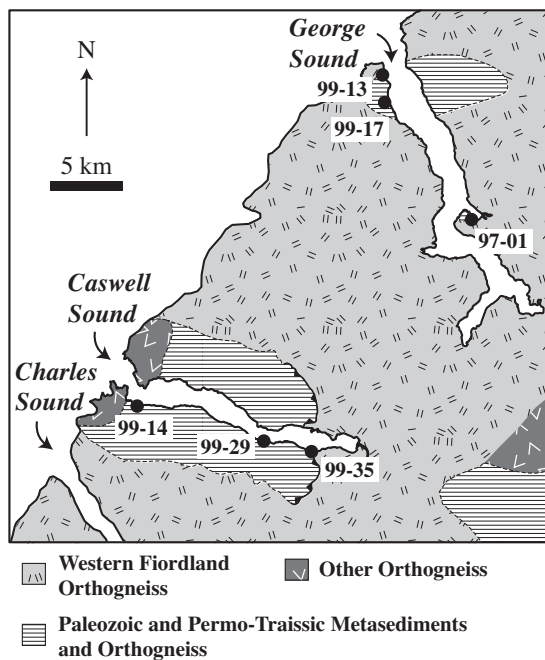


Figure 32. Geologic map showing outcrop localities at George Sound and Caswell Sound. After Daczko et al. (2002a).

The diatexite exposed at the northwestern end of George Sound represents a rare locality within Fiordland where intrusive relationships between the WFO and older host rocks are preserved. Here, migmatite that formed in the metapelitic rafts contain an abundance of leucosome that suggests high melt fractions (>30%) were produced and controlled by the reaction of biotite and muscovite during partial melting (Fig. 35 top). An inhomogeneous diatexite in a metapelitic host near the contact aureole of the Western Fiordland Orthogneiss contains interconnected pockets of leucosome between irregular, joined paleosome. The size and abundance of leucosome increases toward the contact between the batholith and its host where leucosome feeds discordant dikes that were injected back into the dioritic parts of the Western Fiordland Orthogneiss.

Within a few tens of meters of the batholith contact, disconnected rafts of host rock are surrounded by leucosome that infill boudin necks. Differential movement between the rafts relative to gneissic layering in host rock is evident by the discordant pattern of foliations preserved inside them. These relationships suggest that melt, now represented by leucosome, migrated along foliation planes to low-pressure sites. However, apart from the localized boudinage and rotated blocks, this site does not record pervasive subsolidus deformation such as that which affected other parts of the Western Fiordland

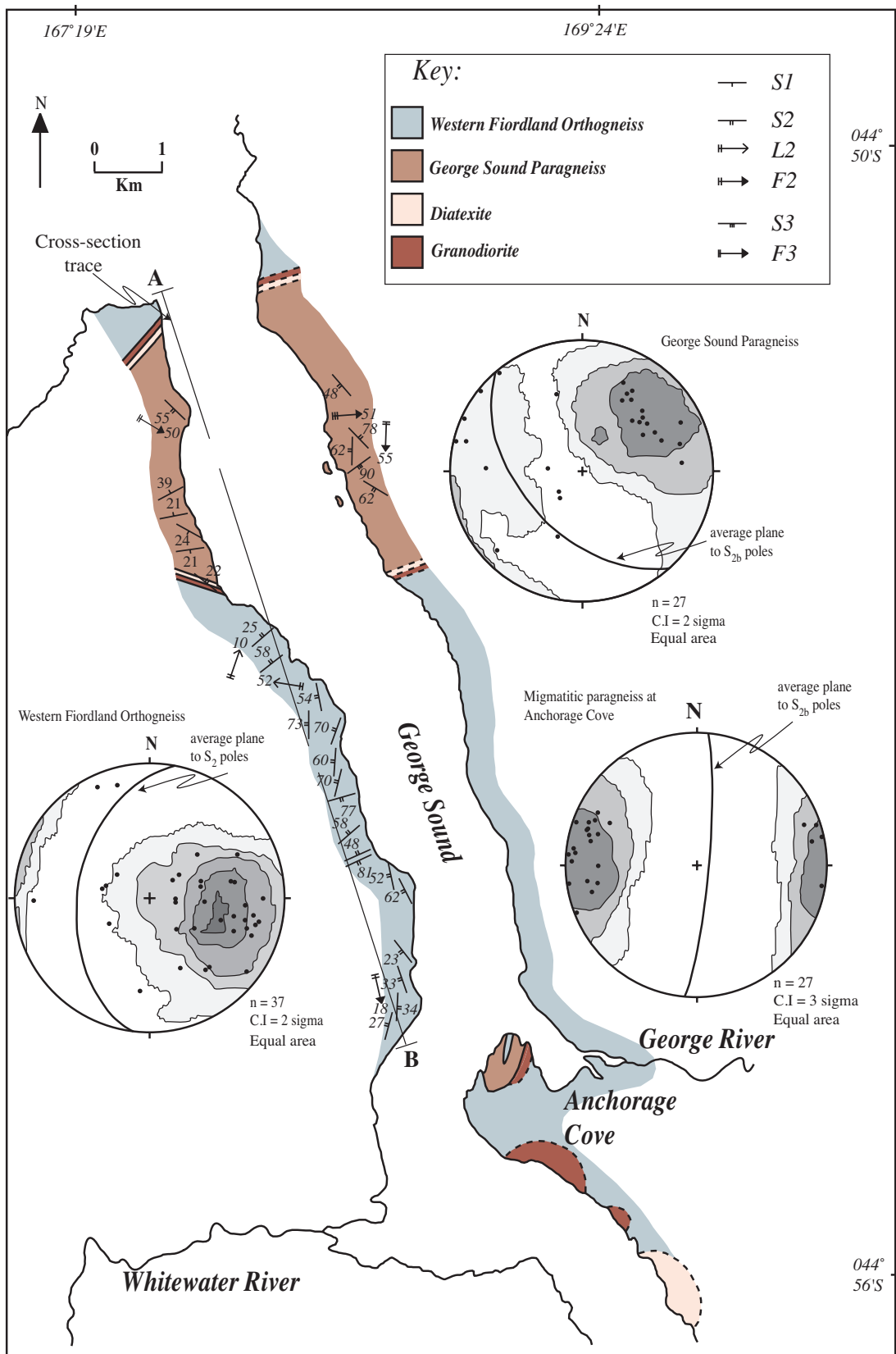


Figure 33. Geologic map and equal-area stereoplots of structural elements from George Sound.

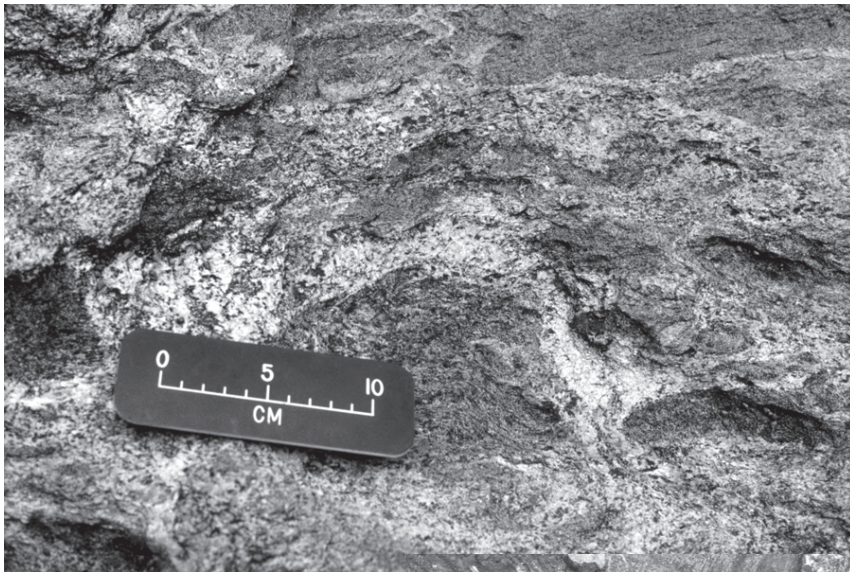


Figure 35. Photograph (top) of a diatexite formed within 200 m of the contact between pelitic schist and the Western Fiordland Orthogneiss at the northwestern end of George Sound. Photograph (bottom) showing a tightly folded subsolidus foliation at Anchorage Cove at George Sound. After Klepeis and Clarke (2003).

Orthogneiss. Daczko et al. (2002a) obtained pressures reflecting the peak of Early Cretaceous metamorphism from 7-9 kbar at this locality suggesting emplacement depths of 25-30 km.

Along the central parts of the sound, dioritic rocks of the WFO contain two-pyroxene igneous assemblages. Orthopyroxene and some clinopyroxene grains are clouded by fine-grained exsolution lamellae of ilmenite, and are inferred to be igneous. Igneous orthopyroxene, with or without igneous clinopyroxene, is separated from plagioclase, quartz and K-feldspar by metamorphic aggregates of clinopyroxene, garnet and rutile. These aggregates may have a weak to well-developed structure involving a small core of igneous orthopyroxene or clinopyroxene, successively mantled by metamorphic clinopyroxene and garnet. Small proportions of hornblende occur intergrown with metamorphic clinopyroxene near the margins of the aggregates.

The degree of subsolidus recrystallization and deformation affecting the interior of batholith was extremely heterogeneous. Inside the WFO foliations form two dominant structural styles. The first style includes magmatic flow foliations defined by the planar alignment of clinopyroxene, hornblende, tabular plagioclase and other minerals. These magmatic foliations show highly variable orientations. The second style includes steeply to moderately dipping subsolidus foliations that are variably developed within the batholith. These foliations form the dominant structural grain observed at Anchorage Cove (Fig. 33) where they envelop lenses of dioritic gneiss and locally cut the older, more gently dipping synmagmatic foliations. A moderately plunging hornblende mineral lineation occurs on some foliation planes. In some places, the foliation parallels the axial planes of upright, south-plunging isoclinal folds of dikes and gneissic layering (Fig. 35 bottom). The tightness of folding and degree of transposition also indicate that this area represents a zone of high strain. The boundaries of this high zone approximately parallel those of the dominant foliation (and Indecision Creek Shear Zone) at Milford Sound.

Emplacement of the Western Fiordland Orthogneiss synchronous with regional deformation and collisional-style orogenesis is illustrated by (i) coeval ages of a post-D1 dyke (*c.* 124 Ma) and its host pluton (*c.* 122 Ma) at Mt Daniel and (ii) coeval ages of pluton emplacement and metamorphism/deformation of proximal paragneiss in George and Doubtful Sounds. Age spectra of detrital zircon populations were characterized for three of these paragneiss units. A paragneiss from Doubtful Sound shows a similar age spectrum to other central Fiordland and Westland paragneiss and SE Australian Ordovician sedimentary rocks, with age peaks at 500-600 and 900-1100 Ma, a smaller peak at *c.* 1400 Ma, and a minor Archaean component. However, some samples of the George Sound Paragneiss exhibit different age spectra. High-pressure kyanite-staurolite-bearing amphibolite facies schists preserved in rafts of the George Sound Paragneiss distal to the Western Fiordland orthogneiss exhibit Permo-Triassic age spectra, some with minor Archaean-Palaeozoic components. The high-pressure mineral assemblages reflect metamorphism and burial by at least 30 km to deep-crustal levels (*c.* 9 kbar) in the Early Cretaceous. Given the timing of deposition of the George Sound Paragneiss (< *c.* 150 Ma) and of Western Fiordland Orthogneiss emplacement (*c.* 120 Ma), burial must have occurred rapidly (at least 1 mm/yr over 30 Ma). The George Sound Paragneiss may have been sourced from Permo-Triassic volcanoclastic rocks of the Eastern Province, or its source region/s, consistent with the close proximity of the Eastern and Western Provinces by the Early Cretaceous.

May 3

Caswell Sound

A Mid-Crustal Fold-Thrust Belt. From east to west, Caswell Sound (Fig. 5, 32, 36) contains three main rock types: (1) Western Fiordland Orthogneiss, (2) Caswell Gneiss and (3) the McKerr monzodiorite. The Western Fiordland Orthogneiss is most commonly weakly deformed hornblende-plagioclase-dominated gabbroic gneiss. Daczko et al. (2002a) obtained peak Early Cretaceous metamorphic pressures of $P=7-9$ kbar from samples collected within the WFO and its contact aureole. The Caswell Gneiss consists of 60% paragneiss and 40% biotite dioritic orthogneiss. The paragneiss is best exposed along the shores of Caswell Sound at its western end near the contact with the McKerr monzodiorite. The paragneiss comprises calcsilicate and mafic gneiss, marble, and metapsammitic schist. All units are interbedded and the thickness of sedimentary layering is highly variable ranging

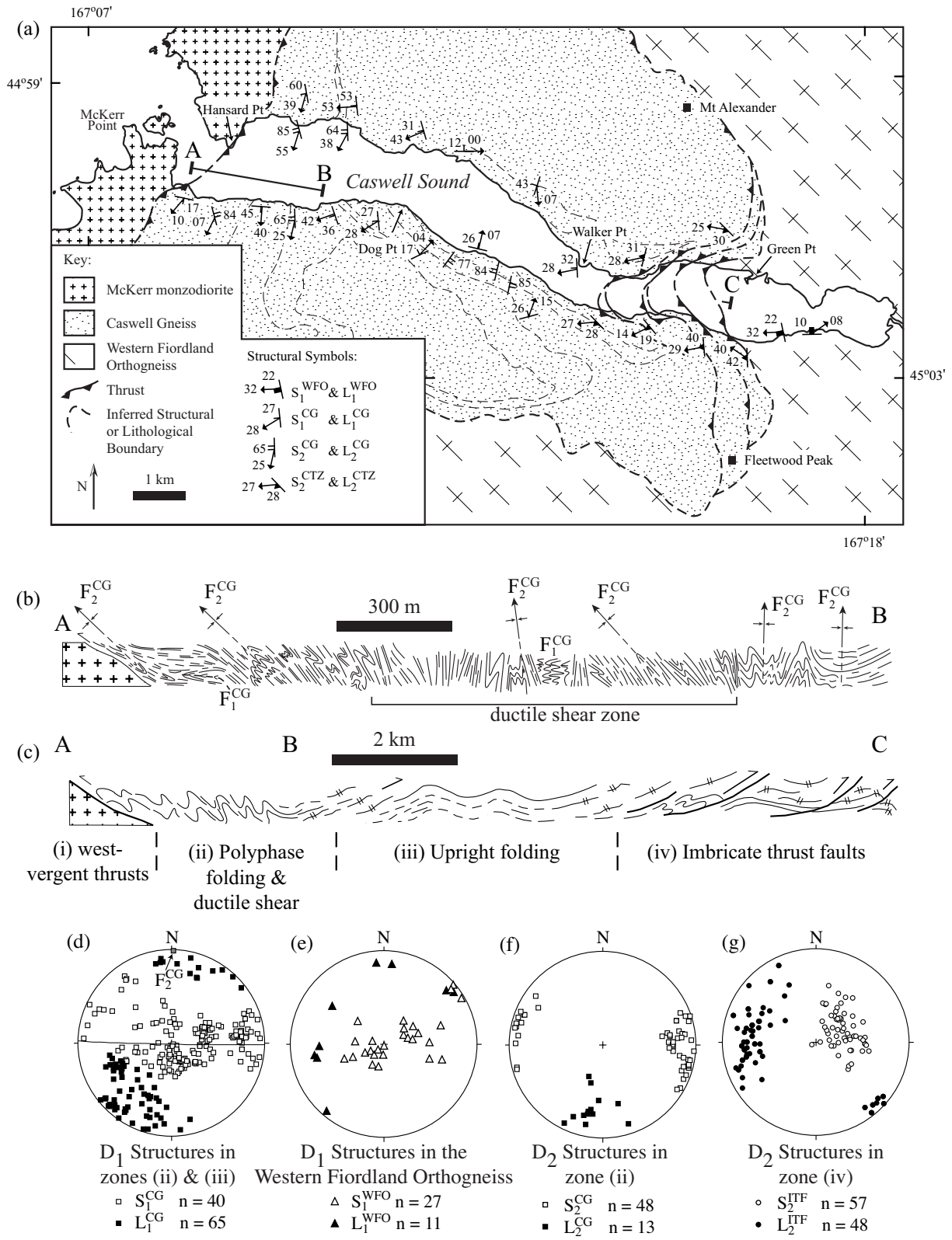


Figure 36. (Structural map of Caswell Sound showing major lithologic divisions and lines of cross-sections. Cross sections and stereoplots of structural elements also shown. After Daczko et al. (2002a).

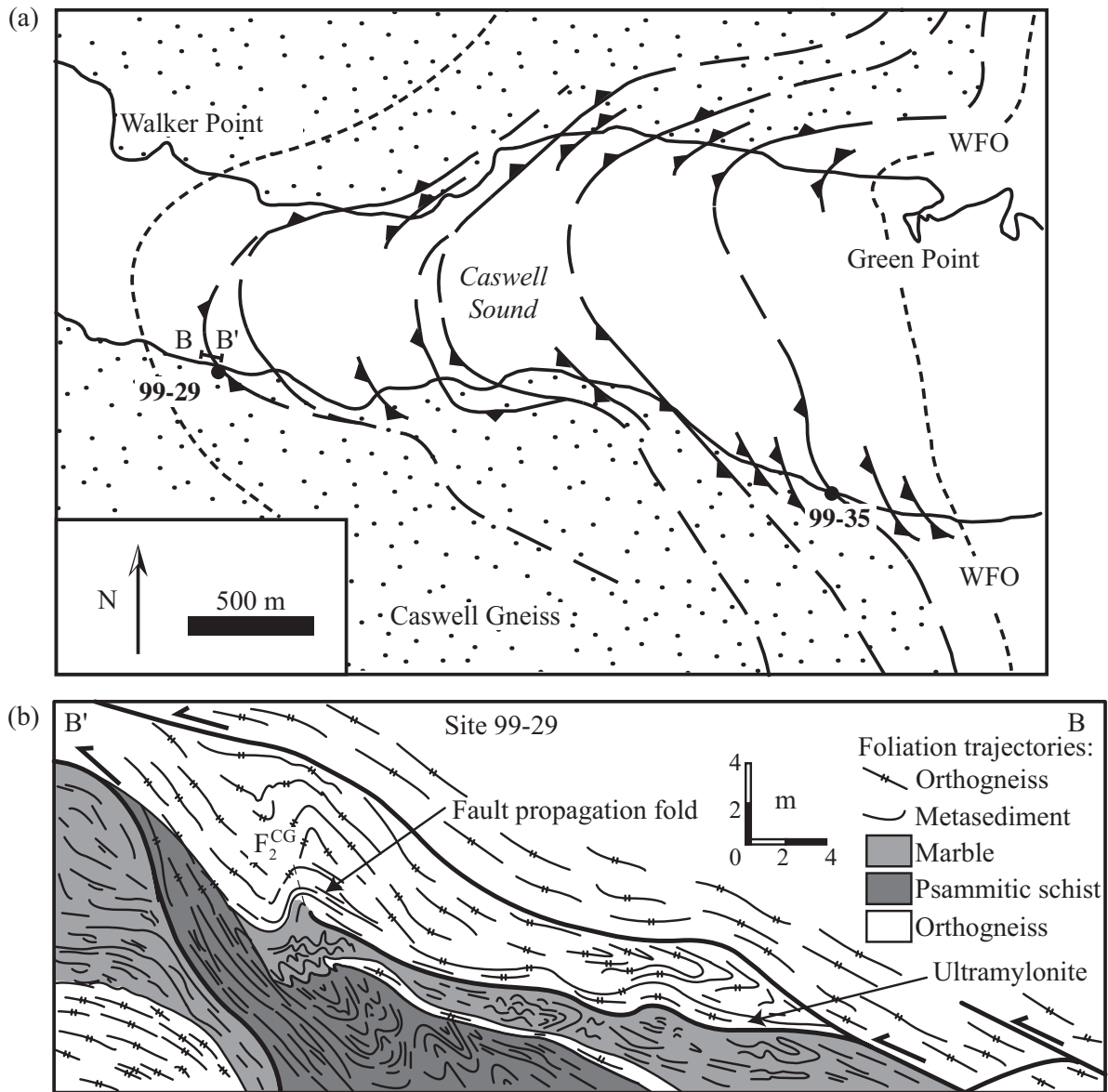


Figure 37. (a) Structural map of the zone of imbricate thrust faults. (b) Vertical section B-B' shown in (a) of a thrust zone viewed perpendicular to transport direction, in the Caswell Gneiss. Note zones of ultramylonite and fault propagation folds. After Daczko et al. (2002a).

from a few centimeters up to in excess of 100m. The biotite-plagioclase-dominated dioritic orthogneiss contains rafts of the paragneiss and is best exposed near Walker Point (Fig. 36a). The orthogneiss forms sill-like intrusions greater than 500 m thick. The McKerr monzodiorite is a very weakly deformed biotite-plagioclase rock that cuts the Caswell Gneiss. The contact with Caswell Gneiss displays clasts of brecciated paragneiss within the monzodiorite that are inferred to represent an igneous breccia.

At the eastern end of the sound, the Western Fiordland Orthogneiss (WFO) is deformed by garnet granulite and amphibolite facies thrusts that sole into a subhorizontal décollement located at and below the contact between the batholith and its host rocks (Fig. 36). Inside the WFO, the detachment is defined by a 1 km thick zone of penetrative subhorizontal, to gently dipping upper amphibolite and garnet granulite facies foliations. The country rocks are composed of calcsilicate gneiss, marble, and

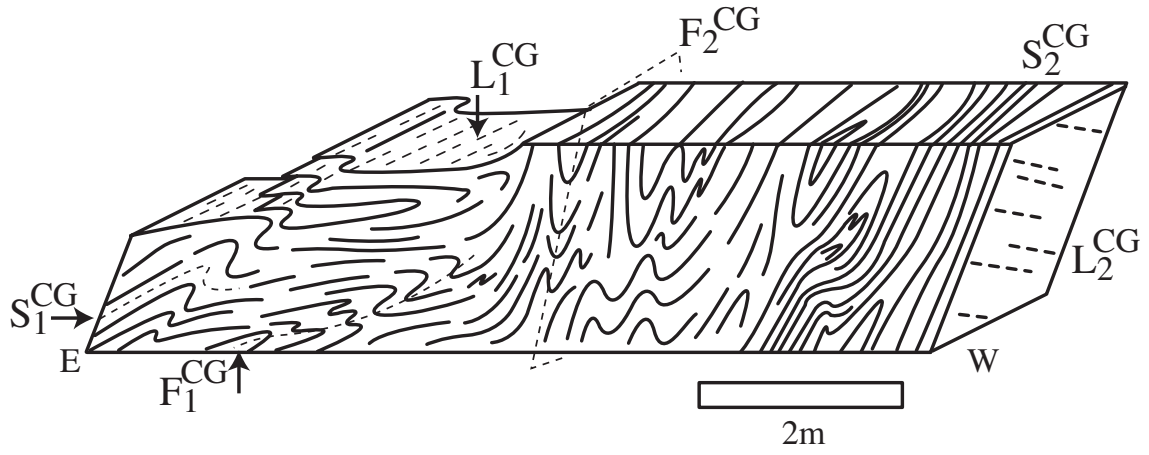


Figure 38. Sketch of polyphase folding in marble shear zone at western end of Caswell Sound.

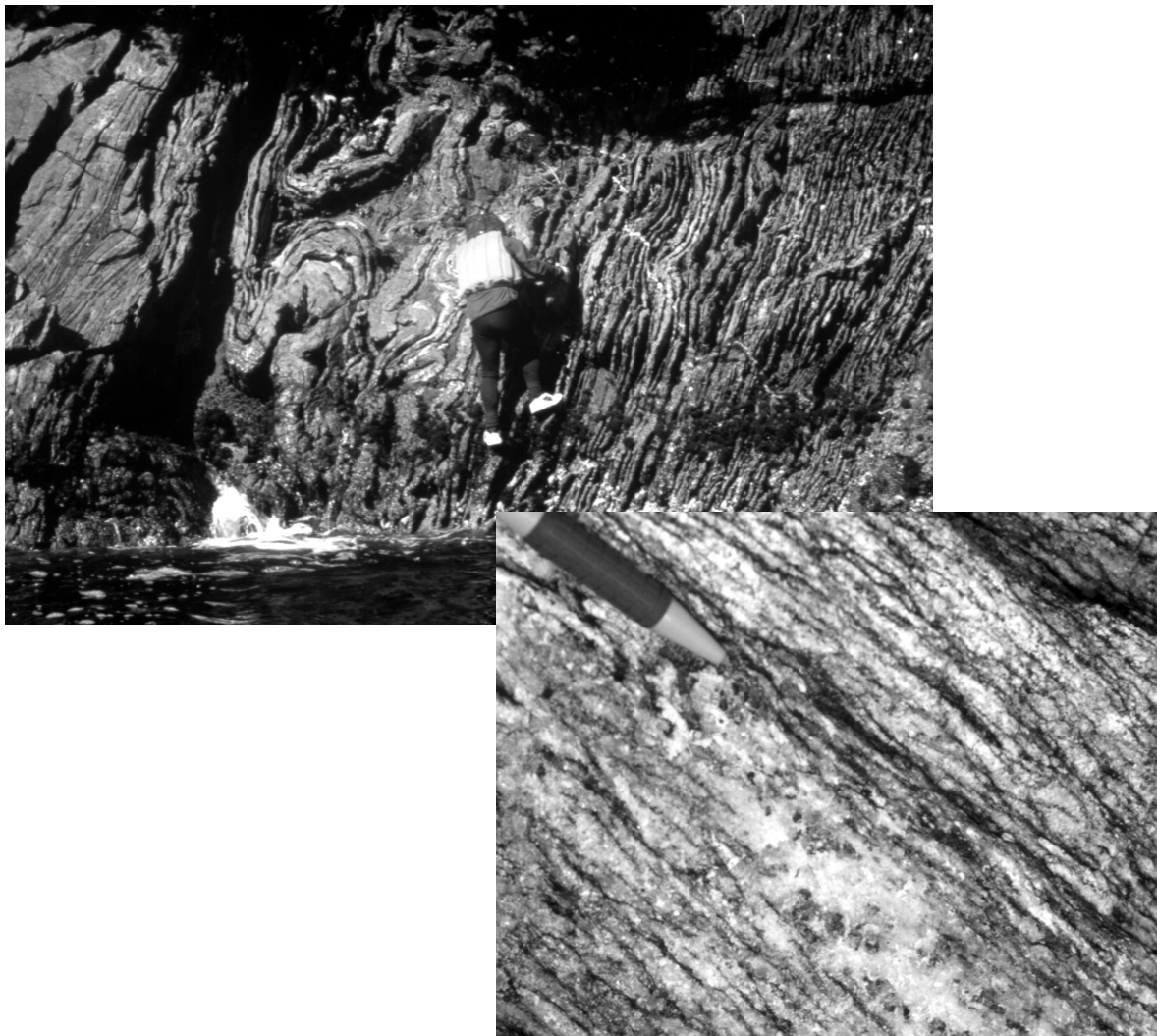


Figure 39. Photograph (top) of tightly folded marble at Caswell Sound. Photograph (bottom) of garnet-bearing leucosome in thrust zone cutting the WFO at Caswell Sound.

metapsammitic schists that form part of the Paleozoic sequences of New Zealand's Western Province. Imbricated, west-dipping ductile thrust splays localized at and above the WFO contact and locally cut across it at the eastern and western ends of the sound (Figs. 36; 37). Tight to isoclinal, south-plunging folds between thrusts deform a penetrative layer-parallel foliation in metasedimentary country rocks. Structurally above and to the west of the imbricate series the geometry of these folds changes from tight and overturned to open and upright, reflecting a decrease in strain intensity above and away from the WFO margin and the basal décollement (Fig. 36c). Steep to vertical upper amphibolite facies foliations cut the layer-parallel foliation and parallel the axial planes of these folds. Farther west (~12 km), the folds gradually tighten and overturn to the east above a major east-dipping thrust fault. This east-dipping thrust separates the high-grade rocks of the thrust belt to the east from weakly deformed McKerr monzodiorite to the west.

The most distinguishing feature of the western part of the thrust belt is a 1.5 km-wide ductile shear zone that deforms a succession of calc-silicate, metapelitic, psammitic and marble units (Fig. 38). The shear zone is characterized by upright, asymmetric, tight to isoclinal folds and a very well developed steeply dipping foliation (Fig. 39 top). This shear zone foliation crosscuts all early shallowly dipping foliations and recumbent folds in the Caswell Gneiss. The tight upright folds are coaxial with the older recumbent folds and produce a macroscopic type 3 interference pattern (fishhooks; Fig. 38). With the exception of an area of 'M-type' symmetrical fold geometry in the central region of this zone, most of these folds are overturned and west-vergent.

Thrust plane foliations inside the WFO are defined by flattened clusters of coarse hornblende, clinozoisite and garnet in a feldspar matrix (Fig. 39 bottom). Inside the WFO and within 500 m of its uppermost contact, feldspar in the thrust zones was dynamically recrystallized along grain boundaries. In contrast, greater than 500 m above the contact, feldspar behaved brittlely during deformation in thrust zones and mylonitic textures are common. Thrust faults greater than 500 m and up to 2.5 km from the contact with the WFO are defined by aligned chlorite, muscovite, quartz, feldspar, clinozoisite and amphibole. This strong link between increasing metamorphic grade, dynamic recrystallization of feldspar, and proximity to the uppermost contact of the WFO suggests that the thrusts were preferentially partitioned into crust that was thermally softened by the emplacement of the batholith. These data also indicate that contraction outlasted emplacement and crystallization of the WFO.

Crosscutting relationships between thrust fabrics in the Caswell detachment and the WFO indicate that contractional deformation there must have occurred during and/or after the interval 126-116 Ma. Klepeis et al. (submitted) confirmed this crosscutting relationship using U-Pb spot analyses on single zircons from the McKerr granodiorite and from a dioritic intrusion that was interlayered with Paleozoic metasediments structurally above the WFO. Zircons were analyzed by George Gehrels with a Micromass Isoprobe multicollector ICPMS at the University of Arizona. These analyses yielded weighted mean ages of 116.8 ± 7.6 Ma and 118.7 ± 7.0 Ma.

May 4-5

Doubtful Sound and Crooked Arm

South of Caswell Sound, the west- and southwesterly dips of the contacts between the WFO and its host rock change to northeasterly, subparallel to the gently dipping Doubtful Sound Shear Zone.

This shear zone is composed of numerous branching splays of upper amphibolite facies mylonite up to several hundred meters thick. The shear zone was originally interpreted as a ductile thrust fault by Oliver and Coggan (1979) and Oliver (1980) but later was reinterpreted as a major extensional detachment fault by Gibson et al. (1988). A U-Pb zircon age of ~119 Ma and K-Ar amphibole and biotite cooling ages of ~93 Ma and ~77 Ma respectively support a mid-Cretaceous age for the Doubtful Sound Shear Zone (Gibson and Ireland, 1995). The deformation has been interpreted to reflect a period of regional extension that resulted in the formation of metamorphic core complexes in the western part of the South Island (Gibson et al., 1988; Tulloch and Kimbrough, 1989). This extension is inferred to have controlled most of the denudation and exhumation of the lower crustal exposures in Fiordland that has occurred since the Early Cretaceous.

The Doubtful Sound Shear Zone is well exposed along the southern shores of Malaspina Reach

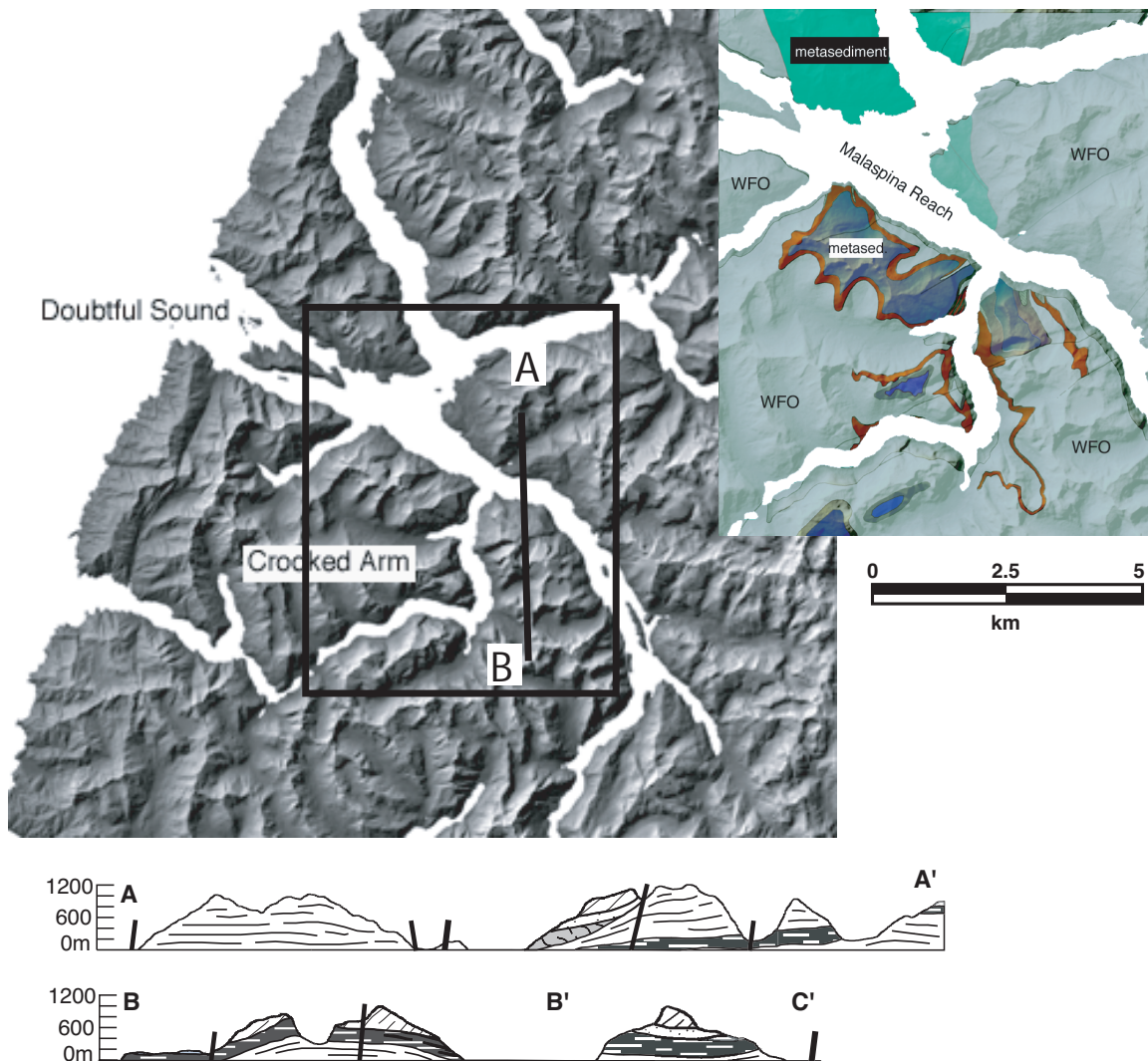


Figure 40. Digital Elevation Map of Malaspina Reach and Crooked Arm. Dark bands in inset and sections show mylonitic parts of the Doubtful Sound Shear Zone. Curved outcrop pattern results from the gentle northerly dip of the shear zone and the steep topography of the sound.



Figure 41. Photograph (top) showing tight, recumbent folds of gneissic layering in the Western Fiordland Orthogneiss at Doubtful Sound. Fold occurs in an asymmetric pod surrounded by zones of mylonite that form part of the Doubtful Sound Shear Zone. East is to the left. Photograph (bottom) showing geometry of asymmetric pods in the Doubtful Sound Shear Zone. East is to the left.

and the headlands at the northern end of Crooked Arm (Fig. 40). Here, subhorizontal and gently NE-dipping upper amphibolite facies mylonite zones that define high strain areas wind in and out of the steep topography of the sound. Two distinctive lithologic units occur along the coast: coarse-grained, pyroxene-, hornblende-bearing gabbro and diorite of the Western Fiordland Orthogneiss, and paragneiss and schists of mostly Paleozoic age. The metasedimentary rocks lie structurally on top of the WFO and, on the southern side of the sound, mostly dip gently to the north and northeast (Fig. 40). Mylonite zones of the Doubtful Sound Shear Zone separate the two units and cut deeply into the batholith near Crooked Arm.

Along Crooked Arm, ultramafic pods and lenses are enclosed by sheets of diorite and gabbro. Some ultramafic pods may also be large intrusions. The ultramafic units are composed mostly of hornblende and pyroxene. Many of the dioritic parts of the WFO display bands of clinopyroxene, orthopyroxene and plagioclase that define igneous layering and parallel the margins of the intrusive sheets. Networks of planar, garnet-, plagioclase-bearing veins cut across all subunits and igneous layering within the WFO. The ultramafic units especially are enriched in garnet. Many of these veins display planar 3-5 cm wide garnet granulite reaction zones along their margins where pink garnet replaces pyroxene and hornblende. These reaction zones record dehydration of host rock assemblages and are similar to those that occur within the Pembroke Valley north of Milford Sound.

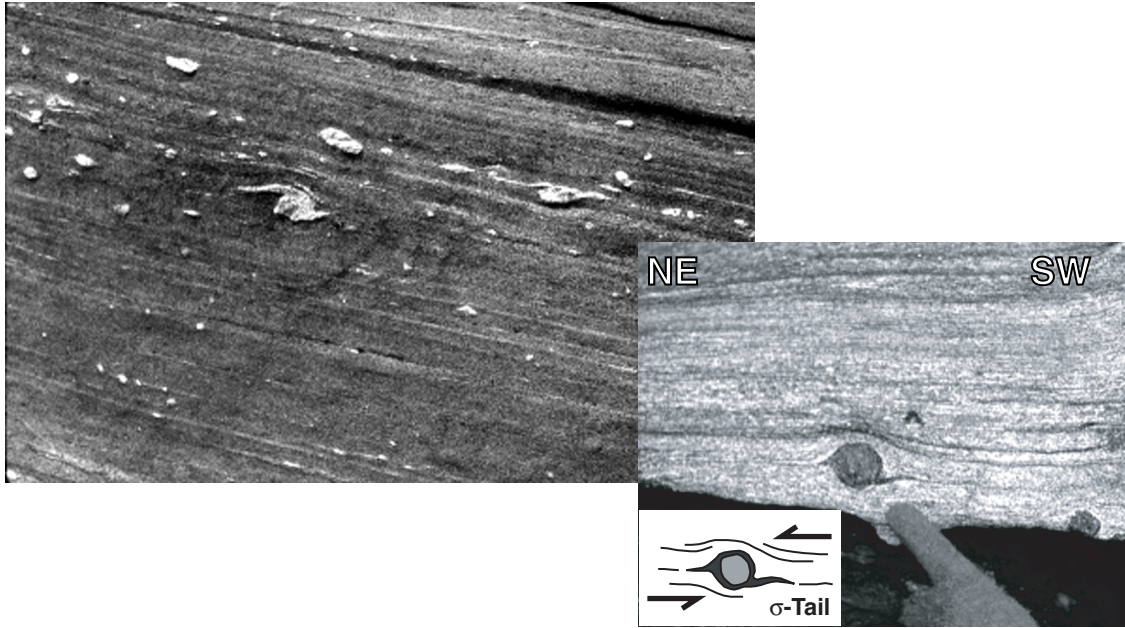


Figure 42. Photograph (top) showing rotated plagioclase porphyroclasts in a hornblende-rich mylonitic matrix in the Doubtful Sound Shear Zone. East is to the left. Photograph (bottom) showing asymmetric biotite tails on rotated garnet porphyroblast the Doubtful Sound Shear Zone. East is to the left.

Retrogressive biotite and hornblende formed from the hydration of pyroxene define the dominant foliation in many parts of the shear zone. Elsewhere garnet granulite facies mineral assemblages define the shear zone foliation. Where the two fabrics occur together in zones of high strain the upper amphibolite facies foliation cuts obliquely across granulite facies foliations and veins in the WFO. Curved zones of mylonite envelop asymmetric pods that preserve older gneissic fabrics and garnet granulite mineral assemblages. These pods typically vary in size from <1 m to >30 m in horizontal length. Inside these pods, mafic dikes and gneissic layering are folded variably (Fig. 41 top and bottom). Some of the folds are tight to isoclinal and recumbent, others are inclined and verge to the southwest. Many of the garnet-bearing vein sets are transposed parallel to upper amphibolite facies mylonitic foliation. Penetrative northeast plunging mineral lineations defined by aggregates of plagioclase, pyroxene and amphibole are well developed on foliation planes in zones of mylonite. These relationships suggest multiple stages of slip at both the garnet granulite facies and the upper amphibolite facies.

Sense of shear indicators in the shear zone also are best preserved in zones of mylonite. In these areas, asymmetric tails of amphibole and quartz around plagioclase grains (Fig. 42 top), hornblende and biotite fish, S-C fabric, and asymmetric tails around rotated garnet porphyroblasts (Fig. 42 bottom) yield top-down-to-the-NE and -ENE senses of shear. Asymmetries associated with these kinematic indicators are best developed on surfaces oriented perpendicular to foliation and parallel to NE-plunging stretching lineations, although other surfaces also display asymmetries. Rotated porphyroblast systems show σ -type, δ -type, and complex σ - δ -type tails that can be used to quantify the ductile flow field in the shear zone. Claypool (2002) found that in zones of mylonite these shapes reflected simple-shear-dominated deformation within a vertically thinning shear zone. However, in some lozenges where strain is lower than in the surrounding mylonite zones, S-C fabric show a top-up-to-the-SW sense of shear. This sense of shear contrasts with the general top-down-to-the-NE kinematics shown

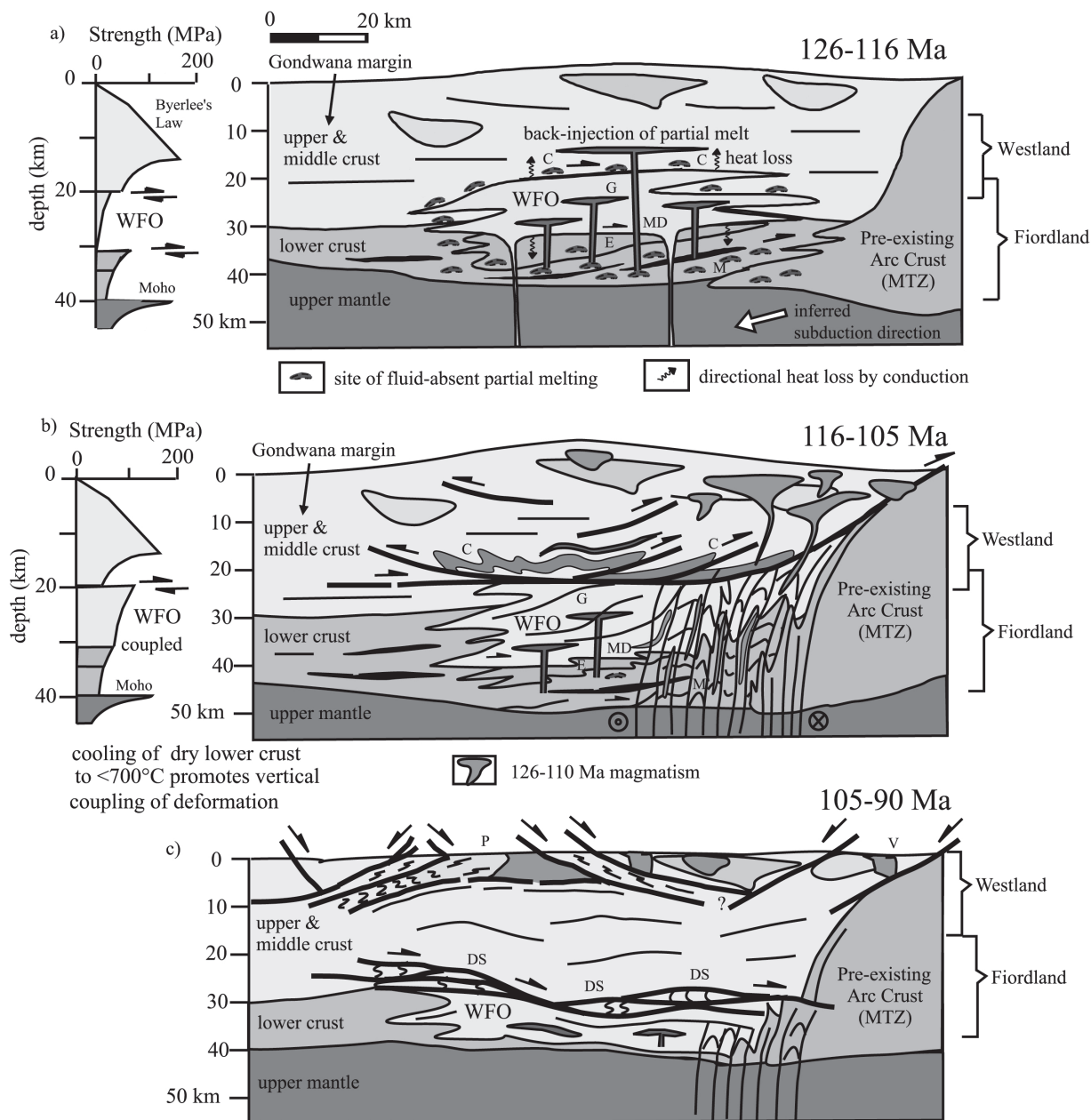


Figure 43. Cartoons illustrating the early Mesozoic tectonic evolution of the South Island's Western Province after Klepeis et al. (2003). a) During interval 126-116 Ma, mafic-intermediate magma (WFO) was added to the middle and lower crust. Upper crust was composed mostly of Paleozoic Gondwana margin rocks and granitoid plutons. Lower crust was composed of older (>126 Ma) arc-related rocks, including parts of the MTZ and Mount Edgar diorite (E) and Paleozoic gneisses of Gondwana. b) Contractional deformation (116-105 Ma) followed magmatism and melt production. c) Late orogenic extension (105-90 Ma) formed metamorphic core complexes (P and V) in mid-upper crust and the Doubtful Sound shear zone (DS) in the lower crust. Schematic strength profiles illustrate variations in the strength of the lower crust during two stages of orogenesis. Lower crust in a) was weakened by magmatism. Lower crust in b) was strengthened by dehydration and the cooling of the WFO to $T < 700^{\circ}\text{C}$.

by most of the shear zone and may reflect an older phase of deformation that pre-dates development of the Doubtful Sound Shear Zone.

Summary of Geologic Relationships and Inferred Processes

Magma emplacement and partial melting in the lower crust

During the period 126-116 Ma, the lower crust of the Fiordland belt accumulated at least 10 km (thickness) of mafic-intermediate magma (Fig. 43a). This period of magmatism formed a >3000 km² tabular batholith called the Western Fiordland Orthogneiss and has been interpreted to have added sufficient heat to the lower crust to partially melt host gneisses. At the time of this intrusion, the lower crust was composed of older (>126 Ma) vertically stratified mafic-intermediate intrusive phases of the early Mesozoic arc and Paleozoic gneisses of Gondwana margin affinity.

Field data show that the spatial distribution of rocks that partially melted following magma emplacement was heterogeneous (Fig. 43a). Above and near the top of the batholith at Caswell and George Sounds, migmatite formed in a narrow zone 200-500 m thick near the batholith-country rock contact. In contrast, below the batholith a region of lower crust at least 10 km thick partially melted (Fig. 43a). Petrologic analyses suggest that the partial melting of mafic-intermediate gneisses below the batholith was patchy and mostly involved hornblende breakdown to form garnet surrounded by leucosome (Daczko et al., 2001b).

Piston-cylinder experiments were performed on an unmelted sample of dioritic gneiss at P=14 kbar and T=800-975°C to test possible mechanisms of melt generation in gneisses below the batholith (Antignano et al., 2001; Antignano, 2002). These experiments suggested that although partial melting occurred in large parts of the section below the batholith, the volume of melt produced probably remained low. These results may explain the low percentage of leucosome observed in mafic lower crust in the field and contrasts with the much higher melt fractions observed in migmatitic paragneiss above the batholith.

Melt segregation and transport

In migmatite formed at paleodepths of 45-50 km, diffuse patches of leucosome parallel gneissic layering and feed laterally into vertical (layer-perpendicular), vein-filled extension fractures. The fracture sets cut across all lithologic boundaries and occur within hundreds of square kilometers of the lower crustal section, including the Pembroke Valley and Crooked Arm. These features provide strong geological evidence that melt segregation and transport were aided by diking and fracture propagation following batholith emplacement.

The physical links that occur between leucosome in migmatitic gneiss and the vein-filled fractures and dikes in the Pembroke Valley suggest that positive volume changes and the development of high melt fluid pressures during melt production helped induce fracturing and melt escape through the lower crust (e.g., Clemens and Mawer, 1992; Davidson et al., 1994). In this scenario, the leucosome observed in the field reflects melt migration along fractures. This hypothesis is supported by metamorphic and geochemical relationships observed in the field and in the laboratory that record how partial melts interacted chemically with gabbroic gneiss during their migration. These relationships led Daczko et al. (2001b) to infer that dehydration of the gabbroic gneiss reflected the scavenging of water by

migrating, water-poor partial melt sourced from the melted diorite gneiss.

Field relationships at Camp Oven Creek also show that fracture propagation and diking were not the only mechanisms of melt transfer following intrusion of the batholith. Foliation planes, lithologic contacts, boudin necks and fold hinges at Camp Oven Creek also contain leucosome. These observations suggest that a combination of fracture networks and deformation in shear zones moved partial melt horizontally and vertically through the crustal column.

Inferred changes in lower crustal strength and rheology

In Fiordland, magma compositions and the liquidus temperature of basalt indicate that the initial intrusion temperatures of the WFO were likely $\geq 1200^{\circ}\text{C}$. Mineral assemblages that formed in the batholith and its host rocks following its emplacement record progressive changes in temperature and fluid activities. Partial melting and granulite facies metamorphism preserved in the Pembroke Valley occurred at $750^{\circ}\text{C} < T < 850^{\circ}\text{C}$ (Daczko et al., 2001b). With time, kyanite- and paragonite-bearing assemblages replaced older garnet-clinopyroxene-plagioclase assemblages reflecting isobaric cooling of the lower crust to $\sim 650^{\circ}\text{C}$ prior to 108-105 Ma (Daczko et al., 2002b). These observations and the well-known dependence of lower crustal strength and rheology on melt fraction, temperature and fluid activity imply that the lower crust must have had a different mechanical strength at different times between 126 and 105 Ma. These changes are illustrated qualitatively in the strength-depth profiles showing a weak lower crust in Figs. 43a and a stronger lower crust in 43b. The results also are consistent with evidence of complex rheological stratifications in sections of arc crust exposed in the U.S. Cordillera (Miller and Paterson, 2001).

Inside the batholith at George Sound and Crooked Arm, magmatic features are cut by the fracture arrays and granulite facies dehydration zones. The fact that these features formed within the batholith (MD, Fig. 43a) provides direct evidence that by ~ 116 Ma the batholith had mostly crystallized. Ductile shear zones that record subsolidus temperatures of $650^{\circ}\text{C} < T < 800^{\circ}\text{C}$ also deform many of the fractures and dikes inside and below the batholith (Daczko et al., 2001a). These transitions suggest that during the period ~ 116 -105 Ma, the lower crust initially was weakened by the addition of heat and magma and later strengthened as melt moved out of the lower crust and the lower crust cooled. Experimental data confirmed the relatively high strengths of lower crustal mafic rocks even as they underwent mineral reactions involving partial melting.

Changing patterns of deformation in the lower crust

One of the most useful features in the study of deformation in Fiordland are the penetrative arrays of extension fractures surrounded by garnet granulite dehydration zones that formed over hundreds of square kilometers of the section, including the batholith. Changes in the angular relationships among these and other vein sets provided a means of defining strain gradients and the kinematic evolution of shear zones from the outcrop to the regional scale. Within the westernmost part of the section, a penetrative, SW-dipping gneissic layering also provided a reference frame that facilitated a comparison of structural styles across the belt. In the west, where Early Cretaceous deformation was weakest, thermobarometric data indicate that this layering was oriented close to horizontal during and after batholith intrusion and fracture sets cut across layering at high angles approaching 90° .

Following partial melting of the lower crust, swarms of vertical, ≤ 1 m thick, E- and NW-striking

shear zones formed at the margins of dikes below the batholith. These shear zones form antithetic (dextral) and synthetic (sinistral) pairs that record arc-parallel (NE-SW) displacements and subhorizontal (layer-parallel) arc-normal (NW-SE) shortening within a dominantly sinistral flow regime (Daczko et al., 2001a). Subsequently, these shear zones were deformed by a series of SE-dipping (avg. 27°), vertically stacked (100 m spacing) shear zones that contain imbricated, asymmetric pods of mylonite. These pods form antiformal stacks that are typical of thrust duplexes and record layer-parallel (subhorizontal) shortening and layer-perpendicular (subvertical) thickening during arc-normal contraction (Daczko et al., 2001a). Mineral assemblages that define foliation planes in these thrusts record metamorphic conditions of $P=14 \pm 1.2$ kbar and $T=674 \pm 36^\circ\text{C}$ (Daczko et al., 2001a). This style of duplex involving simultaneous deformation along steeply and shallowly dipping foliations was also noted by Karlstrom and Williams (in press) as an important mechanism in the middle crust for accommodating strain during synchronous thickening of crust and migration of melt.

As the batholith cooled further and contraction continued, the style of deformation in the lower crust changed. Along the western boundary of the MTZ (below letter M in Fig. 43b), shortening resulted in a vertical, 10-15 km wide, N-striking shear zone that cuts across the entire lower crustal section, including the lower and eastern contact of the batholith. This shear zone records an oblique-sinistral sense of shear. Near vertical foliations that define the shear zone at deep levels (14-16 kbar) underlie a mid-crustal fold-thrust belt that formed at 7-9 kbar at the top of the batholith (Fig. 43b). The mid-crustal fold-thrust belt is well exposed at Caswell Sound and exhibits features that are common in many upper crustal settings including imbricated thrust splays that sole into flat detachments, fault propagation folds, and conjugate thrusts and back thrusts (Daczko et al., 2002a).

Both the mid-crustal fold-thrust belt and the steep lower crustal shear zone below it cut the 126-116 Ma Western Fiordland Orthogneiss and are deformed by a younger set of upper amphibolite facies shear zones, including the Doubtful Sound shear zone (DS, Fig. 43c). These shear zones cut all contractional structures in Fiordland and record decompression and cooling of the granulite belt through the closure temperature of hornblende ($\sim 550^\circ\text{C}$) by ~ 108 -105 Ma and to $\leq 400^\circ\text{C}$ by 90 Ma (Gibson et al., 1988; Gibson and Ireland, 1995; Klepeis et al., 1999; Nathan et al., 2000). These relationships and U-Pb geochronology (Tulloch et al., 2000; Hollis et al., 2003) indicate that as the batholith cooled during the period 116-105 Ma, contraction was coupled at different levels of the crust through an interconnected network of steeply and gently dipping shear zones.

Discussion and Conclusions

Lithospheric-scale interactions among deformation and melt transfer processes

The Fiordland-Westland example provides strong geological evidence that diking and melt-enhanced fracturing was an important mechanism for the segregation and initial ascent of melt out of the lower crust. Similar melt-enhanced fracture systems have been observed in other orogenic belts (Davidson et al., 1994; Roering et al., 1995; Yamamoto and Yoshino, 1998) but to our knowledge none show this behavior on such large scales as in the Fiordland belt.

Once the batholith and its host rocks had cooled to subsolidus temperatures ($T < 820^\circ\text{C}$), structural elements in large vertical shear zones were exploited as pathways for melt transport horizontally and vertically through the crustal column. These observations agree with models that predict the buoyancy of hot felsic magma and the dynamics of transpression can create pressure gradients that help

force magma through the crust (e.g., Robin and Cruden, 1994; de Saint Blanquat et al., 1998).

As transpressional shear zones evolved in the lower crust, granitoids were emplaced into the upper crust at ~118 Ma (Muir et al. 1995; Waight et al. 1998) until ~105 Ma (Tulloch and Kimbrough, 2003). The Separation Point batholith represents the final stages of this process. This batholith consists of sodic, alkali-calcic diorite to biotite-hornblende monzogranite that are similar in composition to Cordilleran adakite suites (Muir et al., 1995). The geochemical and isotopic signatures of these rocks suggest that they were derived either from young, hot subducted oceanic crust or from mafic crust at the root of a thickened (>40 km paleodepths) magmatic arc (Muir et al., 1995; 1998). Our observations support the latter interpretation.

The isotopic (Sr, Nd) composition of the Separation Point suites also suggests that rising magmas experienced little to no interaction with felsic arc crust (Muir et al., 1995; 1998). This implies that the mixing of mantle and crustal components to form shallow-level plutons occurred in the mafic lower crust. Fiordland provides an example where the mixing of mantle and crust components may have occurred beneath a mafic intrusion (e.g., Petford and Gallagher, 2001) and that the rapid ascent of hybrid magmas through fracture networks and shear zones inhibited crustal contamination at shallower levels. Finally, data from Fiordland reconcile the previously tenuous relationship between crustal melting and high-pressure granulite facies metamorphism. The data show that this metamorphism was related directly to the migration of water-poor partial melts through the lower crust.

Transient coupling and decoupling of layers within the lithosphere

High melt volumes (>30%) associated with the emplacement of the WFO and the virtual absence of any Cretaceous deformation outside the batholith and its contact aureoles during emplacement indicate that the lower crust probably was decoupled from the upper and middle crust during the interval 126-116 Ma. Structural patterns indicate that subhorizontal (layer-parallel) flow between layers of colder, less deformed host rock characterized this period and reflected the localization of deformation into areas weakened by melt and heat. However, this period of vertical decoupling was transient, occurring only during the ~10 Ma period before the batholith cooled and crystallized.

By ~116 Ma, the melt enhanced shear zones at the base of the batholith were abandoned. The development of granulite facies fracture arrays inside the batholith and its host indicate that decoupling had ended by this time and that these crustal layers were deforming together at similar high effective viscosities. Evidence that a 10-15 km wide transpressional shear zone in the lower crust evolved simultaneously with and was connected physically to a mid-crustal thrust system following batholith emplacement and crustal melting also indicates that deformation at these levels was coupled from 116-105 Ma. Metamorphic data suggest that strengthening of the lower crust promoted this vertical coupling and was aided by efficient melt extraction and cooling as the batholith crystallized and melt escaped.

Structural features in the upper crust of the arc exposed in Westland also are consistent with a relatively strong, cooling viscous lower crust after ~116 Ma. At shallow levels of the crust contractional deformation occurred within a narrow (50-75 km wide) zone focused along the western side of the MTZ (Tulloch and Challis, 2000). This narrow, focused structural style supports the predictions of numerical models of orogens where a highly viscous lower crust preferentially transmits stresses vertically through the lithosphere (Royden, 1996; Ellis et al., 1998). The style also contrasts with the distributed style of near surface deformation in orogens characterized by a weak middle or lower crust.

Magmatism and late orogenic extension

In some Cordilleran settings, late orogenic extension has been linked to a thermal weakening of the middle or lower crust (Vanderhaeghe and Teyssier, 1997; Ellis et al., 1998). For example, in the Shuswap Ranges of southern British Columbia, crustal melting and magma intrusion decreased crustal viscosity by several orders of magnitude and appear to have aided the development of extensional structures within previously thickened crust (Vanderhaeghe and Teyssier, 2001). However, in Fiordland, the discovery of a vertical transpressional shear zone that formed after batholith emplacement (Fig. 43a) and evidence for a relatively strong lower crust that promoted vertical coupling prior to the onset of extension suggests an alternative mechanism at work. Late orogenic extension in western New Zealand appears to be linked to changes in plate boundary dynamics rather than a change in lower crustal rheology. The shift in structural style in Fiordland from contraction and crustal thickening to crustal thinning and decompression at ~105 Ma corresponds to the end of subduction and a reorganization of plate boundaries outboard of Gondwana (Bradshaw, 1989). This implies that the development of a regional tensile stress field at this time resulted in the extensional failure of the lithosphere rather than a weakening of the lower crust by melt and heat.

These relationships suggest a different type of response to magmatism and melting of the lower crust in Fiordland compared to other orogens that experienced deep crustal melting such as the Shuswap Range. One important reason for the mechanical response of the Fiordland-Westland orogen appears to be the mafic composition of the lower crust and the mineral reactions controlling melt production. In Fiordland, melt production was mostly controlled by hornblende-breakdown which produced relatively low volumes of partial melt that were extracted from the lower crust via fracture networks and ductile shear zones. This situation contrasts with the high melt volumes and widespread development of diatexite in the Shuswap Range where melt production in metapelitic protoliths was controlled by biotite and/or muscovite breakdown. These relationships imply that the hornblende-rich, mafic composition of the lower crust and the mineral reactions controlling melt production strongly influenced the mechanical behavior of the belt following magma emplacement.

In summary, the Fiordland setting provides a natural laboratory within which we can test our understanding of the feedbacks that develop among magmatism, metamorphism and deformation during cycles of orogenesis. In addition, the approach of using parallel field, laboratory, and experimental studies may be one of the most important tools we have to develop a complete picture of coupled processes in the continental lithosphere. In Fiordland, this approach has revealed the mechanisms by which magma was generated and transported through lower continental crust and how these processes affected the evolution of the lithosphere over a 35 Ma cycle.

References

- Allibone, A. H., and Tulloch, A. J., 1997, Metasedimentary, granitoid and gabbroic rocks from central Stewart Island, New Zealand: *New Zealand Journal of Geology and Geophysics*, v. 40, p. 53–68.
- Antignano IV, A., 2002, Experimental constraints on granitoid compositions in convergent regimes: a geochemical study, M.Sc. Thesis, University of Vermont.
- Antignano IV, A., Rushmer, T., Daczko, N. R., Clark, G.L., Collins, W.J., and Klepeis, K.A., 2001. Partial melting of a hornblende-biotite-clinozoisite bearing metadiorite: applications to the deep crust, Fiordland, New Zealand, *Geol. Soc. Amer. Abstracts with Programs*, 33(6), 211.
- Bishop, D.G., Bradshaw, J.D. & Landis, C.A., 1985. Provisional terrain map of South Island, New Zealand. In: D.G. Howell, D.L. Jones, A. Cox & A. Nur (eds), *Tectonostratigraphic terranes of the circum-Pacific region*, Circum-Pacific Council for Energy and Resources, Houston, Texas, 512-522.
- Blattner, P., 1976. Replacement of hornblende by garnet in granulite facies assemblages near Milford Sound, New Zealand. *Contr. Min Pet.*, 55, 181-190.
- Blattner, P., and Graham, I.G., 2000, New Zealand's Darran Complex and Mackay Intrusives – Rb/Sr whole-rock isochrons in the Median Tectonic Zone: *American Journal of Science*, v. 300, p. 603–629.
- Blattner, P., Geology of crystalline basement between Milford Sound and the Hollyford Valley, New Zealand, *NZ J. Geol. Geophys.*, 21, 33-47, 1978.
- Blattner, P., The North Fiordland transcurrent convergence. *NZ J. Geol. Geophys.*, 34, 543-553, 1991.
- Bradshaw, J. D., 1993, A review of the Median Tectonic Zone: terrane boundaries and terrane amalgamation near the Median Tectonic Line: *New Zealand Journal of Geology and Geophysics*, v. 36, p. 117–126.
- Bradshaw, J.D., 1989. Cretaceous geotectonic patterns in the New Zealand region. *Tectonics*, 8, 803-820.
- Bradshaw, J.Y. and Kimbrough, D.L., 1989b. Comment: Age constraints on metamorphism and the development of a metamorphic core complex in Fiordland, southern New Zealand. *Geology*, 17, 380-381.
- Bradshaw, J.Y., 1985. Geology of the northern Franklin Mountains, northern Fiordland, New Zealand, with emphasis on the origin and evolution of Fiordland granulites. Unpublished PhD thesis, University of Otago, Dunedin, New Zealand.
- Bradshaw, J.Y., 1989a. Origin and metamorphic history of an Early Cretaceous polybaric granulite terrain, Fiordland, southwest New Zealand, *Contr. Min. Pet.*, 103, 346-360.
- Bradshaw, J.Y., Geology of crystalline rocks of northern Fiordland: details of the granulite facies Western Fiordland Orthogneiss and associated rock units, *NZ J. Geol. Geophys.*, 33, 465-484, 1990.
- Brown E.H., High-pressure metamorphism caused by magma loading in Fiordland, New Zealand, *J. Metamorphic Pet.*, 14, 441-452, 1996.
- Bull, W.B., and A. F. Cooper, Uplifted marine terraces along the Alpine Fault, New Zealand, *Science*, 240, 804-805, 1986.
- Carter, R.M., Landis, C.A., Norris, R.J. & Bishop, D.G. 1974. Suggestions towards a high-level nomenclature for New Zealand rocks. *Journal of the Royal Society of New Zealand*, 4, 5-18.
- Chase C.G., Plate kinematics: the Americas, East Africa and the rest of the world, *Earth Planet Sci. Lett.*, 37, 355-368, 1978.
- Clarke, G.L., K.A. Klepeis, and N.R. Daczko, 2000. Cretaceous high-P granulites at Milford Sound, New Zealand: metamorphic history and emplacement in a convergent margin setting, *J. Met. Geol.*, 18, 359-374.
- Claypool, A, Klepeis, K., Dockrill, B., Clarke, G., Zwingmann, H., 2002, Structure and kinematics of oblique continental convergence in Northern Fiordland, New Zealand, *Tectonophysics*, 359(3-4), 329-358.
- Claypool, A., 2002, Kinematic evolution and exhumation of Early Cretaceous lower crustal granulites during changes in plate boundary conditions, Fiordland, New Zealand, M.Sc. Thesis, University of Vermont.
- Clemens, J. D. & Mawer, C. K., 1992. Granitic magma transport by fracture propagation. *Tectonophysics*, 204, 339-360.
- Daczko, N. R., K. A. Klepeis, and G. L. Clarke, 2001a. Evidence of Early Cretaceous collisional-style orogenesis in northern Fiordland, New Zealand and its effects on the evolution of the lower crust, *J. Struct. Geol.*, 23, 693-713.
- Daczko, N., K.A. Klepeis, and G.L. Clarke, 2002b. Significance of kyanite- and paragonite-bearing assemblages, northern Fiordland, New Zealand: Rapid cooling at the lower crustal root of a Cretaceous magmatic arc, *J. of Metamorphic Geology*, in press.
- Daczko, N., Klepeis, K. A. and Clarke, G. L., 2002a. Thermomechanical evolution of the crust during convergence and deep crustal pluton emplacement in the Western Province of Fiordland, New Zealand, *Tectonics*, 21(4), 1-18.
- Daczko, N.R., G.L. Clarke, and K.A. Klepeis, 2001b. Transformation of two-pyroxene hornblende granulite to garnet granulite involving simultaneous melting and fracturing of the lower crust, Fiordland, New Zealand, *J. Metamorph. Geol.*, 19, 549-562.

- Daczko, N.R., Stevenson, J.A., G.L. Clarke, K.A. Klepeis, 2002c, Successive hydration and dehydration of high-P mafic granulites involving clinopyroxene-kyanite symplectites, Mt Daniel, Fiordland, New Zealand, *J. of Metamorphic Geology*, **20**(7), 669-682.
- Davey, F.J. and E.G.C. Smith, The tectonic setting of the Fiordland region, south-west New Zealand, *Geophys. J. of the Royal Astron. Soc.*, **72**, 23-38, 1983.
- Davidson, C., Schmid, S.M. and Hollister, L.S. 1994. Role of melt during deformation in the deep crust. *Terra Nova*, **6**, 133-142.
- de Saint Blanquat, M., Tikoff, B., Teyssier, C., Vigneresse, J-L., 1998. Transpressional kinematics and magmatic arcs, In: *Continental transpressional and transtensional tectonics*, Holdsworth, R.E, Strachan, R.A. and Dewey, J.F. (eds). Geological Society Special Publications, **135**, 327-340.
- Degeling, H., Mid-Crustal Response to Syntectonic Pluton Emplacement, George Sound, New Zealand. Unpublished B.Sc. (Honours) thesis, University of Sydney, Sydney, 1997.
- DeMets, C., R. G. Gordon, D. F. Argus, and S. Stein, Current plate motions, *Geophys. J. Int.*, **101**, p. 425-478, 1994.
- Dockrill, B.R., The decompressional history of Northern Fiordland and its relationship to a Cretaceous-Tertiary crustal scale shear zone. Unpublished B.Sc. (Honours) thesis, University of Sydney, Sydney, 2000.
- Ellis, S., Beaumont, C., Jamieson, R. and Quinlan, G., 1998. Continental collision including a weak zone- the Vise model and its application to the Newfoundland Appalachians. *Canadian Journal of Earth Science*, **35**, 1323-1346.
- Gaina, C., Müller, D.R., Royer, J-Y, Stock, J., Hardebeck, J. and Symonds, P. 1998. The tectonic history of the Tasman Sea: A puzzle with thirteen pieces. *Journal of Geophysical Research* **103**, 12413-12433.
- Gibson, G. M., I. McDougall, and T.R. Ireland, 1988. Age constraints on metamorphism and the development of a metamorphic core complex in Fiordland, southern New Zealand, *Geology*, **16**, 405-408.
- Gibson, G. M., Uplift and exhumation of middle and lower crustal rocks in an extensional tectonic setting, Fiordland, New Zealand, in *Exposed Cross-Sections of the Continental Crust*, edited by Fountain, M.H. and D. M. Salisbury, Kluwer Academic, Dordrecht, 71-101, 1990.
- Gibson, G.M. and Ireland, T.R., 1995. Granulite formation during continental extension in Fiordland. *Nature*, **375**, 479-482.
- Hill, E.J, A deep crustal shear zone exposed in western Fiordland, New Zealand. *Tectonics*, **14**, 1172-1181, 1995.
- Hollis, J.A., Clarke, G.L., Klepeis, K.A., Daczko, N., Ireland, T.R., 2003. Geochronology and Geochemistry of high-pressure granulites of the Arthur River Complex, Fiordland, New Zealand: Cretaceous Magmatism and Metamorphism on the Palaeo-Pacific Margin. *Journal of Metamorphic Geology*, **21**, 299-313.
- Hollis, J.A., Clarke, G.L., Klepeis, K.A., Daczko, N., Ireland, T.R., submitted, U-Pb zircon geochronology of Fiordland granulites, New Zealand: Rapid burial and uplift along the Mesozoic Pacific Gondwana margin, *Journal of Metamorphic Geology*.
- Holyoke, C. III and Rushmer, T., 2002. An experimental study of grain-scale melt segregation mechanisms in crustal rocks. *Journal of Metamorphic Geology*. v. **20**, pp. 493-512.
- Ireland, T.R. and G.M., Gibson, 1998. SHRIMP monazite and zircon geochronology of high-grade metamorphism in New Zealand, *J. Metamorphic Geol.*, **16**, 149-167.
- Karlstrom, K.E. and Williams, M.L., 2002. Nature of the middle crust-heterogeneity of structure and process due to pluton-enhanced tectonism: an example from Proterozoic rocks of the North American Southwest, in Brown, M. and Rushmer, T.(eds.), *Evolution and differentiation of the continental crust*, Cambridge University Press, in press.
- Kimbrough, D.L., A.J. Tulloch, D.S. Coombs, C.A. Landis, M.R. Johnston, and J.M. Mattinson, 1994. Uranium-lead zircon ages from the Median Tectonic Zone, New Zealand. *NZ J. Geol. Geophys.*, **37**, 393-419.
- Kimbrough, D.L., Tulloch, A.J., Geary, E., Coombs, D.S. & Landis, C.A., 1993. Isotopic ages from the Nelson region of South Island, New Zealand; crustal structure and the definition of the Median Tectonic Zone. *Tectonophysics*, **225**, 443-448.
- Klepeis, K.A. and Clarke, G. L., 2003. Evolution of an exposed lower crustal attachment zone in Fiordland, New Zealand, *Geol. Soc. of London Spec. Pub.*, in press.
- Klepeis, K.A., Clarke, G.L., & Rushmer, T., 2003, Magma Transport and Coupling Between Deformation and Magmatism in the Continental Lithosphere, *GSA Today*, **13**, 4-11.
- Klepeis, K.A., N.R. Daczko, and G.L. Clarke, 1999. Kinematic vorticity and tectonic significance of superposed mylonites in a major lower crustal shear zone, northern Fiordland, New Zealand, *J. Struct. Geol.*, **21**, 1385-1405.
- Lamarche, G., J.-Y. Collot, R.A. Wood, M. Sosson, R. Sutherland, and J. Delteil, The Oligocene-Miocene Pacific-Australia plate boundary, south of New Zealand: evolution from oceanic spreading to strike-slip faulting, *Earth and Planet. Sci Lett.*, **148**, 129-139, 1997.
- Landis, C. A. & Coombs, D. S., 1967. Metamorphic belts and orogenesis in southern New Zealand. *Tectonophysics*, **4**, 501-518.
- MacKinnon, T. C., 1983. Origin of the Torlesse terrane and coeval rocks, South Island, New Zealand. *Geological Society of*

- American Bulletin, **94**, 967-985.
- Mattinson, J.L., D.L. Kimbrough, and J. Y. Bradshaw, 1986. Western Fiordland orthogneiss: Early Cretaceous arc magmatism and granulite facies metamorphism, New Zealand, *Contrib. Min. Pet.*, **92**, 383-392.
- McCulloch, M.T., J.Y. Bradshaw, and S.R. Taylor, 1987. Sm-Nd and Rb-Sr isotopic and geochemical systematics in Phanerozoic granulites from Fiordland, Southwest New Zealand. *Contrib. Min. Pet.*, **97**, 183-195.
- Miller, R.B., and Paterson, S.R., 2001. Influence of lithological heterogeneity, mechanical anisotropy, and magmatism on the rheology of an arc, North Cascades, Washington, *Tectonophysics*, **342**, 351-370.
- Mortimer, N., A.J. Tulloch, R. Spark, N. Walker, E. Ladley, D.L. Kimbrough, and A.H. Allibone, 1999. Overview of the Median Batholith, New Zealand: a new interpretation of the geology of the Median Tectonic Zone and adjacent rocks, *J. of African Earth Sci.*, **29**, 257-268.
- Muir, R. J., Weaver, S. D., Bradshaw, J. D., Eby, G. N. & Evans, J. A., 1995. The Cretaceous Separation Point batholith, New Zealand: granitoid magmas formed by melting of mafic lithosphere. *Journal of the Geological Society, London*, **152**, 689-701.
- Muir, R.J., Ireland, T.R., Weaver, S.D., Bradshaw, S.D., Evans, J.A., Eby, G.N. and Shelley, D., 1998. Geochronology and geochemistry of a Mesozoic magmatic arc system, Fiordland, New Zealand. *Journal of the Geological Society, London*, **155**, 1037-1053.
- Nathan, S., C. Thurlow, P., Warnes, and R., Zucchetto, 2000. Geochronology database for New Zealand rocks (2nd edition): 1961-1999, *Inst. Geol. Nuc. Sci. rep.* 2000, **11**, 51.
- Norris, R.J. and A.F. Cooper, Late Quaternary slip rates and slip partitioning on the Alpine Fault, New Zealand, *J. of Struct. Geol.*, **23**, 507-520, 2001.
- Oliver, G. J. H., 1977. Feldspathic hornblende and garnet granulites and associated anorthosite pegmatites from Doubtful Sound, Fiordland, New Zealand. *Contributions to Mineralogy and Petrology*, **65**, 111-121.
- Oliver, G.J.H. and J.H. Coggon, Crustal Structure of Fiordland, New Zealand, *Tectonophysics*, **54**, 253-292, 1979.
- Oliver, G.J.H., Geology of the granulite & amphibolite facies gneisses of Doubtful Sound, Fiordland, New Zealand, *NZ J. Geol. Geophys.*, **1**, 27-41, 1980.
- Peford, N. and Gallagher, K., 2001. Partial melting of mafic (amphibolitic) lower crust by periodic influx of basaltic magma, *Earth and Planet. Sci. Letters*, **193**, 483-499.
- Robin, P.-Y.F. and Cruden, A.R., 1994. Strain and vorticity patterns in ideally ductile transpressional zones. *Journal of Structural Geology*, **16**, 447-466.
- Roering, C., van Reenen, D. D., Smit, C. A., Du Toit, R., 1995. Deep crustal embrittlement and fluid flow during granulite metamorphism in the Limpopo Belt, South Africa. *Journal of Geology*, **103**, 673-686.
- Royden, L., 1996. Coupling and decoupling of crust and mantle in convergent orogens: Implications for strain partitioning in the crust. *Journal of Geophysical Research*, **101**, 17,679-17,705.
- Rushmer, T., 1995. An experimental deformation study of partially molten amphibolite: Applications to low-fraction melt segregation. In: *Segregation of Melts from Crustal Protoliths: Mechanisms and Consequences*. Brown, M., Rushmer, T. and Saywer, E. W. (eds). *Journal of Geophysical Research*, **100**, 15,681-15,696.
- Spell, T. L. McDougall, I., Tulloch, A.J., 2000. Thermochronologic constraints on the breakup of the Pacific Gondwana margin: the Paparoa metamorphic core complex, South Island, New Zealand. *Tectonics*, **19**, 433-451.
- Sutherland, R., Displacement since the Pliocene along the southern section of the Alpine fault, New Zealand, *Geology*, **22**, 327-330, 1994.
- Sutherland, R., F. Davey, and J. Beavan, Plate boundary deformation in South Island, New Zealand, is related to inherited lithospheric structure, *Earth and Planet. Sci. Let.*, **177**, 141-151, 2000.
- Tulloch, A. J., 1988, Batholiths, plutons and suites: nomenclature for granitoid rocks of Westland-Nelson, New Zealand: *New Zealand Journal of Geology and Geophysics*, v. 31, p. 505-509.
- Tulloch, A. J., and Rabone, S. D. C., 1993, Mo-bearing granodiorite porphyry plutons of the Early Cretaceous Separation Point Suite west Nelson, New Zealand: *New Zealand Journal of Geology and Geophysics*, v. 36, p. 401-408.
- Tulloch, A.J. and D.L. Kimbrough, 1989. The Paparoa metamorphic core complex, New Zealand: Cretaceous extension associated with fragmentation of the Pacific margin of Gondwana, *Tectonics*, **8**, 1217-1234.
- Tulloch, A.J. and D.L. Kimbrough, 2003, Paired plutonic belts in convergent margins and the development of high Sr/Y magmatism: the Peninsular Ranges Batholith of California and the Median Batholith of New Zealand, *Geological Society of America Special Paper*, in press.
- Tulloch, A.J., and Challis, G.A., 2000. Emplacement depths of Paleozoic-Mesozoic plutons from western New Zealand estimated by hornblende-Al geobarometry, *New Zealand J. of Geology and Geophys.*, **43**, 555-567
- Tulloch, A.J., T.R., Ireland, N.W., Walker, and D.L., Kimbrough, 2000. U-Pb zircon ages from the Milford Orthogneiss, Milford Sound, northern Fiordland: Paleozoic igneous emplacement and Early Cretaceous metamorphism, *Inst. Geol. Nucl. Sci. Rep.*, **6**, 17.
- Turnbull, I.M., 2000. Geology of the Wakatipu area. Institute of Geological & Nuclear Sciences 1:250 000 Geologic Map

18. 1 sheet + 72 p. Lower Hutt, New Zealand. Institute of Geological & Nuclear Sciences Ltd.
- Vanderhaege, O. and Teyssier, C., 1997. Formation of the Shuswap metamorphic complex during late-orogenic collapse of the Canadian Cordillera: Role of ductile thinning and partial melting of the mid- to lower crust. *Geodynamica Acta*, 10, 41-58.
- Vanderhaege, O. and Teyssier, C., 2001. Crustal-scale rheological transitions during late orogenic collapse. *Tectonophysics*, 335, 211-228.
- Waight, T.E., Weaver, S.D., Muir, R.J., 1998. Mid-Cretaceous granitic magmatism during the transition from subduction to extension in southern New Zealand: a chemical and tectonic synthesis, *Lithos*, 45, 469-482.
- Walcott, R.I., Modes of oblique compression: Late Cenozoic tectonics of the South Island of New Zealand, *Rev. Geophys.*, 36, 1-26, 1998.
- Walcott, R.I., Plate motions and shear strain rates in the vicinity of the Southern Alps, in *The Origin of the Southern Alps*, edited by Walcott, R.I., M.M. Creswell, Roy. Soc. NZ Bull., 18, Wellington, 5-12, 1979.
- Wandres, A.M., S.D., Weaver, D., Shelley, and J.D., Bradshaw, Change from calc-alkaline to adakitic magmatism recorded in the early Cretaceous Darran Complex, Fiordland, New Zealand, *NZ J. Geol. Geophys.*, 41, 1-14, 1998.
- Weissel, J.K., D.E. Hayes, and E.M. Herron, Plate tectonics synthesis: the displacements between Australia, New Zealand, and Antarctic since the late Cretaceous, *Marine Geology*, 25, 231-277, 1977.
- Wellman, H.W., 1953. Data for the study of recent and late Pleistocene faulting in the South Island of New Zealand, *New Zealand Journal of Science and Technology*, B34, 270-288.
- Williams, J.G., and C.T. Harper, 1978. Age and status of the Mackay Intrusives in the Eglinton-Upper Hollyford area, *New Zealand Journal of Geology and Geophysics*, 21, 733-742.
- Wood, B.L., Metamorphosed ultramafites and associated formations near Milford Sound, New Zealand, *NZ J. Geol. Geophys.*, 15, 88-128, 1972.
- Yamamoto, H. and Yoshino, T., 1998. Superposition of replacements in the mafic granulites of the Jijal Complex of the Kohistan Arc, northern Pakistan; dehydration and rehydration within deep arc crust. *Lithos*. 43, 219-234.